

**THE ROLE OF MEDIATOR COMPLEX SUBUNIT 12 (*MED12*) IN THE  
MURINE REPRODUCTIVE TRACT**

by

Priya Mittal

B.Tech, Vellore Institute of Technology, India, 2010

Submitted to the Graduate Faculty of  
Graduate School of Public Health in partial fulfillment  
of the requirements for the degree of  
Doctor of Philosophy

University of Pittsburgh

2015

UNIVERSITY OF PITTSBURGH  
GRADUATE SCHOOL OF PUBLIC HEALTH

This dissertation was presented

by

Priya Mittal

It was defended on

October 23, 2015

and approved by

**Dissertation Advisor:** Aleksandar Rajkovic, MD, PhD, Professor, Obstetrics and Gynecology, School of Medicine, University of Pittsburgh

Zsolt Urban, PhD, Associate Professor, Human Genetics, Graduate School of Public Health, University of Pittsburgh

Urvashi Surti, PhD, Professor, Pathology and Obstetrics and Gynecology, School of Medicine, University of Pittsburgh

Michael. M. Barmada, PhD, Associate Professor, Human Genetics, Graduate School of Public Health, University of Pittsburgh

Quasar Padiath, PhD, Assistant Professor, Human Genetics, Graduate School of Public Health, University of Pittsburgh

Copyright © by Priya Mittal

2015

**THE ROLE OF MEDIATOR COMPLEX SUBUNIT 12 (*MED12*) IN THE MURINE REPRODUCTIVE TRACT**

Priya Mittal, PhD

University of Pittsburgh, 2015

**ABSTRACT**

Uterine leiomyomas are benign neoplasms arising from smooth muscle cells of the uterus. They are clinically diagnosed in 25% of women and are associated with significant morbidity. Whole exome approaches have identified heterozygous somatic mutations in the mediator complex subunit 12 (*MED12*) in about 70% of leiomyomas with a majority harboring in exon 2 of *MED12* with c.131G>A being the most common SNV. *MED12* protein is part of the large mediator complex and is involved in transcriptional regulation of RNA Polymerase II. To elucidate the role of *MED12* exon 2 variants in leiomyomagenesis, we generated three different mouse models of *Med12*; loss-of-function, dominant-negative and gain-of-function mouse models.

The loss-of-function females lacked any leiomyoma-like lesions, instead the reproductive tracts were hypoplastic and the females were infertile.

We engineered a model where we conditionally floxed *Med12* c.131G>A cDNA and inserted into the *ROSA26* locus to generate *Med12 ROSA* knock-in mice. *Amhr2-cre* was used to drive the expression of the mutant *Med12* from the *ROSA* locus either in the absence (gain-of-function) or presence (dominant-negative) of X-chromosome wild-type *Med12* in the uterine mesenchyme. Uteri from (gain-of-function) females displayed leiomyoma-like lesions in about 87% of females. Similar characterization of uteri of dominant negative females revealed the development of leiomyoma-like lesions, but with appearance of smaller lesions and lower penetrance (50% of females) as compared to the gain-of-function model, leading us to conclude

that the *Med12* exon 2 variants are likely to cause uterine leiomyomas via gain-of-function mechanism.

Array comparative genomic hybridization (aCGH) of mouse tumors displayed genome wide aberrations, affecting general tumor pathways. Interestingly, several regions previously implicated in human leiomyomas were also shared by the mouse leiomyomas, revealing the similarities between human and mouse leiomyomas. This data suggests that *Med12* exon 2 mutations are precursors to genomic rearrangements leading to an unstable genome. The public health significance of this work includes the successful development of the first animal model for uterine leiomyomas, which will be an invaluable tool to understand the role of *MED12* in leiomyoma genesis, as well as provide a unique platform to test targeted therapeutics as an alternative to hysterectomies.

## TABLE OF CONTENTS

<b>PREFACE</b> .....	<b>xiii</b>
<b>1.0 INTRODUCTION</b> .....	<b>1</b>
<b>1.1 UTERINE LEIOMYOMAS</b> .....	<b>1</b>
<b>1.1.1 Epidemiology and risk factors</b> .....	<b>2</b>
<b>1.1.2 Diagnosis and treatment</b> .....	<b>3</b>
<b>1.1.3 Histopathology and molecular characteristics</b> .....	<b>6</b>
<b>1.2 GENESIS OF UTERINE LEIOMYOMAS</b> .....	<b>9</b>
<b>1.2.1 Ovarian hormones and leiomyomagenesis</b> .....	<b>10</b>
<b>1.2.2 Myometrial stem cells and leiomyomagenesis</b> .....	<b>11</b>
<b>1.3 GENETICS OF LEIOMYOMAS</b> .....	<b>12</b>
<b>1.3.1 Cytogenetics of leiomyomas</b> .....	<b>13</b>
<b>1.3.1.1 12q14-15 translocations</b> .....	<b>13</b>
<b>1.3.1.2 Deletions of 7q</b> .....	<b>15</b>
<b>1.3.1.3 6p21 rearrangements</b> .....	<b>15</b>
<b>1.3.1.4 Other cytogenetic aberrations</b> .....	<b>16</b>
<b>1.3.1.5 Monoclonality of leiomyomas</b> .....	<b>16</b>
<b>1.3.1.6 Copy number alterations and gene expression profiling in                 leiomyomas</b> .....	<b>17</b>

1.3.2	Leiomyomas and associated syndromes .....	18
1.3.2.1	Hereditary leiomyomatosis and renal cell cancer ( <i>HLRCC</i> )..	18
1.3.2.2	Leiomyomas associated with other syndromes .....	19
1.3.3	Molecular genetics of leiomyomas.....	20
1.3.3.1	Genome wide association studies.....	20
1.3.3.2	Whole exome sequencing; <i>MED12</i> exon 2 variants and leiomyomas .....	21
1.3.3.3	<i>MED12</i> mutations and genomic alterations .....	25
1.3.3.4	<i>MED12</i> mutations in other benign and malignant tumors ....	27
1.3.4	<i>MED12</i> germline mutations .....	28
1.3.5	Mediator complex subunit 12 ( <i>MED12</i> ).....	29
1.3.6	Animal models of leiomyomas .....	33
1.3.7	Public health significance.....	35
1.3.8	Summary.....	35
2.0	<b>LOSS OF MED12 CAUSES INFERTILITY BUT DOES NOT STIMULATE TUMORIGENESIS.....</b>	<b>37</b>
2.1	<b>INTRODUCTION .....</b>	<b>37</b>
2.2	<b>MATERIALS AND METHODS .....</b>	<b>38</b>
2.3	<b>RESULTS .....</b>	<b>43</b>
2.3.1	Generation of conditional loss of function model of <i>Med12</i> .....	43
2.3.2	<i>Med12</i> cKO females have atrophic uteri.....	46
2.3.3	<i>Med12</i> cKO females are infertile .....	48

2.3.4	Ovulation occurs under external gonadotropic stimulus in <i>Med12</i> cKO females .....	50
2.3.5	<i>Med12</i> is a maternal effect gene important for somatic cell but not germ cell development .....	53
2.3.6	<i>Med12</i> cKO uteri infrequently develop tumors other than leiomyomas .....	55
2.4	DISCUSSION .....	58
3.0	<b>MED12 GAIN OF FUNCTION MUTATION CAUSES LEIOMYOMAS AND GENOMIC INSTABILITY.....</b>	<b>60</b>
3.1	INTRODUCTION .....	60
3.2	MATERIALS AND METHODS .....	61
3.3	RESULTS .....	66
3.3.1	Generation of mutant <i>Med12 Rosa</i> knock in mice (c.131G>A)	66
3.3.2	Expression of the <i>Med12</i> c.131G>A variant on the background of conditional <i>Med12</i> knockout causes leiomyomas.....	69
3.3.3	<i>Med12</i> c.131G>A variant can cause uterine leiomyomas on WT background.....	75
3.3.4	<i>Med12</i> mouse mutations and genomic instability .....	80
3.3.5	Expression of mutant <i>Med12</i> in myometrial cells using the Myosin heavy chain 11- cre ( <i>Myh11-cre</i> ) .....	84
3.4	DISCUSSION .....	86
3.5	ACKNOWLEDGEMENTS .....	89
4.0	OVERALL SUMMARY AND CONCLUSIONS.....	91

**APPENDIX: ABBREVIATIONS AND TABLES .....95**  
**BIBLIOGRAPHY .....103**

## LIST OF TABLES

Table 1.1 WHO based pathological classification of uterine leiomyoma variants. ....	8
Table 1.2 List of missense, splice-site variants and indels in exon 2 of <i>MED12</i> .....	24
Table 3.1 Table of logarithmic signal intensity ratios to interpret aCGH data .....	80
Table 3.2 Regions shared between human and mouse leiomyomas .....	84
Table 4.1 List of abbreviations.....	95
Table 4.2 Regions of aberrations in mouse leiomyomas.....	98
Table 4.3 Syntenic regions between mouse aberrations and human chromosomes.....	101

## LIST OF FIGURES

Figure 1.1 MRI image of an intramural uterine leiomyoma .....	4
Figure 1.2 Histopathology of conventional leiomyomas .....	7
Figure 1.3 Histopathological variants of uterine leiomyoma .....	9
Figure 1.4 <i>MED12</i> exon 2 variants associated with uterine leiomyomas .....	23
Figure 1.5 <i>MED12</i> as part of the <i>CDK8</i> kinase module in the mediator complex.....	30
Figure 2.1. Evaluation of <i>Amhr2-cre</i> activity, <i>Med12</i> recombination and expression in loss of Med12 uteri .....	45
Figure 2.2. <i>Med12<sup>fl/fl</sup> Amhr2-cre</i> females have hypoplastic reproductive tract .....	47
Figure 2.3. Evaluation of breeding in <i>Med12</i> cKO males and females.....	49
Figure 2.4. Assessment of ovarian histology and ovulation assay .....	52
Figure 2.5. Breeding schemes to generate <i>Med12<sup>fl/-</sup></i> females and evaluation of <i>Med12<sup>fl/fl</sup> Zp3-cre</i> ovaries .....	55
Figure 2.6. Solid tumors in <i>Med12</i> cKO uteri .....	57
Figure 3.1. Generation of <i>ROSA26 Med12</i> mice that conditionally express <i>Med12</i> c.131G>A variant.....	67
Figure 3.2 Models and breeding schemes of mice used in Chapter 3 .....	68
Figure 3.3. Histological evaluation of uteri from nulliparous <i>Med12<sup>fl/+</sup> Med12<sup>R<sup>mt/+</sup></sup> Amhr2-cre</i> females.....	71

Figure 3.4. Multiparous *Med12<sup>fl/+</sup> Med12R<sup>mt/+</sup>Amhr2-cre* females develop spectacular leiomyoma-like lesions similar to human leiomyomas ..... 72

Figure 3.5. Molecular characterization of leiomyoma-like lesions ..... 72

Figure 3.6. Histological evaluation of uteri from *Med12<sup>fl/fl</sup> Med12R<sup>mt/+</sup> Amhr2-cre*, *Med12<sup>fl/fl</sup> Amhr2-cre* and *Med12<sup>fl/fl</sup> Med12R<sup>mt/mt</sup> Amhr2-cre* females ..... 74

Figure 3.7. Histological evaluation of uteri from nulliparous *Med12R<sup>mt/+</sup>Amhr2-cre* females ..... 77

Figure 3.8 Multiparous *Med12R<sup>mt/+</sup> Amhr2-cre* uteri develop prominent leiomyomas ..... 78

Figure 3.9 Histological evaluation of uteri from nulliparous and multiparous *Med12R<sup>mt/mt</sup>Amhr2-cre* females ..... 79

Figure 3.10 Representative array profiles of *Med12<sup>fl/+</sup>Med12R<sup>mt/+</sup> Amhr2-cre* tumors..... 82

Figure 3.11 Representation of human syntenic mapping of uterine rearrangements in mouse *Med12<sup>fl/+</sup> Med12R<sup>mt/+</sup> Amhr2-cre* females ..... 83

Figure 3.12 Evaluation of 12-week *Med12R<sup>mt/+</sup> Myh11-cre* uteri ..... 85

## **PREFACE**

My journey through the Ph.D. was made possible by the support of steadfast friends and accomplished scientists. Writing this in a formal acknowledgment will hardly justify the immense gratitude that I hold for all the people, who have contributed towards my accomplishments.

My deepest gratitude goes to my advisor, Dr. Aleksandar Rajkovic, who has enthusiastically supported, counseled, inspired and encouraged me throughout the course of my Ph.D. Over the past five years, you taught me invaluable lessons, both in science and life, which I will cherish forever. You have been a great example of a dedicated, focused, productive, perceptive and a brilliant scientist, and I will always strive to be more like you. Thank you for steering me through graduate school and for being the most instrumental person behind my scientific accomplishments.

I would like to thank my dissertation committee members Dr. Zsolt Urban, Dr. Urvashi Surti, Dr. Michael Barmada and Dr. Quasar Padiath for their discussions, suggestions, constructive criticism and guidance.

I am grateful to the Rajkovic lab members both old and new, for providing me with an enjoyable work environment. I had the privilege of working with some of my good friends, Megan, Kayla, Andrew, and Archana who were also my colleagues. I really appreciate all the intellectual and non-intellectual guidance, laughs and support you have offered over the years.

My warmest acknowledgements goes to Alexander Yatsenko, Yu Ren, Yonghyun-shin, Hitomi Suzuki, Huiyang Jiang and Michelle Wood-Trageser for their scientific discussions, mentorship and technical assistance. I would also like to thank Drs. William Walker and Anthony Zeleznik from the Magee-Womens Research Institute for their stimulating scientific discussions and for their guidance.

A big thank you to my collaborators, Carlos Castro for collaborating on the pathology aspects of the mouse leiomyomas and Svetlana Yatsenko for teaching and collaborating with me on the array CGH projects.

Above all, I could not have accomplished my journey without the unwavering support of my parents and friends. I thank my parents for their inspiration, motivation, encouragement and especially my grandmom to whom I dedicate this thesis.

I would like to sincerely thank my friends Advaita, Swati, Mainpal, Savita and Cressida for their constant encouragement, advice, and support and for making my PHD life a little smoother.

Finally, I would like to acknowledge the Department of Human Genetics for my graduate fellowship and the department faculty members, especially Candace Kammerer for running a very successful and a high-quality graduate training program.

## **1.0 INTRODUCTION**

### **1.1 UTERINE LEIOMYOMAS**

Uterine leiomyomas (fibroids or myomas) are benign neoplasms arising from the smooth muscle layer of the uterus. Leiomyomas are one of the most common gynecological tumors occurring in women, with a frequency of occurrence ranging from 20-50% of women of reproductive age (1). This number can be even as high as 77% as majority of leiomyomas maybe asymptomatic and hence go undiagnosed (2). They are clinically diagnosed in about 25% of women and depending on their location in the uterus may be classified as subserous, submucosal or intramural. Grossly, leiomyomas often appear to be smooth, spherical and firm and can be as large as 20 cm (3). Larger leiomyomas may undergo degenerative changes including hemorrhage (dark red), necrosis (demarcated by yellow regions), cystic changes or even calcification. The size, location and number of tumors in the uterus often, determines the presentation and intensity of symptoms. Leiomyomas requiring treatment are often associated symptoms such as dysmenorrhea (painful menstruation), menorrhagia (heavy menstrual bleeding), infertility, miscarriage, ascites, anemia and polycythemia (4-6). On the other hand, leiomyomas growing outside or in between uterine walls (subserous and intramural) are very common and can cause pelvic discomfort or may even pressurize surrounding organs (7). The recurrence, size and unclear etiology of leiomyomas

makes their management difficult, making hysterectomies the only available long-term treatment option for women with leiomyomas (8).

### **1.1.1 Epidemiology and risk factors**

Leiomyomas are usually prevalent after menarche, peak during reproductive years and regress after menopause (9, 10). The evidence strongly suggests a strong link between ovarian steroids and tumor progression in women. Further, factors such as early menarche in women, increases the risk for leiomyomas, while late onset of menarche and longer duration of lactation decreases the risk respectively (11-14). One hypothesis suggests that early menarche could expose the uterus to longer duration of menstruation and hormones, thereby increasing the number of cell divisions and a higher chance of accumulation of mutations in the myometrium. On the other hand, later age of menarche and lactation reduces the risk to leiomyomas as the lifetime exposure of the uterus to cyclical changes decreases (11).

Race and ethnicity differences also play a crucial role in determining the incidence, presentation and severity of uterine leiomyomas. Studies conducted on North American women have shown ~10% higher incidence and a younger age of diagnosis of leiomyomas in African-American women as compared to Caucasian women (9, 15). African-American women also had higher uterine weight, larger and more number of leiomyomas causing more severe symptoms, ultimately leading to a younger age at hysterectomy (16, 17). The cause for this racial disparity in tumor incidence and presentation is not understood. A few studies have attributed a difference in estrogen metabolism as a possible explanation for the disparity of leiomyoma presentation between the two races (18).

Sibling and other family studies have strongly indicated a genetic predisposition for leiomyomas (19). First-degree relatives of women with leiomyomas have a two time higher risk of developing leiomyomas in their lifetime. Other environmental and lifestyle factors may also influence the development and outcomes of these tumors. The risk of leiomyomas increases with factors such as obesity, caffeine, alcohol, diabetes and hypertension. Interestingly, smoking reduces the incidence of leiomyomas (12, 20-24). Few studies have indicated a link between vegetarian diet and overall better prognosis of uterine leiomyomas (25).

Xenoestrogens are compounds with the capability of disrupting estrogenic functions by acting as an agonist or an antagonist (26). Few such xenoestrogens have also been associated with the development of leiomyomas. For example, DDT (dichlorodiphenyltrichloroethane) has been determined to be present at significantly higher levels in leiomyomas as compared to normal myometrium (27). DES (Diethylstilbestrol) is another such xenoestrogen that has been shown to cause leiomyomas both through *in-vivo* models (28) and human data (29).

Larger cohort studies looking at environmental and lifestyle factors and their influence on tumorigenesis are required to have a deeper understanding of their contribution to disease progression.

### **1.1.2 Diagnosis and treatment**

Leiomyomas can be diagnosed during a bimanual pelvic exam and are perceived by an enlarged, firm or an irregularly shaped uterus. The initial diagnosis is followed by either an ultrasonography, saline-infusion sonohysterography, or by magnetic resonance imaging (MRI) (30). Ultrasonography or ultrasound is a relatively cheap imaging technique that is most frequently used to carry out differential diagnosis on intramural or subserous leiomyomas, but is

inefficient in detecting the exact number or position of leiomyomas (31, 32). Saline-infusion sonography can be used to detect submucosal leiomyomas as this technique uses saline to distend the uterine cavity, therefore allowing more accurate information to be obtained from the mucosal lining of the uterus. The most robust of these techniques is the use of MRI for diagnosis of leiomyomas (31, 33). Although, more expensive than a trans-vaginal ultrasound, it provides more precise information on the number, position (subserous, intramural, submucosal) and the size of leiomyomas with a sensitivity to detect even 5mm lesions (Figure 1.1). Precise diagnostic information on the number, size and position of leiomyomas can be crucial for determining the treatment and management of the disease (34).

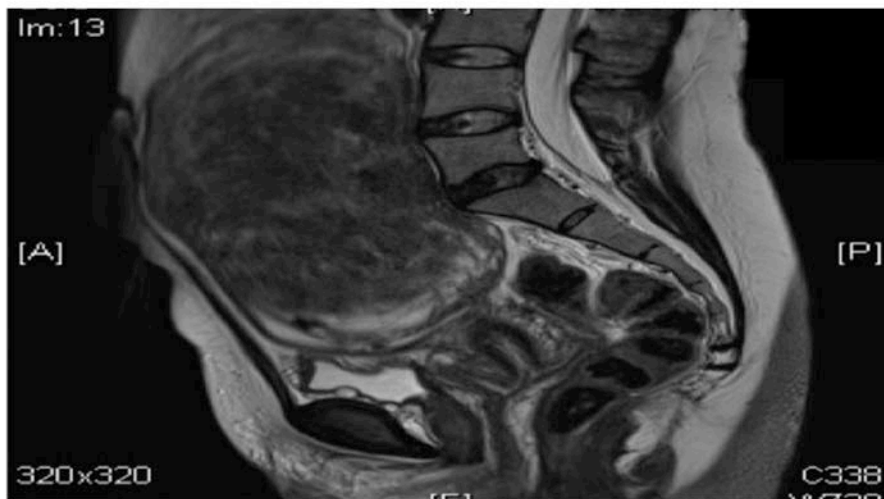


**Figure 1.1 MRI image of an intramural uterine leiomyoma**

(Reproduced from Khan et al., 2014) (32)

The management of the disease depends on the severity of symptoms, skills of the surgeon, reproductive age and decision of the patients. The kind of treatments currently available for leiomyomas includes, medical therapy, minimally invasive procedures and surgery (32).

Medical therapies include short-term treatments used to provide either symptomatic relief or maybe used as a preoperative measure. These treatments are usually not used in the long-term as they often have either long-term risks associated with them, or they lack evidence on the health risks posed by their long-term use. Patients for symptomatic relief are often prescribed nonsteroidal anti-inflammatory (NSAIDs) drugs (pain) or tranexamic acid to control menorrhagia (32). Combined oral contraceptives, levonorgestrel-releasing intra-uterine devices (Mirena), aromatase inhibitors or gonadotropin-releasing hormone analogs (GnRHa) are currently used as a pre-operative adjunct. Estrogen and especially progesterone receptor modulators are gaining popularity as an effective treatment option to reduce myoma volumes and associated symptoms. Mifepristone (RU486) and Ulipristal acetate are two such examples of progesterone receptor modulators, which have been subjected to clinical trials and are now being used clinically as a pre-operative measure in both the U.S and Europe (35, 36).

Surgical therapy is currently, the only long-term and gold standard treatment available for uterine leiomyomas. For women of prime reproductive age or with a desire for future pregnancies, myomectomy (open or minimally invasive) is usually performed (depending on the physician). In the recent years, minimally invasive techniques are providing women not only with the option of preserving their uterus and fertility, but also reduce morbidity and recovery time in comparison to open surgery (32). Minimally invasive techniques include, uterine artery embolization (UAE), Magnetic resonance-guided focused ultrasound surgery (MRgFUS) and combined sonography and radiofrequency therapy (VizAblate). UAE is an image-guided technique through which the blood to the leiomyomas is blocked resulting in their shrinking (37). MRgFUS is a method of thermal ablation using high intensity ultrasound waves for shrinking fibroids, but is not widely available to women. The newest of these techniques is using a

combination of sonography and radiofrequency waves for treatment of fibroids using a transcervical device (VizAblate) (38). Although these techniques are helpful, they are not effective in preventing recurrent fibroids. The only definitive solution to the treatment of fibroids is a hysterectomy, which is effective in permanently alleviating the symptoms and the fibroids themselves. Other than ending a women's fertility, hysterectomy carries serious risks such as damage to the excretory system, pelvic abscess, hemorrhage during surgery or pulmonary embolism (39). Thus there is a dire necessity to understand the etiology of this disease and develop a model to help better understand the tumor process as well as develop drugs as a definitive solution as an alternative to hysterectomies.

### **1.1.3 Histopathology and molecular characteristics**

Leiomyomas are composed of whorled, uniform, fusiform plump smooth muscle cells forming fascicles. The spindle-shaped cells have indistinct borders, with blunt elongated nuclei, finely dispersed chromatin and small nucleoli. Leiomyomas often consist of disorderly arranged smooth muscle fibers interspersed abundantly with extracellular matrix deposits (collagen, fibronectin, proteoglycan) (Figure 1.2). Hyaline fibrosis and edema are also quite common in leiomyomas (3). About 10% of leiomyomas pathologically vary and present as heterogeneous lesions, mimicking malignant aspects (Table 1.1). Although, the histology presentation resembles malignant lesions, they are clinically diagnosed to be benign and are managed similar to conventional leiomyomas (Figure 1.3) (40).

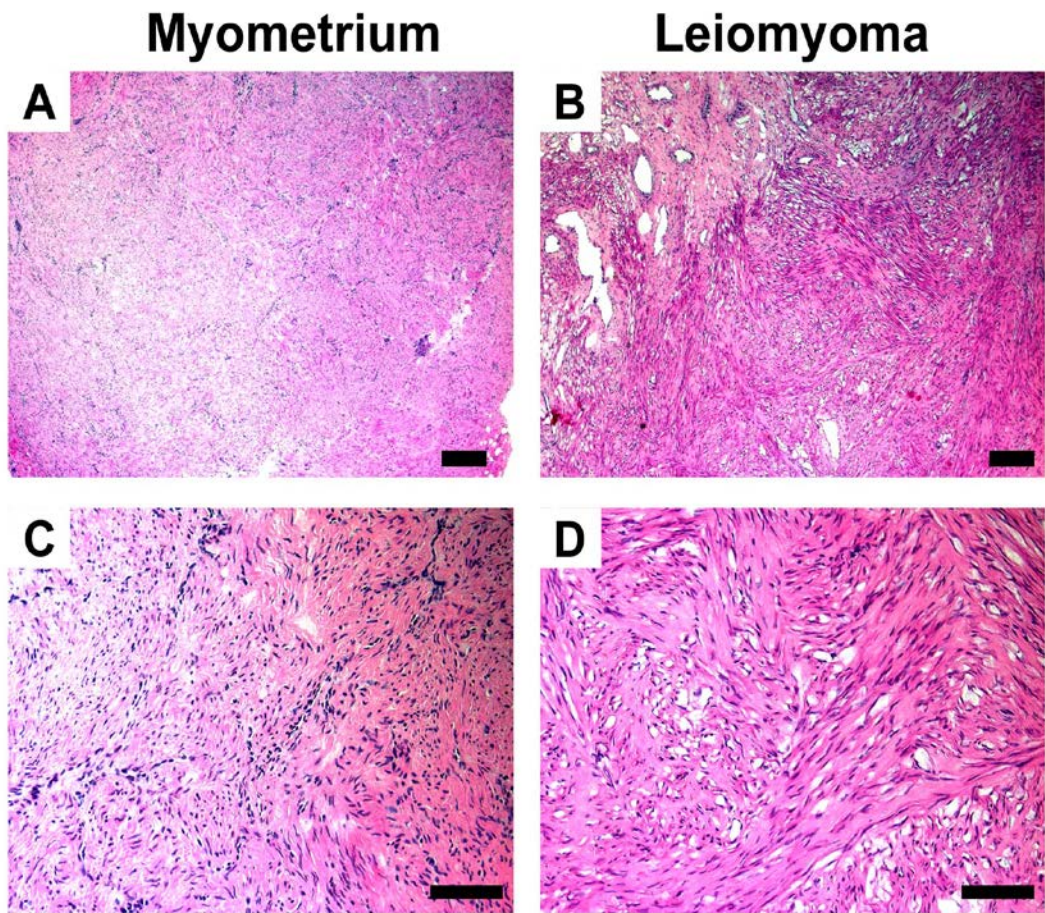


**Figure 1.2 Histopathology of conventional leiomyomas**

(A) Normal myometrium showing arrangement of smooth muscle fibers. (B) Pathology of typical leiomyoma lesion marked by fibrosis, disorganized nuclei and ECM deposits. Higher magnification of (A) and (B) are shown respectively in (C) and (D). Scale bars= Scale Bars = 0.5 $\mu$ m (A, B), 100 $\mu$ m (C, D).

**Table 1.1 WHO based pathological classification of uterine leiomyoma variants.**

<b>Leiomyoma variant</b>	<b>Features</b>
<b>Cellular Leiomyoma</b>	<p>Significantly increased cellularity compared to the surrounding medium</p> <p>Lack of nuclear atypia</p> <p>Infrequent mitotic figures</p> <p>Usually irregular borders mimicking invasion</p>
<b>Atypical Leiomyoma</b>	<p>Focal occurrence of highly atypical cells in a conventional leiomyoma</p> <p>Infrequent mitotic figures</p>
<b>Lipoleiomyoma</b>	<p>Presence of adipocytes in conventional leiomyoma</p>
<b>Myxoid leiomyoma</b>	<p>Smooth muscle cells separated by myxoid material</p> <p>Lack of cytological atypia</p> <p>Infrequent mitotic figures</p>
<b>Epitheloid Leiomyoma</b>	<p>Epithelial-like appearance in tumor cells</p>
<b>Intravenous leiomyomas</b>	<p>Smooth muscle cells within vascular spaces outside a leiomyoma</p> <p>Infrequent mitotic figure</p>

(Adapted from Oliva et al., 2014) (40)

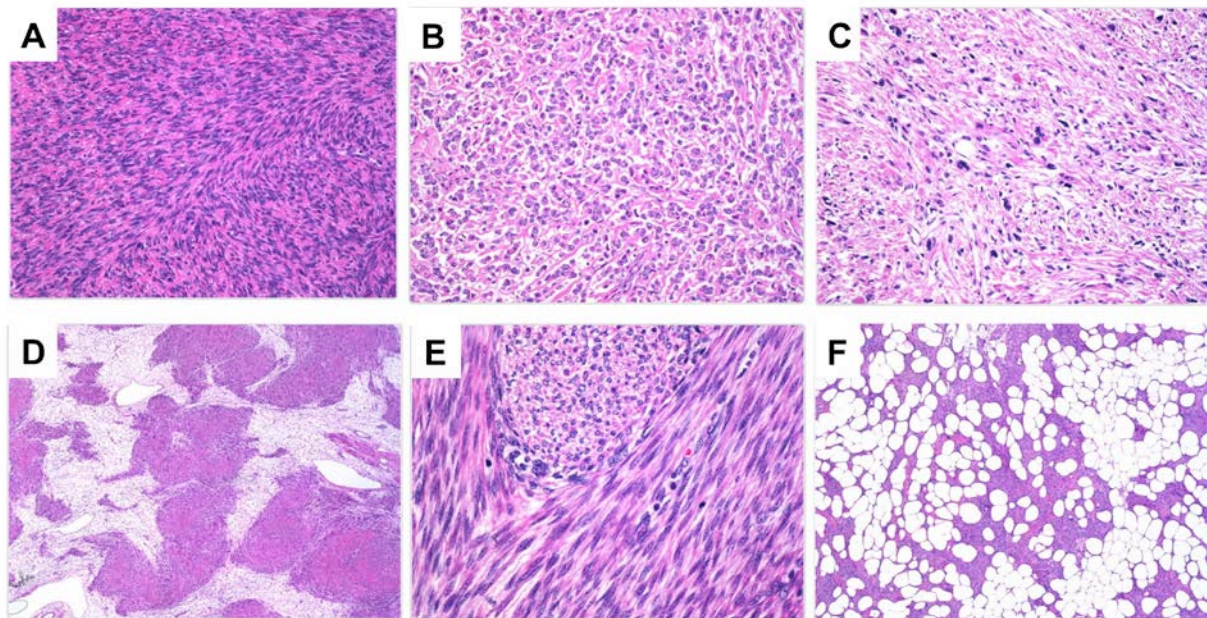


**Figure 1.3 Histopathological variants of uterine leiomyoma**

(A) Cellular leiomyoma. (B) Epithelioid leiomyoma (C) Atypical leiomyomas (D) Myxoid leiomyomas. (E) Mitotically active leiomyoma (F) Lipoleiomyomas. These images were reproduced from webpathology (<http://www.webpathology.com/case.asp?case=570>)

## **1.2 GENESIS OF UTERINE LEIOMYOMAS**

Leiomyomas are known to arise from a single cell of the uterus (monoclonal in origin) i.e. each fibroid nodule consists of a single type of active X-allele, though independent nodules may have different active X alleles (41-44). The initiation of leiomyomas or leiomyomagenesis, involves transformation of a normal cell into a neoplastic myometrial cell, which may be influenced by genetic, epigenetic, hormonal or remodeling due to monthly cyclical changes.

### 1.2.1 Ovarian hormones and leiomyomagenesis

A large body of literature and circumstantial evidence show an important role of ovarian hormones (estrogen and progesterone) in the development of leiomyomas. The regression of fibroids after menopause, and the dramatic changes in leiomyomas associated with hormonal changes during early pregnancy or postpartum, are compelling pieces of evidence supporting the role of estrogen and progesterone in leiomyomas (9, 10, 45, 46). The mechanisms through which ovarian hormones influence the growth of these tumors are not clearly understood but several hypotheses suggesting a role of these hormones in tumor initiation and progression exist. One such initiation theory suggests the role of estrogen and progesterone in increasing the proliferative activity of cells ultimately leading to the rapid accumulation of somatic mutations (47). Alternatively, underlying anomalies in normal myometrium may result in an enrichment of estrogen receptors and altered estrogen metabolism in leiomyomatous uteri compared to normal myometrium (48). Estrogen metabolism is also altered in leiomyomatous uteri (10) through reduced levels of 17 $\beta$ -hydroxysteroid dehydrogenase catalyzing estradiol to estrone conversion leading to estradiol accumulation, or increased levels of aromatase, catalyzing the conversion of androgens into estrogens (49-52).

*In-vivo* graft models, where human fibroid tissues are placed under the kidney capsule in mice, have shown the importance of progesterone and its receptor, as grafted human fibroid tissues show proliferation, accumulation of extracellular matrix and cellular hypertrophy under the influence of exogenous progesterone (53). Based on its proliferative role during pregnancy, progesterone is more likely to have a function in clonal expansion of tumor cells. It may mediate these effects through progesterone receptor, effecting and regulating hundreds of genes (54).

Progesterone also prevents apoptosis by increasing the levels of BCL2 in the fibroid tissue thereby contributing further to growth and progression of the tumor (55).

The effects of estrogen and progesterone are often mediated by growth factor such as Transforming growth factor- $\beta$  (TGF- $\beta$ ), basic fibroblast growth factor (bFGF), insulin-like growth factor (IGF), platelet-derived growth factor (PDGF), epidermal growth factor (EGF), and vascular endothelial growth factor (VEGF) (56) and are often present at higher concentrations in leiomyomas as compared to normal myometrium (10). Each of the growth factors may contribute to different aspects of tumorigenesis including ECM expansion, angiogenesis or clonal proliferation of cells. For example: Increased TGF- $\beta$  may promote cell proliferation and ECM production (57) whereas FGF promotes angiogenesis in leiomyomas and cell proliferation, ultimately leading to tumor growth (58).

### **1.2.2 Myometrial stem cells and leiomyomagenesis**

In the last few years, there have been emerging reports about the role of stem cells/ progenitor cells from human myometrium as a source of origin for human leiomyomas (59). Both human and mouse myometrium generate stem cells via asymmetric division, which are capable of differentiating into mature smooth muscles cells under the influence of estrogen and progesterone. This process is responsible for myometrial regeneration in a normal uterus (59, 60). In an event of a genetic alteration, a myometrial cell may transform into a fibroid stem cell. These fibroid stem cells proliferate continuously to then give rise to a leiomyoma (61). Fibroid stem cells lacking ER and PR, often require surrounding myometrial cells rich in ER, PR, and ligands to support self-renewal of fibroid stem cells in a paracrine manner (61, 62). Thus steroids not only influence development of leiomyomas directly but also influence them indirectly via

supporting stem cell renewal and tumor progression. Another hypothesis suggests the role of injuries such as hypoxia induced ischemic injury to play a role in initiation of tumors (63). In vitro data shows that the myometrial stem cells are capable of differentiating into mature smooth muscle cells under hypoxic conditions (64), which would suggest that the stem cells under hypoxic conditions may give rise to differentiated leiomyoma cells. As leiomyomas are believed to have stem cells of their own, in much lower percentage than normal myometrium, it is also possible that the hypoxic environment could possibly cause the myometrial stem cells to convert into fibroid stem cells and thus contribute to tumorigenesis (61).

### **1.3 GENETICS OF LEIOMYOMAS**

The etiology of fibroids has long been elusive. Twin studies, familial studies and hereditary syndromes have suggested a strong genetic component involved in leiomyomagenesis. In the past years cytogenetic analysis using classical karyotyping methods have shown 40-50% of tumors having tumor specific chromosomal aberrations such as inversions, deletions, duplication and translocations (65, 66). Though chromosomal aberrations and the inherited syndromes account for a fraction of leiomyomas, the genetic basis for the majority of leiomyomas remains unexplained. In this section I will discuss in detail the advances in understanding the molecular genetics and cytogenetics of leiomyomas using next generation sequencing technologies.

### **1.3.1 Cytogenetics of leiomyomas**

Chromosomal aberrations in uterine leiomyomas often associate with larger size tumors and are specific to the location of the tumor (67, 68). For example, the tumor size of leiomyomas with 7q deletions is much smaller in size compared to the size of tumors with 12q14 rearrangements (69). Similarly, intramural and subserous leiomyomas display more chromosomal aberrations than submucous leiomyomas (70).

#### **1.3.1.1 12q14-15 translocations**

About 20% of uterine leiomyomas display 12q14-15 rearrangements, making it one of the most common karyotypic abnormalities in these tumors (70). The 12q14-15 rearrangements, mostly occur as a simple translocation,  $t(12;14)(q15;q23-24)$  but can have other complex rearrangements (71-77). Rearrangements in other benign mesenchymal tumors, such as angiomyxomas, breast fibroadenomas, endometrial polyps, hemangiopericytomas, lipomas, pulmonary chondroid hamartomas, and salivary gland adenomas, also have shown the importance of this region in tumorigenesis (78). The 12q breakpoint in uterine leiomyomas maps to a region identified as an evolutionarily conserved, high mobility group AT-hook 2 (*HMGA2*) gene, belonging to the high-mobility group A (HMGA) protein family (79, 80). The HMGA group of proteins are both positive and negative transcriptional regulators of genes. They indirectly regulate gene expression by bringing about conformational changes in the DNA and influencing the accessibility of DNA binding proteins (81). They play a role in diverse processes such as proliferation, differentiation, growth, and apoptosis (82, 83). HMGA2 protein is abundant and expressed ubiquitously during embryonic development, but is almost undetectable in adult tissues, except in the lungs and the kidneys (84-86). A majority of chromosome 12

breakpoints, in uterine leiomyomas, carrying t(12;14)(q15;q23-24) map to the 5' region of *HMGA2* and a minority map to the 3' region, suggesting impaired *HMGA2* expression (75, 87). This may explain the aberrant overexpression of *HMGA2* in leiomyomas (84, 88). It is possible that the translocation may either disrupt regulatory elements or place the gene near an effective promoter causing the aberrant expression. Let7-miRNAs directly regulate *HMGA2* by binding to the 3' UTR region and inhibiting *HMGA2* expression. Removal of *HMGA2* 3' binding site may provide another mechanism of *HMGA2* overexpression (88-91). There is also a positive correlation between larger tumor sizes and the presence of t(12;14)(q15;q23-24), *HMGA2* overexpression and low expression let-7 miRNA (68, 90, 92). Evidence also supports the notion that overexpression of *HMGA2* may be important for proliferation and maintenance of the transformed state of the cell (78).

The breakpoints on chromosome 14 involved in t(12;14)(q15;q23-24) in leiomyoma were mapped to identify the genes in this region (70, 93, 94). *RAD51* paralog B (*RAD51B*) at the 14q23~q24 emerged as a strong candidate translocation partner for *HMGA2* (95, 96). *RAD51B* plays an essential role in homologous recombination mediated DNA damage repair (97). *HMGA2* and *RAD51B* fusion transcripts occur in a small percentage of leiomyomas, but the underlying pathogenesis of majority of t(12;14)(q15;q23-24) is not understood (96, 98). In some leiomyomas, aberrant expression of *HMGA2* may occur without the 12q14-15 rearrangements (99), suggesting an independent role in leiomyoma pathogenesis (75).

### **1.3.1.2 Deletions of 7q**

Interstitial deletions of chromosome 7, del(7)(q22-32), occurs in about 17% of karyotypically abnormal leiomyomas (78). The deletions on the long arm of chromosome 7 have been narrowed down to the 7q22 band and are somewhat specific to uterine leiomyomas as compared to other solid tumors. The frequent LOH indicates the presence of tumor suppressor genes in this region (100-104). The identification of the target sequences in this region has been a challenge due to the dense cluster of genes in this region. *CUX1* (cut-like homeobox 1) has been identified as one of the candidate tumor suppressor genes in this region, with diverse roles in cell proliferation, cell motility/invasiveness, and apoptosis (105, 106). This gene has also been identified as a frequent target in myeloid neoplasms (107, 108). Few other candidate genes in the 7q22 such as *ORC5L*, *PCOLCE*, and *ZNHIT1* in the 7q22 region have also been identified in uterine leiomyomas; yet fail to consistently be in leiomyomagenesis (91, 109-111). The 7q deletions may either occur independently or sometimes co-exist with t(12;14) rearrangements in some leiomyomas (112). Cells from such leiomyomas persist in culture, compared to leiomyoma cells with 7q deletions as the sole cytogenetic anomaly (113). This may indicate the role of 7q deletions as a secondary cytogenetic change necessary for the progression of leiomyomas.

### **1.3.1.3 6p21 rearrangements**

Rearrangements of 6p21 locus recurrently occur in a variety of benign mesenchymal tumors, such as lipomas, pulmonary chondroid hamartomas, and endometrial polyps (78). The 6p21 rearrangements also occur in uterine leiomyomas with a frequency of <5%, with the majority of the rearrangements consisting of translocations and inversions (114-117). The high mobility group AT-hook 1 (*HMGAI*) gene has been identified as one of the targets of rearrangements at

the 6p21 locus (118, 119). Breakpoints on *HMGA1* have also been demonstrated in pulmonary chondroid hamartomas and hamartomas of the breast (120, 121). The *HMGA1* gene encodes a protein belonging to the HMGA family and also acts as a transcriptional regulator (71). Although, HMGA1 and HMGA2 belong to the same protein family, and have sequence and structural similarities but correlate with a substantially different expression pattern and phenotypic outcome, suggesting different functional roles of HMGA1 from HMGA2. For example, in uterine leiomyomas the relative overexpression of HMGA2 is more than HMGA1 (78). Also, HMGA1 overexpression usually correlates with a more malignant outcome as observed in other epithelial tumors and leukemia (122).

#### **1.3.1.4 Other cytogenetic aberrations**

Trisomy of chromosome 12 affects about 10% of karyotypically abnormal leiomyomas (123). This may result in a copy number gain of *HMGA2* resulting in overexpression of HMGA2 in leiomyomas (78). Other chromosomal aberrations such as deletion 10q, disrupting the K(lysine) acetyltransferase 6B (*KAT6B*) gene (124) or aberrations on chromosome 1,3, 13 and X also occur in uterine leiomyomas, but at a much lower frequency (78). These aberrations often occur with other cytogenetic rearrangements, indicating as a secondary change, acquired during multi-step tumorigenic process. The presence of multiple aberrations in individual tumors may also be suggestive of genomic instability in uterine leiomyomas.

#### **1.3.1.5 Monoclonality of leiomyomas**

Analyses of multiple tumors from a single uterus often display different cytogenetic aberrations across different tumors, suggesting the independent origins of each tumor (125). The process of lyonization or X-chromosome inactivation is where either of the X allele is inactivated in all

female somatic cells during embryonic development (126). The same X-inactivated allele is maintained throughout the lifecycle of a cell and is accordingly passed on to daughter cells. The process of X-chromosome inactivation has been used to study the clonality of leiomyomas. Tumors are monoclonal if they have the same X-allele inactivated in all of its cells, whereas polyclonal tumors arise from a mixture of cells. X-inactivation studies in leiomyomas have been carried out using various approaches, including glucose-6-phosphate dehydrogenase isoenzyme, X-linked androgen receptor CAG-repeats polymorphism, or phosphor-glycerokinase (*PGK*). All of the approaches have shown that independent leiomyomas in a uterus arise from a single cell, where independent tumors in the same uterus, exclusively have either of X-alleles inactivated (41, 43, 44, 127).

#### **1.3.1.6 Copy number alterations and gene expression profiling in leiomyomas**

Classical cytogenetics has been used for a long time to detect chromosomal aberrations in leiomyomas, but with the advent of newer technologies such as array comparative genomic hybridization (CGH), the genomic landscape can be analyzed at a much higher resolution. The array CGH technology allows the detection of submicroscopic copy number gains and losses, which were not previously, detected using standard karyotyping (G-banding) techniques. Few studies using array CGH have been conducted on leiomyomas and have shown additional copy number gains and losses including gains in chromosomes 9q and 19 and losses in chromosome 22q. These gains and losses were present in addition to the classically detected aberrations but also did not commonly occur in leiomyomas (128-131).

Series of gene expression microarray studies were also conducted on leiomyomas and normal myometrium to potentially identify differentially regulated genes and associated pathways in leiomyomas. Though the expression profiles were variable, genes involved in cell

proliferation, extra cellular remodeling, retinoic acid metabolism and apoptosis have been linked with leiomyomagenesis. Few examples of relevant genes include *ADH1*, *30 EGRI*, *C-FOS*, *IGF2*, and *TGFBR2*. The results from these studies were often inconsistent, and failed to indicate any causal genes associated with tumorigenesis. The inconsistencies in the results could have been due to differences in microarray techniques, data analysis methods, ethnicity differences, or the genetic status of leiomyoma samples.

Therefore, determining and validating novel genes associated with the initiation and progression of leiomyomas is key to developing successful therapeutic strategies against uterine leiomyomas.

### **1.3.2 Leiomyomas and associated syndromes**

Hereditary cancer syndromes such as hereditary leiomyomatosis and RCC (HLRCC), tuberous sclerosis complex (TSC), and Birt-Hogg-Dubé (BHD) syndromes also predispose patients for developing leiomyomas, implicating a role of genes such as fumarate hydratase (*FH*), Tuberous sclerosis 2 (*TSC2*) and Birt-Hogg-Dubé (*BHD*) in a small subset of leiomyomas.

#### **1.3.2.1 Hereditary leiomyomatosis and renal cell cancer (HLRCC)**

Hereditary leiomyomatosis and renal cell cancer (HLRCC; MIM 150800, HLRCC; Gene Reviews), also known as multiple cutaneous and uterine leiomyomatosis (MCUL), is a rare disorder, with a dominant pattern of inheritance. Only about 100 families around the world are reported to have this condition. Individuals tend to develop benign tumors such as cutaneous and uterine leiomyomas and are at high risk of developing renal cell cancer (132). Cutaneous leiomyomas are benign neoplasms arising from the muscles surrounding hair follicles. Cutaneous

lesions may grow as bumps throughout the trunks and limbs, and are sensitive to touch or temperature and maybe painful (133). Affected women also develop multiple large uterine leiomyomas, with severe symptoms and an earlier age of onset as compared to the general population (134). Only about 10-16% of women with this disorder develop renal cell cancer (132, 133, 135, 136) but the malignant lesions are often very aggressive and can metastasize very quickly making diagnosis and management of cancer very difficult.

HLRCC is primarily caused due to heterozygous germline mutations in *FH* located on chromosome 1(1q42) (137). *FH* gene encodes fumarase or fumarate hydratase, an enzyme catalyzing the conversion of fumarate to malate in the tricarboxylic acid cycle (TCA cycle), important for generation of energy in the mitochondria. Germline mutations in *FH* gene may occur as heterozygous missense (~58%), nonsense (~11%), or frameshift mutations (~18%) (133, 138). A second hit or biallelic inactivation of *FH* mostly occurs due to loss of heterozygosity events triggered by environmental factors, but may rarely be caused by a second point mutation (132, 139). It is thought that the biallelic inactivation of *FH* may render fumarase inactive, causing a buildup of fumarate or succinate in the cell (140). Excessive fumarate stabilizes the HIF1 creating a “pseudohypoxic” condition (141, 142). HIF1 in turn regulates genes responsible for vascularization, glycolysis, and glucose transport, contributing to tumorigenesis. Only about 1.3% of *FH* mutations contribute to leiomyoma pathogenesis (143-145).

### **1.3.2.2 Leiomyomas associated with other syndromes**

Uterine leiomyomas may also be associated with hereditary syndromes such as Tuberous sclerosis complex, Birt-Hogg-Dubé (*BHD*), and Cowden syndrome. TSC is a multi-organ rare dominant disorder caused due to heterozygous germline mutations in the *TSC1* or *TSC2* genes

located on chromosome 16 (146). The Eker rat, an animal model for the TSC, carrying heterozygous *TSC2* mutations have shown spontaneous incidence of uterine leiomyomas (147, 148). The details of this model will be further discussed in section 1.3.6. Similarly, German Shepherd canine models for Birt-Hogg-Dubé syndrome, carrying germline mutations in *Bhd* gene also spontaneously develop leiomyomas (149). Cowden syndrome is caused due to germline mutations in *PTEN* tumor suppressor gene resulting in multiple benign growth or hamartomas (150). About 50% of these patients also develop uterine leiomyomas (151). These syndromes although genetically associated with leiomyomas, only explain the etiology for a very small fraction of leiomyomas.

### **1.3.3 Molecular genetics of leiomyomas**

#### **1.3.3.1 Genome wide association studies**

In the past two decades, twin studies and familial aggregation studies have suggested a strong genetic component in the occurrence of leiomyomas. Genome wide association studies have revealed three chromosomal loci (10q24.33, 22q13.1, and 11p15.5) associated with incidence of leiomyomas in Japanese women (152). These findings could not be consistently replicated across various other ethnicities (153-155). Another genome wide association study conducted on a cohort of European Caucasian women, suggested a novel risk allele on chromosome 17q25.3, coding for fatty acid synthase (FASN) (153). Supporting this evidence, the expression level of fatty acid synthase was significantly higher in leiomyomas as compared to surrounding myometrium. Previously, fatty acid synthase has been associated with other tumors and has been known to promote tumorigenesis (156-158). These associations are still pending confirmation.

### 1.3.3.2 Whole exome sequencing; *MED12* exon 2 variants and leiomyomas

In the past five years, the rapid advancement of next generation sequencing (NGS) has revolutionized the field of cancer genomics, allowing us to discover and explore previously unknown somatic alterations such as point mutations, indels (insertion and deletions) in tumor pathogenesis. Others and we have utilized whole exome technologies to identify novel somatic candidate drivers associated with uterine leiomyomas to improve our understanding of genetics underlying the development of tumors.

The first whole exome sequencing studies were conducted on 18 uterine leiomyomas from 17 Finnish women (Finnish population) (159). Upon analysis, *MED12* was identified as the only recurrently mutated tumor specific gene. All of the identified mutations were heterozygous and were located in the exon 2 of *MED12*, with majority of the single nucleotide variants occurring specifically in codon 44 of exon 2. To verify the *MED12* exon 2 variants, Sanger sequencing was performed on the initial eighteen leiomyomas, and an additional 207 leiomyomas. The results revealed about 70% (159/225) of leiomyomas harboring *MED12* exon 2 mutations. About 70% of the *MED12* exon 2 variants were located in codon 44 including all six base pair substitutions. The most common non-synonymous missense variant was a c.131G>A causing a glycine (G) to aspartic acid (D) amino acid change (pG44D) (159). The glycine on codon 44 is conserved across 39 different species including plants and fungi (one of the most conserved residues). Other *MED12* mutations were observed in codons 36 and 43 of exon 2. Indels were also observed in 15% of *MED12* mutated leiomyomas. Mutant *MED12* allele expression (active X) was also confirmed in the cDNA of all leiomyomas.

*MED12* positive mutation status also correlated with smaller tumor sizes and gene expression profiling of *MED12* positive leiomyomas showed unique clustering of genes affecting

focal adhesion, ECM receptor and Wnt signaling pathways. Makinen and colleagues also confirmed the presence of 50% *MED12* exon 2 heterozygous variants in leiomyomas from women of another ethnic background (South African), although the sample sizes were small (160).

We conducted whole exome sequencing in parallel to the Finnish group, and performed targeted sequencing studies on 148 leiomyomas from mixed cohort of North American women (120 white American and 23 Black American). We also discovered novel *MED12* exon 2 heterozygous variants in 70% (100/148) of leiomyomas and none in the normal myometrium (161). Similar to Makinen et al., studies published from our lab showed 68 out 76-missense variant occurring at positions 130 and 131 in the 44<sup>th</sup> codon, exon 2 of *MED12* (Table 1.2). Remarkably, in our study as well, the most commonly observed non-synonymous single nucleotide variant was the c.131G>A, p. G44D, heterozygous variant (Figure 1.4). Higher frequency of *MED12* mutations correlated with the presence of multiple tumors per uterus as opposed to a single tumor. *MED12* exon 2 variants were detected in leiomyomas from both white American and African American women (66% and 78% respectively), suggesting a universal role of *MED12* exon 2 variants in leiomyoma pathogenesis regardless of ethnicity or race. *MED12* mutation status was also equally distributed among, karyotypically normal and abnormal leiomyomas and therefore we could not conclude if the *MED12* mutations are true precursors to cytogenetic alterations (161).

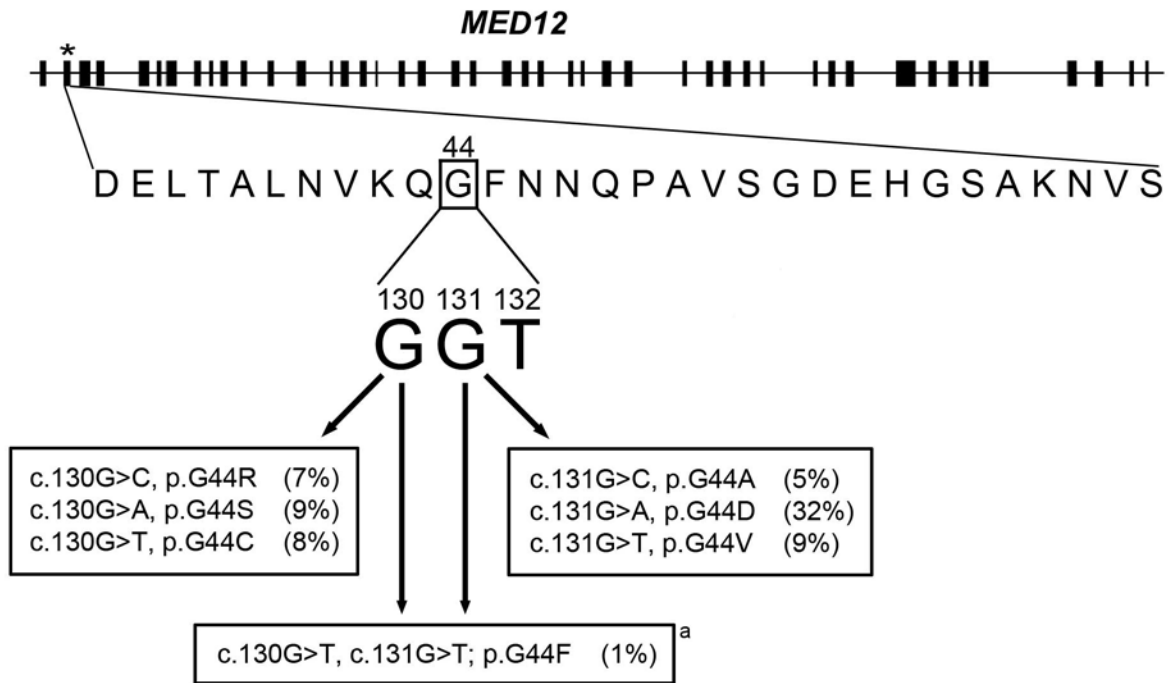


**Figure 1.4 *MED12* exon 2 variants associated with uterine leiomyomas**

Illustration of all 45 coding exons of the *MED12* gene. The asterisk denotes the mutations determined in exon 2 of *MED12* in leiomyomas from North American women. 71% of these non-synonymous variants occurred in codon 44 of exon 2 affecting the Glycine residue. The most common missense variant was c.131G>A variant causing a glycine to aspartic amino acid change.

(Figure has been reproduced from McGuire et al., 2012) (161)

**Table 1.2 List of missense, splice-site variants and indels in exon 2 of *MED12***

Variant type	Nucleotide change	Protein change	Number of mutated leiomyomas <sup>a</sup>
Missense	c.107T>G	p.L36R	3 (2.0% / 3.0%)
(Exon 2)	c.128A>C	p.Q43P	5 (3.4% / 5.0%)
	c.130G>C	p.G44R	7 (4.7% / 7.0%)
	c.130G>A	p.G44S	9 (6.1% / 9.0%)
	c.130G>T	p.G44C	8 (5.4% / 8.0%)
	c.131G>C	p.G44A	5 (3.4% / 5.0%)
	c.131G>A	p.G44D	32 (21.6% / 32.0%)
	c.131G>T	p.G44V	9 (6.1% / 9.0%)
	c.130G>T; c.131G>T	p.G44F	1 (0.7% / 1.0%)
Splice Site	IVS1-8T>A	p.E33_D34insPQ	2 (1.4% / 2.0%)
(Intron1-Exon2)	IVS1-1_139del41	Lose splice acceptor	1 (0.7% / 1.0%)
	IVS1-2_141del44insAG	Lose splice acceptor	1 (0.7% / 1.0%)
Deletions	c.103_138del36	p.E35_N46del	1 (0.7% / 1.0%)
(Exon 2)	c.107_111del5insGC	p.L36_T37delinsR	1 (0.7% / 1.0%)
	c.111_155del45	p.A38_S52del	1 (0.7% / 1.0%)
	c.113_121del9	p.A38_N40del	1 (0.7% / 1.0%)
	c.117_122del6	p.N40_V41del	1 (0.7% / 1.0%)
	c.118_132del15	p.N40_G44del	1 (0.7% / 1.0%)
	c.118_134del17insTA	p.N40_F45delinsY	1 (0.7% / 1.0%)
	c.118_146del29insTT	p.N40_P49delinsF	1 (0.7% / 1.0%)
	c.122_148del27	p.V41_P49del	1 (0.7% / 1.0%)
	c.122_163del42	p.V41_D54del	1 (0.7% / 1.0%)
	c.123_152del30	p.K42_V51del	1 (0.7% / 1.0%)
	c.126_131del6	p.K42_G44delinsN	1 (0.7% / 1.0%)
	c.126_140del15	p.K42_F45del	1 (0.7% / 1.0%)
	c.129_137del9	p.Q43_N46delinsH	1 (0.7% / 1.0%)
	c.129_143del15	p.G44_Q48del	1 (0.7% / 1.0%)
	c.133_144del12	p.F45_Q48del	1 (0.7% / 1.0%)
	c.149_163del15	p.A50_D54del	1 (0.7% / 1.0%)

(Table reproduced from McGuire et al., 2012) (161)

<sup>a</sup> The number of leiomyomas with each variant is followed in parentheses by the percentage of the total number of leiomyomas under study (148) and the percentage of the total number of mutated leiomyomas (100), respectively.

Multiple groups have now validated and replicated the presence of *MED12* exon 2 mutations, in leiomyomas from ethnically diverse women including German, Korean, Japanese, Dutch and Hispanic cohorts (162-174). The *MED12* mutation rates ranged from 50% to 80%, which may

vary due to location or the size of leiomyomas analyzed. Rarely, somatic *MED12* exon 1 mutations consisting of in-frame insertion-deletions have been reported in a few *MED12* exon 2 negative leiomyomas (175). Yet, the majority of the *MED12* mutations occur as hotspot mutations in exon 2 of the *MED12* gene, underlying their significance in the development of uterine leiomyomas.

Majority of *MED12* mutations seem to occur only in conventional leiomyomas, with rare clinical histological subtypes including cellular leiomyomas, HLRRC leiomyomas and leiomyomas with bizarre nuclei, harboring only 5-17% of *MED12* exon 2 mutations (168, 176). Mitotically active leiomyomas had *MED12* mutation rates (38%) very similar to that of conventional leiomyomas. About half of the *MED12* variants occurring in the histopathological leiomyoma variants were in codon 44 of exon 2 of *MED12*, signifying the importance of this codon in leiomyoma pathogenesis irrespective of the clinical sub-type. Interestingly, leiomyomas from HLRCC patients showed that *MED12* mutations and biallelic loss of *FH* were mutually exclusive events (173, 176).

### **1.3.3.3 *MED12* mutations and genomic alterations**

Whole genome sequencing provides the most comprehensive sequence data on the genome including coding and non-coding genetic variation, copy-number alterations, and structural rearrangements (177). Mehine and colleagues performed whole genome sequencing on 38 uterine leiomyomas including sixteen *MED12* positive leiomyomas, four *FH* deficient leiomyomas, and eighteen leiomyomas lacking *MED12* and *FH* mutations (91). The study found no new recurrently mutated somatic point mutations but found typical cytogenetic alterations associated with leiomyomas such as t(12;14)(q15;q24) and deletions in chromosome 7q. The genome of leiomyomas lacked any large amplified segments (<100 kb) or high-level genomic

amplifications, suggesting a mechanism protecting the genome from malignant degeneration (91). The most interesting finding was the common occurrence of complex chromosomal rearrangements called chromothripsis in both *MED12* positive (3/16) and *MED12* negative leiomyomas (12/16) (91, 178). Chromothripsis is defined as a single genetic event leading to shattering and random reassembly of an entire chromosome (179).

To determine if the recurrent *MED12* mutations synergistically acted with other cytogenetic alterations, Markowski et al., investigated the association of *MED12* mutations in leiomyomas with specific recurrent cytogenetic alterations. The findings of the study showed that the *MED12* mutations and frequent cytogenetic alterations such as the deletion of long arm of chromosome 7 and the 6p21 rearrangements coexist (163). This would suggest that the *MED12* mutations are precursors to some of these genetic alterations and the observed cytogenetic changes may be more of a secondary change, occurring during the course of disease progression. Interestingly, multiple studies have highlighted a clear distinction between *MED12* mutated leiomyomas and leiomyomas with *HMGA2* rearrangements, signifying different pathways of *MED12* mutated and *HMGA2* mediated leiomyomagenesis (91, 172). It is quite fascinating to note that *MED12* mutations and *HMGA2* rearrangements could possibly explain 85% of the cases.

Based on gene expression analysis, several reports have suggested that *MED12* mutations have a unique effect on global transcription patterns. Makinen et al., showed the effect of *MED12* mutations on pathways associated with focal adhesion, extra cellular matrix remodeling, and *WNT* signaling pathways (159). Markowski et al., investigated the expression of *WNT4*, as it is present in the mesenchyme and is also located at the chromosomal locus, which is altered in leiomyomas (1p36). Analysis of *WNT4* in leiomyomas with *MED12* mutations showed higher

expression compared to *HMGA2* rearranged leiomyomas or normal myometrium, thus justifying its role as a probable target and mediator of *MED12* for affecting WNT signaling in the myometrium (163). Gene expression studies conducted by Mehine et al., have also shown *RAD51B*, a DNA repair gene, also to be up-regulated in leiomyomas, implicating oncogenic stress in the smooth muscle cells possibly caused by *MED12* mutations (91).

#### **1.3.3.4 *MED12* mutations in other benign and malignant tumors**

Ever since the discovery of recurrent *MED12* exon 2 mutations in uterine leiomyomas, series of investigations have been conducted to detect the presence of *MED12* mutations in a host of other benign and malignant tumor types. To begin with, the frequency of *MED12* exon 2 variants was examined in malignant counterparts of leiomyomas; i.e. leiomyosarcomas. Uterine leiomyosarcomas are clinically rare, aggressive, highly recurrent tumors with poor prognosis and survival (176-178, 180). Reports addressing the origins of leiomyosarcomas are often contradictory; with some reports indicating a *de novo* event versus others indicating *MED12* altered precursor leiomyomas as the underlying cause (181-184). Recurrent *MED12* exon 2 variants were discovered only in a limited number of leiomyosarcomas (5-20%), suggesting a different pathway of pathogenesis as compared to *MED12* positive leiomyomas (162, 164-167, 169, 172, 185). Smooth muscle tumors with uncertain malignant potential (STUMP) are a group of heterogeneous tumors, with an uncertain benign or malignant pathological diagnosis. *MED12* exon 2 variants were determined in STUMPs also with a low frequency (11%) (164). Strikingly *MED12* expression was found to be undetectable in a majority of leiomyosarcomas and STUMPs, including leiomyosarcomas harboring *MED12* exon 2 variants. Contrary to the malignant tumors, *MED12* mutated leiomyomas, expressed *MED12* irrespective of the *MED12* mutation status (164, 167, 172). This suggests that *MED12* variants are more common in benign

tumors than their malignant counterparts, and the *MED12* exon 2 variants may exert completely different effects in benign versus malignant tumors.

Other than human leiomyomas, *MED12* exon 2 variants have recently been discovered as the sole recurrent mutations in other benign tumors such as fibroadenomas and phyllodes tumors of the breast. Remarkably, the *MED12* mutation rates in these tumors were very similar to that of uterine leiomyomas, with 59% of fibroadenomas (186) and 80% of phyllodes tumors harboring the *MED12* exon 2 variants, suggesting common mechanisms of pathogenesis (187-190). Interestingly, *MED12* c.131G>A was again the most common missense variant discovered in these tumors as well (186, 187). This suggests a very specific role of the *MED12* exon 2 variants in steroid-driven benign tumors in females.

*MED12* exon 2 variants have been rarely described in few carcinomas such as colon carcinomas (0.3-0.5%) (162, 185), basal triple-negative carcinomas (191) and chronic lymphatic leukemias (<1%) (CLL) (192). Other than *MED12* exon 2 variants, somatic mutations have also been observed in other regions of *MED12* gene, in hormone related prostate and adrenocortical carcinomas (193, 194), but the pattern of these variants are slightly different from the exon 2 variants, indicating distinct pathways of *MED12* between malignant and benign tumors. Nonetheless, the high recurrence rate of *MED12* exon 2 variants in uterine leiomyomas, fibroadenomas, and phyllodes tumors highlights the importance of understanding the role of *MED12* variants in tumorigenesis.

#### **1.3.4 *MED12* germline mutations**

Prior to the association of *MED12* with uterine leiomyomas, germline mutations in the C-terminus of *MED12* have been linked with three X-linked mental retardation syndromes; namely

Opitz Kaveggia syndrome (MIM 305450) (195, 196), Lujan-Fryns syndrome (MIM 309520) (197), and Ohdo syndrome (Maat-Klevit-Brunner type) (198). All of the above syndromes occur in an X-linked recessive fashion, mostly affecting males and have missense mutations in the leucine-serine-rich (LS) domain of *MED12*. For example, *MED12* c.2881C>T, c.3020A>G missense variants are associated with Lujan-Fryns syndrome, c.5185 C>A is associated with Ohdo syndrome, and c.2873 G>A is associated with Opitz Kaveggia syndrome (195-198). Patients with these syndromes often exhibit intellectual disability (mild to severe), behavioral problems, dysmorphic facial features and hypotonia. There have been no reports describing uterine leiomyomas in patients with these syndromes. Contrary to somatic *MED12* exon 2 variants associated with leiomyomas, C-terminal germline *MED12* variants are extremely rare and are believed to have very different molecular pathogenesis. It is hypothesized that the germline *MED12* mutations may affect REST-imposed epigenetic silencing of neuronal gene expression by disrupting mediator and RE1- silencing elements causing the rare mental retardation syndromes (198, 199).

### **1.3.5 Mediator complex subunit 12 (*MED12*)**

The *MED12* gene is located on X chromosome (Xq13) and consists of 45 exons, encoding a 250kDa protein (2177 amino acids) (191, 196). The *MED12* protein is highly conserved amongst eukaryotes, specifically in mammals (200). The protein is divided into four domains based on sequence similarity: a leucine-rich (L), leucine-serine-rich (LS), proline-glutamine-leucine-rich (PQL), and an odd-paired (Opa) domain, though not much is known about the function of each domain. *MED12* has ubiquitous expression in adult human tissues, but has higher expression during fetal development (201, 202).

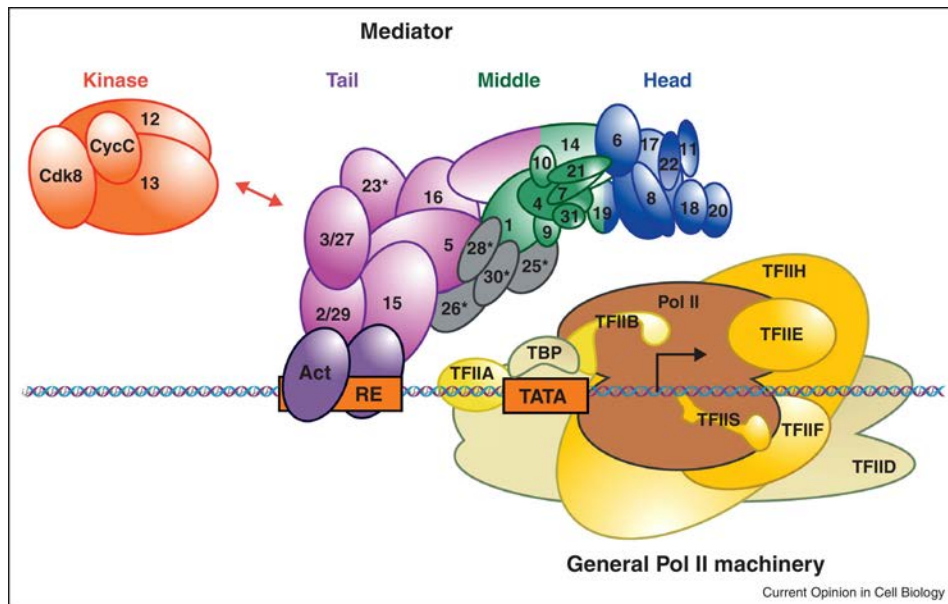


**Figure 1.5** *MED12* as part of the *CDK8* kinase module in the mediator complex

Schematic representation of the mediator complex subunits (denoted by different colors) and the RNA pol II transcriptional machinery. The core mediator consists of the head (blue), middle (green), tail (purple) and the kinase module (orange). *MED12* is part of the CDK8 sub-complex (orange) and reversibly associates with the core mediator complex. The mediator complex acts as a bridge between DNA regulatory elements and the transcriptional machinery. Components present only in higher eukaryotes are denoted by asterisk.

(Reproduced from Larivière et al., Science Direct 2012; with copyright permission from Elsevier, 2015) (203).

*MED12* is a part of a large complex of mediator proteins and is involved in transcriptional regulation of RNA polymerase II complex in eukaryotic cells (204, 205). The mediator complex acts as an intermediate between transcription factors and RNA Pol II and relays regulatory information from transcription factors to RNA Pol II, which is an essential step during initiation and elongation process of transcription (202-204). The structure of the Mediator complex consists of head, middle, tail sub-complexes and a separate kinase (CDK8) sub-complex. The head and the middle sub-complex bind to Pol II, whereas the tail sub-complex binds to other transcription factors and undergoes conformational changes to form the “foot” or

the “hook” domain respectively (204, 206, 207). The kinase sub-complex reversibly associates with the mediator complex and brings about large structural changes to the core mediator complex (Figure 1.5) (203, 208). When the kinase sub-complex disassociates from the core sub-complex, head and the middle mediator sub-complex binds to RNA Pol II whereas the tail sub-complex binds to transcription factors or co-activators, leading to highly efficient transcription in the cells (207, 208). To render the complex inactive, kinase sub-complex attaches itself to the core sub-complex, bringing about structural changes such that it allosterically inhibits the interaction of the core mediator and RNA Pol II, thereby inhibiting transcription (209). It is believed that the mediator complex can carry out gene specific transcription based on its interaction with specific co-regulatory transcription factors, which in turn would mediate its effect through cell specific targets in the mediator (204). Given the large structure and the complexities of the mediator complex, its role in cell specific gene regulation is not clearly understood.

The kinase sub-complex consists of *MED12*, *MED13*, *CDK8*, and *Cyclin C* as its subunits, which can act as a transcriptional activator or repressor of gene transcription (206, 210). The kinase sub-complex can also phosphorylate the C-terminus of the Pol II subunit, thereby affecting transcription carried out by the RNA Pol II complex (209). The kinase module “hooks” onto the core mediator complex via *MED13* (211). *MED12* is also essential in the kinase module for the kinase activity of CDK8, but *MED12* can carry out functions independent of CDK8 kinase (212). *MED12* has been shown to interact with a variety of pathways including WNT, nuclear hormone receptor, beta-catenin, and sonic hedgehog pathways through various targets (213-216). For example, *MED12* binds to  $\beta$ -catenin through its C-terminal  $\beta$ -catenin binding domain.  $\beta$ -catenin is a nuclear effector of the canonical Wnt pathway. *MED12* and  $\beta$ -

*catenin*, together affect the transcription of targets in the WNT canonical signaling (214). MED12 directly binds to Gli-3, affecting the sonic hedgehog pathways. MED12 also contributes to epigenetic silencing of RE1-silencing transcription factors (REST) via G9a histone methyltransferase in non-neuronal cells (199). Zebra fish models have shown that Med12 can interact with Sox9 and Sox10 to carry out gene specific functions during embryonic development, possibly suggesting a role as a co-regulator of certain specific transcription factors (217-219).

Rocha and colleagues examined the role of *Med12* in mouse embryonic development by engineering loxP sites flanking exons 1-7 of *Med12* and developing *Med12<sup>fllox</sup>* mice (220). Using the *Med12<sup>fllox</sup>* mice, they generated both *Med12* hypomorphs and *Med12* null models. Both these models resulted in embryonic lethality; but had different timelines of embryonic arrest. *Med12<sup>hyp</sup>* embryos (90% *Med12* truncated) had severe defects in neural tube closure, heart defects, axis elongation, and somitogenesis, which resulted in lethality at E9.5. Whereas, the *Med12<sup>δ1-7</sup>* embryos were arrested earlier by E7.5 due to aberration of the Wnt/  $\beta$ -catenin and Wnt/ planar cell polarity (PCP) signaling pathways. This implied a role of *Med12* in activating canonical Wnt/ $\beta$ -catenin signaling and its gene specific transcription during development. Similar effects were observed upon mosaic expression of *Med12* during development, with embryonic lethality occurring at E9.5 to E12.5 (221). The *Med12<sup>fllox</sup>* mice have been used in this thesis for the purpose of generating *Med12* conditional knockouts (220).

Interestingly, with evolution of species (mammals), the kinase module subunits; *MED12*, *MED13* and *CDK8* have undergone gene duplication to give rise to paralogs as *MED12L*, *MED13L* and *CDK19* respectively with high sequence similarity (222, 223). *MED12L*, *MED13L* and *CDK19* are part of the mammalian mediator complex, but their functions remain elusive.

The addition of these paralogs to the complex may indicate towards the extended functions of the mediator complex, including gene-specific or tissue-specific regulation (176).

### **1.3.6 Animal models of leiomyomas**

Currently, no good animal model for uterine leiomyomas exists, posing a challenge in understanding of leiomyomagenesis as well as in development and testing of new drugs. In this section we will discuss three such animal models, which were generated with some relevance to leiomyoma biology and in an attempt to develop a model with a phenotype similar to that of human leiomyomas. Unfortunately, most of the phenotypes displayed by these rodent models were confined to myometrial hyperplasia and small lesions with ECM deposits.

The Eker rat, carrying a heterozygous germline mutation in  $Tsc2^{Ek/+}$  was the first model characterized, where leiomyomas were coincidentally observed in 65% of  $Tsc2^{Ek/+}$  female carrier rats by 18 months of age (147). The model was developed initially to study the tuberous sclerosis complex and in addition to leiomyomas, this model develops renal cell carcinomas and hemangiosarcomas. The leiomyomas in this model often have aberrant expression of HMGA2 and were also responsive to steroid hormones (148). ELT Cell lines were also developed from leiomyomas of the Eker rat model to facilitate an in-vitro model for leiomyomas. Unfortunately, the rare occurrence of the tuberous sclerosis syndrome in humans and the long tumor latency period in the rodent model neither made this model clinically applicable nor feasible for studying uterine leiomyomas.

Similar to the Eker rat model, a mouse model conditionally expressing  $Tsc2$  mutation in the uterine mesenchyme was generated. In this model,  $Tsc2$  conditional knock-out (cKO) led to constitutive activation of mTORC1/S6 pathway in uteri causing myometrial hyperplasia and

disorganized cells. These lesions were also responsive to steroid hormones, especially to estrogen as assessed by ovariectomy followed by estrogen supplementation (224).

The next model for leiomyomas was generated by constitutive activation of  $\beta$ -catenin in uterine myometrial cells using *Amhr2-cre* recombinase (225). Females expressing a stable form of  $\beta$ -catenin (constitutively activated) in the uterus developed smooth muscle tumors, characterized by hyperplasia and ECM deposition and low mitotic index. The severity of the phenotype was also affected by age and parity. As *Amhr2-cre* is also expressed in the stromal compartment of the uterus (226), constitutive activation of  $\beta$ -catenin in the uterine stroma also lead to the development of endometrial stromal sarcoma-like lesions. Though the model shows the effect of sustained activation of WNT signaling on mesenchymal tumors, the development of stromal tumors and indirect mechanistic relevance to human data increase the challenges of using this model to successfully study leiomyomas.

Yet another approach of generating a transgenic mouse model was by overexpressing h*GPR10*-driven with calbindin-*D9K* promoter (227). This approach stemmed from the fact that human leiomyomas had higher expression of GPR10 (neuronal specific G protein coupled receptor) due to aberrant loss of REST in the uterus, potentially affecting the PI3K-AKT-mTOR signaling. Yet again, the GPR10 model showed hyperplasia and ECM deposits, but no significant large lesions were observed. Thus a lack of good models to understand leiomyomagenesis encouraged us to develop such a model, which would not only provide us a tool to study leiomyomas but would also provide a platform to test targeted therapeutics against leiomyomas.

### **1.3.7 Public health significance**

Uterine leiomyoma or fibroids are some of the most common clinically relevant solid tumors occurring in women of reproductive age. More than five million women in the U.S suffer from fibroids. The prevalence of this condition may be as high as 70% taking into account the occurrence of asymptomatic leiomyomas (2). About 25% of leiomyomas are clinically diagnosed and can cause severe morbidity in women including heavy menstrual bleeding and associated anemia, pelvic pain, infertility (4-7, 15). Due to the recurring nature of these tumors, a partial myomectomy or hormonal antagonists only help with temporary management. Currently, a hysterectomy is the only permanent solution to recurrent fibroids (15, 228).

About 300,000 hysterectomies per year are associated with fibroids in the United States (8, 229). This also results in humongous health care costs with approximately \$4.1-9.4 billion spent every year (surgery, hospital admissions, outpatient visits, and medications) on the treatment of leiomyomas (230). However, the lack of an understanding of the etiology or the lack of a clinically relevant model makes it difficult to develop new treatment alternatives to hysterectomies. Our current approach on developing animal models for fibroids will be an essential step in understanding the role of MED12 in uterine leiomyomas, which together with the models will be an invaluable tool for developing new treatment strategies against leiomyomas as an alternative to hysterectomy.

### **1.3.8 Summary**

Ever since uterine leiomyomas have been studied, there have been more speculations than evidence regarding the etiology of these tumors. The most promising cytogenetic etiological

evidence in the past two decades has implicated chromosome 12q14-15 translocations, 7q deletions and 6p21 rearrangements in the etiology of a subset of leiomyomas (78). The advent of next generation sequencing technologies, including whole genome and whole exome sequencing has revolutionized the era of cancer genomics and we, like many others sought these technologies to discover novel variants associated with leiomyoma formation. The discovery of *MED12* exon 2 variants in 70% of leiomyomas transformed the field, by providing a novel candidate driver gene to pursue. We set out to functionally validate this variant by generating animal models for *Med12* variants. Thus, my thesis work focuses on tackling the following questions:

- a) Can *Med12* exon 2 variants cause leiomyomas?
- b) Do *Med12* exon 2 variants cause leiomyomas via loss of function or gain of function mechanisms?
- c) Is *Med12* important for maintaining fertility and the normal functionality of the uterus?
- d) Can *Med12* exon 2 variants cause the underlying cytogenetic abnormalities associated with uterine leiomyomas?

As means to address the above questions, we have generated and characterized conditional loss of function and gain of function mouse models of *Med12* exon 2 variants. This dissertation work will discuss the various phenotypes observed in both of these models, revealing the role of *Med12* in fertility, leiomyomagenesis and genomic instability.

## 2.0 LOSS OF MED12 CAUSES INFERTILITY BUT DOES NOT STIMULATE TUMORIGENESIS

Part of the work in Chapter 2 have been published in the Journal of Clinical Investigation.

### 2.1 INTRODUCTION

Uterine leiomyomas are the most common gynecological tumors occurring in women of reproductive years, yet the genetic factors associated with the causation and progression of these tumors are not well understood. Using whole exome sequencing approaches, others and we have shown that *MED12* exon 2 mutations are strongly associated with leiomyomas (159, 161). As *Med12* is present on the X chromosome, there has been speculation regarding the mechanism of these mutations causing tumors via loss of function or a gain of function mechanism. Presently, no good *in vitro* models exist as *MED12* mutated cells do not survive in culture (231). Neither an *in vivo* model nor an *in-vitro* with *Med12* mutations replicating the human condition is presently available. *Med12* has already been shown to be important during development as *Med12* null embryos are arrested at E7.5 due to impaired mesoderm formation and defective Wnt/ $\beta$ -catenin signaling pathway (220). Although *Med12* is part of the CDK8 sub-complex, it can carry out functions independent of CDK8 kinase activity (212). Currently, we understand that the gene is important for development, but what role *Med12* plays in uterine development, function or in the

development of uterine leiomyomas remains unknown. To understand the roles of *Med12*, we decided to generate mouse models of *Med12*, as it would allow us to study genotype phenotype effects without confounding variables (environment). Also, developing *in vivo* models are advantageous in tumor studies as they provide a “niche” a microenvironment essential for the progression of the tumor. The embryonic lethality of *Med12* global knockouts required us to use conditional knockout mice (220). *Med12* is highly conserved among all eukaryotes, allowing us to develop mouse models as a means to study the function of *Med12* in a tissue specific manner. We utilized the *Med12* floxed (flanked by loxP) (*Med12<sup>fl/fl</sup>*) animals (220) along-with anti Mullerian receptor type II cre (*Amhr2-cre*) (226) animals to generate a loss of function model of *Med12*, by deleting *Med12* exon 1-7 in the uterine mesenchyme. The aim of this study was to systematically analyze the phenotypic effects of loss of *Med12* in the uterine mesenchyme with regards to either tumorigenic changes or any other functional effects on the female reproductive tract.

## 2.2 MATERIALS AND METHODS

### *Animal care and experimentation*

Experiments involving mice were approved by the University of Pittsburgh Institutional Animal Care and Use Committee and in accordance with the NIH guidelines for humane care of animals. Dr. Heinrich Schrewe generously donated the *Med12<sup>flox</sup>* mice (220). The *Amhr2-cre* mice were a kind gift of Dr. Richard Behringer (226). The *mT/mG* mice (GT(ROSA)26Sor<sup>tm4</sup>(ACTB-tdTomato,-EGFP)<sup>Lox</sup>) and the *Zp3-cre* (Tg(*Zp3-cre*)93Kw/J) mice were obtained from the Jackson Laboratory (Stock #007576, # 003651). The *Gdf9-cre* Tg(*Gdf9-icre*)5092Coo/J mice were a kind gift of Dr. Austin

Cooney (232). The DNA from tail biopsies was used to confirm the genotypes, using standard PCR protocols. The primer sets and the PCR protocol used to distinguish *Med12* wild-type and the recombined alleles in tissue genomic DNA have previously been described (220). Jackson laboratory PCR protocols were followed for *Amhr2-cre*, *Gdf9-cre*, and *Zp3-cre* mice. The *Med12<sup>fllox</sup>*, *Amhr2-cre*, *Zp3-cre*, *Gdf9-cre* lines were maintained on a C57BL/6/129Sv hybrid background. Litters were weaned at 3 weeks, and breeding pairs were set up at 6 weeks of age. All animals were housed under a 12-hour light, 12-hour dark schedule and provided food and water ad libitum.

### ***Histological analyses***

Gross morphology and histology assessments were performed on greater than six weeks of age adult females. Prior to harvesting uteri, all females were estrous synchronized with intraperitoneal injections of 5 IU PMSG followed by 5 IU of hCG after 48 hours. Females were euthanized 20 hours after hCG administration, and uteri were fixed in 10% formalin, processed, embedded in paraffin, serially sectioned (6  $\mu$ m), and stained with hematoxylin and eosin. For frozen sections, tissues were embedded in optimal cutting temperature compound and were snap-frozen in liquid nitrogen. Sections were obtained using a Leica cryostat (6  $\mu$ m). At least four pairs of uteri of each genotype were subjected to gross and microscopic analysis for each time point. Images were acquired using an Axio Scope.A1 microscope (Zeiss) equipped with a digital camera (Zeiss) and an AxioVision (v4.8) imaging software.

### ***Histomorphometric analysis***

For histomorphometric analyses, every fifth section was obtained from the long axis of the ovary (n=3), stained with periodic-acid and schiff base, photographed and oocytes containing nuclei

were scored. The mean of the total score of oocytes for all the sections was considered as the oocyte count per ovary. Primordial follicles were defined as small oocytes (<20µm) surrounded by flat epithelial cells. Primary follicles were defined as having larger oocytes surrounded by a single layer of cuboidal granulosa cells; secondary follicles defined by two or more layers of granulosa cells and pre-antral follicles by the presence of antral fluid (233).

### ***Med12 antibody generation***

Med12 antigen was produced by cloning the C-terminus of mouse *Med12* (561 bp) in the pET-23b vector (His tag) and expressing the Med12 protein under optimized conditions. The expressed protein was purified using nickel resin columns (Novagen). The purified antigen was used to immunize guinea pigs. Immunization of guinea pigs was carried out at Cocalico Biologicals (Reamstown, PA). Exsanguination serum containing Med12 antibodies was used for further downstream applications.

### ***Immunofluorescence***

Immunofluorescence was performed on 6-µm frozen sections and subjected to antigen retrieval using 10 mM sodium citrate (PH 6.0) for 20 min. Sections were blocked with 3% bovine serum albumin for 45 min, followed by incubation with anti- smooth muscle actin (A5228, Sigma Aldrich) and anti-Med12 antibodies (custom designed) at 4°C overnight. Following primary antibody incubation, sections were washed and incubated in secondary Alexa Fluor 488 (Life Technologies) and Alexa Fluor 647 (Life Technologies) and co-stained with DAPI. The sections were mounted with Vectashield mounting medium containing DAPI. Images were taken with a

Nikon A1 confocal microscope equipped with a digital camera and NIS-Elements software (Nikon). For quantitation of Med12 expression, about 300 uterine mesenchyme cells were counted for Med12 positive cells in three independent uteri (two cross-sections each).

To assess the fluorescent signals in the *mT/mG* reporter mice, frozen sections were washed three times in PBS and stained with DAPI. mT (Tomato) and mG (Green) signals were analyzed and scored in 300 uterine myometrial cells.

### ***Reverse transcription and quantitative real-time PCR***

Total RNA was isolated from frozen uteri using the RNeasy Mini Kit (Qiagen). One microgram of total RNA was reverse transcribed using Superscript III reverse transcriptase (Invitrogen). *Med12* gene expression was analyzed by real-time quantitative polymerase chain reaction. A SYBR Green detection system (Bio-Rad CFX96 PCR Detect System) was used, along with customized *Med12* primer sets: Med126-7F: CTGACTTGGGTGCTTGAGTGTT and Med12 6-7R: CCAATCTCCGGGTACAGAAGTA. Melt curve analysis was performed when using SYBR Green to verify a single amplification peak. Data were normalized to an endogenous reference (*GAPDH*) and then relative mRNA expression was calculated using the  $2^{-\Delta\Delta CT}$  method.

### ***Superovulation***

Superovulation was carried out on 3-5 week old mutant and control female mice with IP injections of 5 IU PMSG (Sigma-Aldrich) followed by 5IU hCG after 46-48 hours. Twenty hours following hCG administration, females were euthanized, and their oviducts were removed. The cumulus-oocyte complexes were separated from the ampulla region of each oviduct by puncturing the oviduct. Cumulus cells were then released by incubating the complex in 0.5mg/ml

hyaluronidase (Sigma-Aldrich) in DMEM media (Invitrogen). Isolated oocytes were assessed for morphology and scored.

### ***Fertility and Copulation Studies***

The fertility status of mice was examined by housing female mice with a proven male stud and vice-versa for at least a period of six months. Data such as litter size, litters per month and the pup sexes were recorded over successive pregnancies for a period of at-least 6 months. Copulation studies were conducted on estrous synchronized females (administering 5IU PMSG followed by hCG) with proven stud males overnight. Following morning the males and females were separated and the females were examined for the presence of seminal plugs. The presence of the seminal plugs was considered as 0.5dpc.

### ***Statistical analysis***

Two-tailed Student's t-test was applied to determine the difference of means between two groups and one-way ANOVA test was used to determine the differences among multiple groups using GraphPad Prism 4.0 software. Significance was defined at  $p < 0.05$ .

## 2.3 RESULTS

### 2.3.1 Generation of conditional loss of function model of *Med12*

We first determined whether the conditional inactivation of *Med12* causes leiomyomas. Since *Med12* is expressed from the X chromosome, random X-chromosome inactivation will lead to random expression of either the paternal or maternal *Med12* locus in uterine myometrial cells. We chose *Amhr2*- driven cre recombinase (226) to delete *Med12* from the uterine mesenchyme and granulosa cells of the ovary at E13.5. Since *Amhr2-cre* acts well after X-chromosome inactivation is established (E6.5) (234), loss of *Med12* function will not lead to skewed X-inactivation in mouse uteri. One of the key parameters of our experimentation was the efficiency of the cre allele used to delete the floxed allele. To assess the cre-recombination in our hands, we crossed the *Amhr2-cre* mice with the double-fluorescent cre- reporter *mT/mG* mice (235), which express red fluorescence in all tissues and green fluorescence upon cre- mediated recombination. Based on our results, (Figure 2.1A, B), about 60% of uterine mesenchymal cells underwent Cre-mediated excision. As 60% Cre efficiency was sufficient for our experiments, we went ahead and utilized the *Amhr2-cre* mice to generate *Med12* cKO animals.

We crossed *Amhr2-cre* with *Med12<sup>fl/fl</sup>* animals to generate *Med12<sup>fl/+</sup>Amhr2-cre* (het cKO) females and crossed *Med12<sup>fl/y</sup>Amhr2-cre* with *Med12<sup>fl/fl</sup>* animals to generate *Med12<sup>fl/fl</sup>Amhr2-cre* animals (*Med12* cKO) (Figure 2.1C). We used different breeding schemes to generate het *Med12* cKO and *Med12* cKO animals to introduce the cre alleles from the males and avoid nonspecific maternal cre effects (236). In the *Med12<sup>fl/+</sup>Amhr2-cre* females we studied the effects of *Med12* in a subpopulation of cells, where the expression of the *Med12* floxed allele or the *wild-type* allele was dependent on random X chromosome inactivation. In the *Med12<sup>fl/fl</sup>Amhr2-cre* females we

could circumvent this problem, as both alleles were floxed. In our models, *Amhr2-cre* acts to delete the floxed sites flanking *Med12* exons 1-7, resulting in ablation of Med12 in the uterine mesenchyme and the granulosa cells of the ovary at E13.5.

Recombination of the *Med12<sup>fllox</sup>* allele was shown in the uteri of both *Med12<sup>fl/+</sup>Amhr2-cre* and *Med12<sup>fl/fl</sup>Amhr2-cre* females (Figure 2.1D). The *Amhr2-cre*-mediated floxed allele recombination was also specific to the uterus and did not occur in other organs (Figure 2.1E). Quantitative real time PCR analysis showed that *Med12* mRNA levels were decreased in *Med12<sup>fl/+</sup>Amhr2-cre* uteri (Figure 2.1F). We had also generated custom Med12 antibodies to determine Med12 localization and expression in the uterus. Utilizing the Med12 antibody we performed immunofluorescence and co-stained with  $\alpha$ -SMA (cytoplasmic) and DAPI (nuclear) (Figure 2.1G). Interestingly, Med12 seemed to be mostly expressed in the myometrial layer of the uterus with cytoplasmic expression as observed by the Sma and Med12 merge (orange) and nuclear pattern of expression as observed by Med12 and DAPI merge (light blue). The nuclear-cytoplasmic shuttling pattern has also been observed in a variety of cancer cell lines including lung and colon cancer cell lines (237). Quantification of cells expressing Med12 in *Med12<sup>fl/fl</sup>*, *Med12<sup>fl/+</sup>Amhr2-cre* and *Med12<sup>fl/fl</sup>Amhr2-cre* uteri showed a 20-25% decrease of Med12 in *Med12<sup>fl/+</sup>Amhr2-cre* uteri and 40% decrease in *Med12<sup>fl/fl</sup>Amhr2-cre* uteri, both with statistical significance (Figure 2.1H).

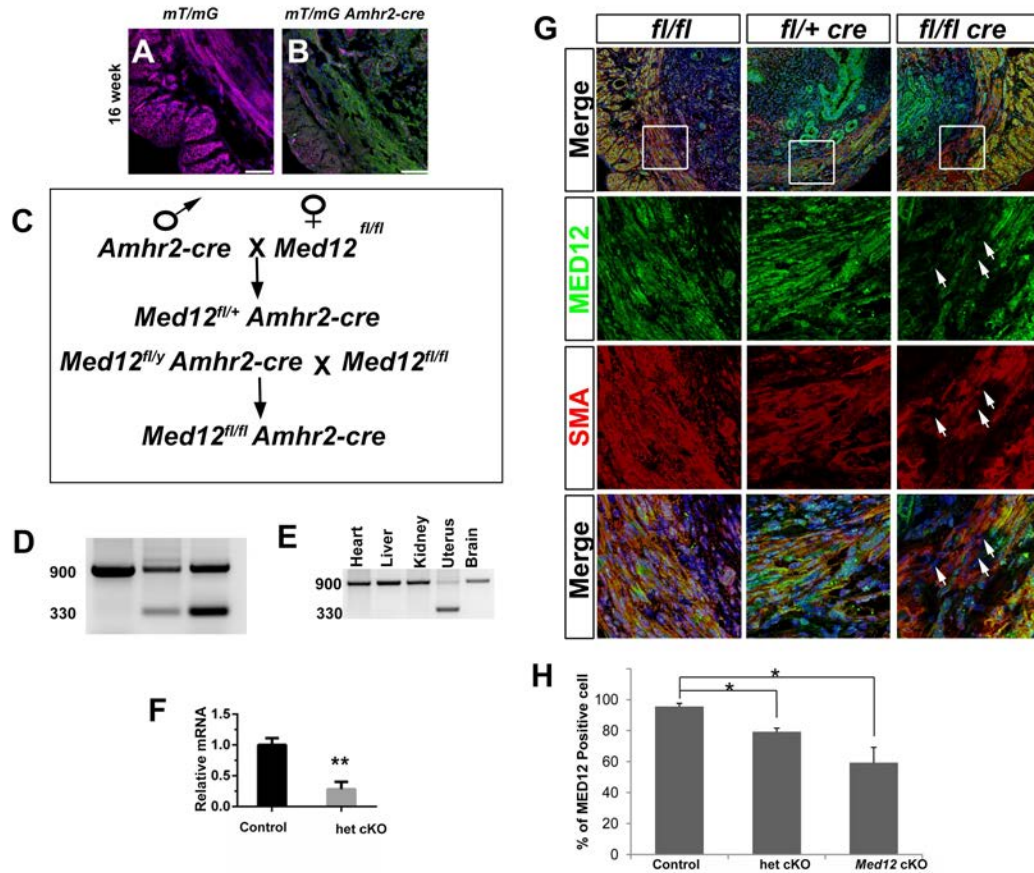


**Figure 2.1. Evaluation of *Amhr2-cre* activity, *Med12* recombination and expression in loss of *Med12* uteri**

We used *mT/mG* mice to assess the efficiency of *Amhr2-cre* recombination. (A) 16-week-old *mT/mG* mice displaying ubiquitous mT (Tomato) expression prior to recombination. (B) 16-week-old *mT/mG Amhr2-cre* uteri display mG (Green) expression in cells having undergone cre-mediated excision. The non-recombined cells still display mT expression. (C) Schematic representation of the breeding strategy used to generate *Med12* het cKO (*Med12<sup>fl/+</sup> Amhr2-cre*) and *Med12* cKO (*Med12<sup>fl/fl</sup> Amhr2-cre*) females (D) Recombination of *Med12* floxed alleles in uterine genomic DNA of *Med12<sup>fl/+</sup> Amhr2-cre* (Lane 2) and *Med12<sup>fl/fl</sup> Amhr2-cre* (Lane 3) females. *Med12* recombined bands are detected at 330 bp in the genomic DNA of cKO (Lane 2 & 3) but not in the uterine genomic DNA of controls (*Med12<sup>fl/fl</sup>*). (E) The recombined bands (330 bp) were only detected in the genomic DNA of the uterus and not in other tissues such as the liver, heart, or kidneys. (F) Relative *Med12* mRNA levels are down-regulated (5-fold) in uteri of het cKO (n=4) as compared to *Med12<sup>fl/fl</sup>* uteri (n=4) ( $p < 0.05$ ). (G) Sections from *Med12<sup>fl/fl</sup>*, *Med12<sup>fl/+</sup> Amhr2-cre* and *Med12<sup>fl/fl</sup> Amhr2-cre* uteri were co-stained with Med12 antibody, SMA and DAPI and analyzed for Med12 expression pattern using immunofluorescence. The white arrows in (G) indicate regions with loss Med12 in the uterine myometrial cells (H) About 20% of *Med12<sup>fl/+</sup> Amhr2-cre* cells and about 45% of *Med12<sup>fl/fl</sup> Amhr2-cre* uterine cells lack Med12 compared to controls, with statistical significance ( $p < 0.05$ ) (n=3). Student's t test was applied to (F) and ANOVA was carried out to compare the groups in (H). Data is presented as mean  $\pm$  SEM. Scale bars = 50  $\mu$ m (A, B, G).

### 2.3.2 *Med12* cKO females have atrophic uteri

We first evaluated the uteri of *Med12<sup>fl/+</sup> Amhr2-cre* females starting at 6 weeks of age and continued to evaluate at 12, 16, 24 and 32-week time points (n=4 at each time point). The morphology and histology of *Med12<sup>fl/+</sup> Amhr2-cre* (Figure 2.2 D, G) uteri appeared normal at all time points. We did not observe any leiomyoma formation or hyperplasia either in the nulliparous or multiparous *Med12<sup>fl/+</sup> Amhr2-cre* females (Figure 2.2B, D, G). These results indicated that loss of *Med12* was not the likely mechanism of leiomyoma formation. As random X chromosome inactivation may play a role in influencing the results observed in the *Med12<sup>fl/+</sup> Amhr2-cre* animals, we decided to generate animals where both *Med12* alleles are floxed. Similar to the het cKO females, we evaluated the uterine morphology and histology of *Med12<sup>fl/fl</sup> Amhr2-cre* (*Med12* cKO) females at 6,12,16,24 and 32-week age time points. We did not observe any pathological changes associated with leiomyoma formation but on the contrary we observed hypoplastic reproductive tracts of *Med12* cKO females (Figure 2.2A) and correspondingly the uterine weights of the *Med12* cKO were 50% lesser than that of controls ( $p<0.01$ ) (Figure 2.2B). Histological evaluation also corroborated these findings as the uterine myometrial layer was severely diminished (Figure 2.2E, H). In addition, there was a noticeable reduction in the number of glandular epithelium (Figure 2.2H). It is possible that the loss of *Med12* can affect glandular development as the reporter cre experiments show cre recombination occurring in glandular epithelium as well (Figure 2.1A).

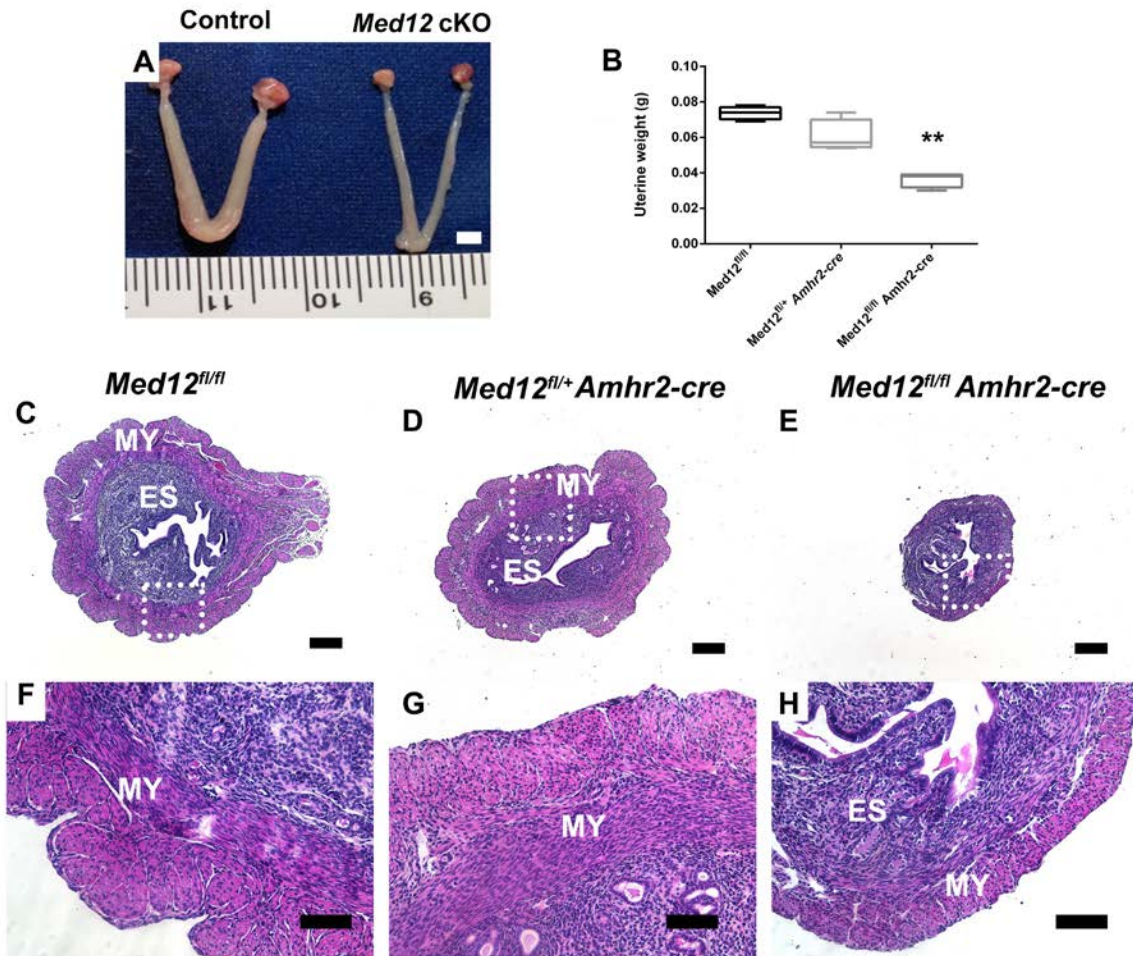


**Figure 2.2. *Med12*<sup>fl/fl</sup> *Amhr2-cre* females have hypoplastic reproductive tract**

(A) Gross morphology of 12-week old reproductive tracts, showing healthy control (*Med12*<sup>fl/fl</sup>) uteri as compared to reproductive tracts of *Med12* cKO females (*Med12*<sup>fl/fl</sup> *Amhr2-cre*). Uterine weights of control (n=7), het cKO (n=7) and *Med12* cKO (n=7) corroborate these findings with a 50% drop in uterine weights of *Med12* cKO females as compared to controls ( $p < 0.01$ ) (t-test), whereas the uterine weights of *Med12*<sup>fl/fl</sup> *Amhr2-cre* mice (n=7) did not significantly differ from that of *Med12*<sup>fl/fl</sup>. Histological evaluation was conducted on uteri from 8, 12, 16, 24, 32-week control, het cKO and *Med12* cKO females. At 12-weeks control uteri (C) (*Med12*<sup>fl/fl</sup>) were normal. (D) Uteri of het cKO (*Med12*<sup>fl/fl</sup> *Amhr2-cre*) also lacked any gross abnormalities or leiomyoma-like lesions. (E) Corroborating the gross morphology, the uteri of *Med12* cKO, displayed a hypoplastic uterus, with diminished myometrial thickness and a decrease in the number of glandular epithelia. The white dotted regions in (C), (D) and (E) are shown at higher magnification in panels (F), (G) and (H), respectively. Data are presented as means  $\pm$  SEM. ES-endometrial stroma; MY-myometrium; EM-endometrium. Scale bars = 2000 $\mu$ m(A) 0.5 $\mu$ m (C,D,E), 100 $\mu$ m (F,G,H).

### 2.3.3 *Med12* cKO females are infertile

We next investigated the reproductive and the fertility outcomes of *Med12* cKO and het cKO females by breeding them with proven male studs for a period of six months. Interestingly, the *Med12* cKO females were infertile and het cKO females were sub-fertile ( $p < 0.001$ ) (Figure 3.3A). If the *Med12* floxed allele is expressed and excised, then the cell is likely to behave like a *Med12* cKO, whereas if the cell expresses the wild-type *Med12* allele then we would expect the cell to behave like wild type. Thus the random pattern of X inactivation in het cKO uteri would explain the mosaicism observed in the fertility outcomes of het cKO females (Figure 2.3A). Another interesting aspect of our findings is the slight sub-fertility of the *Med12* cKO (*Med12*<sup>fl/y</sup> *Amhr2-cre*) males ( $p < 0.05$ ) (Figure 2.3B). Previous reports have shown that in addition to the female reproductive tracts, *Amhr2-cre* is also expressed in Leydig cells (somatic) of the testis (238) and the loss of *Med12* in these cells could affect male fertility. We also observed an unexpected discrepancy in the number of males to females with a tendency of higher number of males born in each litter. The sex ratio was determined to be about 3:2 ( $p < 0.05$ ) (Figure 2.3C). The possibility of sex reversal as a cause of sex ratio discrepancies was ruled out by confirming the presence of SRY (sex-determining region Y) gene in several sets of male pups born from the *Med12*<sup>fl/y</sup> *Amhr2-cre* and *Med12*<sup>fl/fl</sup> mating.

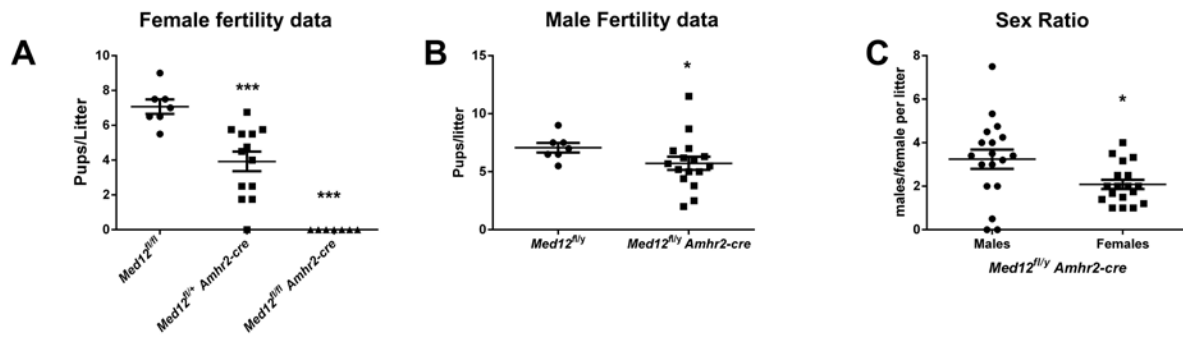


**Figure 2.3. Evaluation of breeding in *Med12* cKO males and females**

(A) Fertility data collected from *Med12<sup>fl/fl</sup>*, *Med12<sup>fl/+</sup> Amhr2-cre* and *Med12<sup>fl/fl</sup> Amhr2-cre* females by breeding them with wild-type stud males for a period of six months. The *Med12<sup>fl/+</sup> Amhr2-cre* females are sub-fertile and *Med12<sup>fl/fl</sup> Amhr2-cre* females are infertile ( $p < 0.001$ ). (B) Male fertility data collected from *Med12<sup>fl/y</sup> Amhr2-cre* males also show slight sub-fertility as compared to controls (*Med12<sup>fl/y</sup>*) when mated with *Med12<sup>fl/fl</sup>* females. (C) Representative dot plot graph showing the skewed sex ratios in pups born from *Med12<sup>fl/y</sup> Amhr2-cre* x *Med12<sup>fl/fl</sup>* mating. The observed male to female sex ratio is 3:2 ( $p < 0.05$ ) ( $n=10$ ). Data are represented as mean  $\pm$  SEM.

### 2.3.4 Ovulation occurs under external gonadotropic stimulus in *Med12* cKO females

*Amhr2-cre* is expressed in the uterine mesenchyme, oviduct and granulosa cells of the ovary (226). Hence, deletion of *Med12* in the above regions of the female reproductive tract may either contribute individually or collectively to the infertility phenotype observed in *Med12* cKO females. To define the cause of fertility, we examined the ovarian morphology and histology of adult females. Upon histological evaluation, control ovaries (n=5) (*Med12<sup>fl/fl</sup>*) at 12-weeks of age appeared normal and contained follicles at various stages of follicular development (Figure 2.4 A, D). Similar to the controls, het cKO ovaries also had normal stages of follicular development but had the presence of unique “follicular nest” like structures, described as hyper chromatically stained, solid, disorganized cells associated with dying follicles (Figure 2.4 B, E)(239). Interestingly, the *Med12* cKO ovaries appeared to be of normal size, but there were a number of “follicular nests” accompanied by dying follicles suggesting a block in follicular development. We next tested the ovulatory response of het cKO and *Med12* cKO ovaries, using external gonadotropic stimulus. Superovulation was performed on three-four week age het cKO, *Med12* cKO and control mice. No significant differences were seen in the oocyte numbers recovered from the ampulla region of the oviduct between the mice of various genotypes (Figure 2.4G). Correspondingly, the histology of superovulated *Med12* cKO ovaries appeared normal with follicles of all developmental stages and corpora lutea (CL) present in the ovaries (Figure 2.4H). These results suggest that despite normal ovulatory response under external gonadotropic stimulus, reproductive function is affected. To determine the number of follicles in the *Med12* cKO ovaries, we quantitated non-atretic follicles at secondary, pre-antral, large antral, preovulatory, corpora lutea and total atretic follicles in 6-week control (*Med12<sup>fl/fl</sup>*) (n=3) and *Med12* cKO (n=3) ovaries. Upon quantitation, it became evident that the numbers of antral,

preovulatory and large antral follicles in the *Med12* cKO ovaries were few. There were also a remarkably large number of atretic follicles in these ovaries (Figure 2.4I). These results suggest a block in follicular development at the secondary follicular stage in the absence of external gonadotropic stimulus.

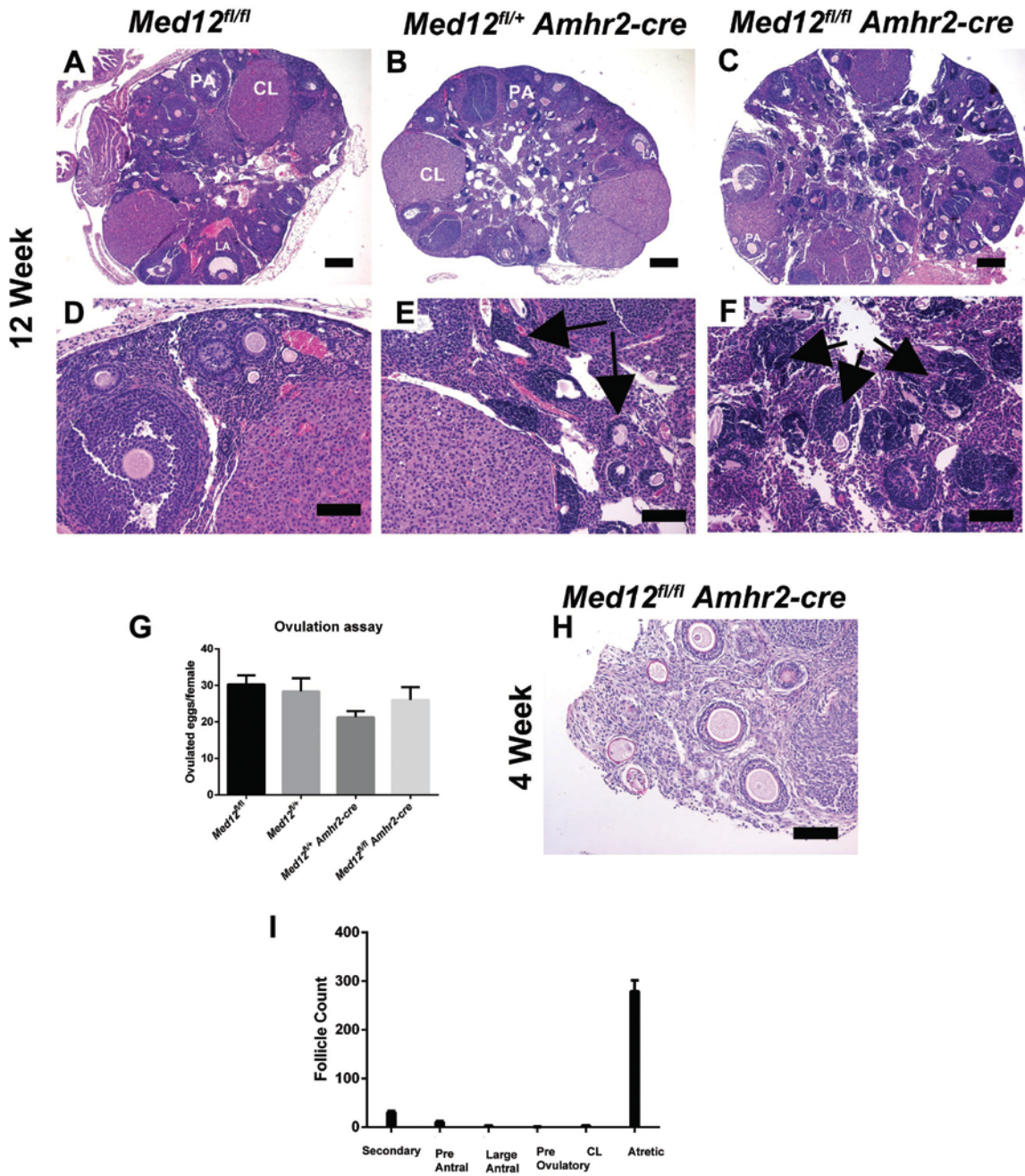


**Figure 2.4. Assessment of ovarian histology and ovulation assay**

(A) Ovarian histology of 12 week control, *Med12<sup>fl/fl</sup>* females (n=5) (B) *Med12<sup>fl/+</sup> Amhr2-cre* females n=5) (C) *Med12<sup>fl/fl</sup> Amhr2-cre* females. Higher magnification of (A-C) is shown in (D-F), respectively. (F) Black arrows indicate the presence of hyper chromatically stained granulosa cells and accompanying dying follicles indicated by the collapsing *zona pellucida* layers in *Med12* cKO ovaries. (G) Upon performing superovulation assays the number

of ovulated eggs did not significantly differ between control (*Med12<sup>fl/fl</sup>*) (n=5), *Med12* het cKO (n=5) and *Med12* cKO (n=5) females. (H) Histology of 4 week PMSG- hCG treated ovaries. (I) Quantification of secondary, pre-antral (PA), large-antral (LA), corpus luteum (CL) and atretic follicles in 6-week *Med12* cKO ovaries (n=3 pairs). Data are presented as mean  $\pm$  SEM. Scale bars = 0.5 $\mu$ m (A,B,C), 100 $\mu$ m (D,E,F,H).

### **2.3.5 *Med12* is a maternal effect gene important for somatic cell but not germ cell development**

In section 2.3.1, we had shown the *Amhr2-cre* recombinase activity was about 60%. To increase the efficiency of floxed allele deletion in the myometrium and decrease the incidence of mosaicism, we utilized oocyte specific growth differentiation factor driven cre (*Gdf9-cre*) (232) and *zona pellucida* driven-cre (*Zp3-cre*) (240) to generate *Med12<sup>fl/-</sup>* females. The generation of *Med12<sup>fl/-</sup>* animals is advantageous as the Cre recombinase would have to eliminate floxed allele from only 50% of cells.

We tried generating *Med12<sup>fl/+</sup> Gdf9-cre* mice by mating *Med12<sup>fl/fl</sup>* females with *Gdf9-cre* males (Figure 2.5A). Unfortunately we were unable to generate *Med12<sup>fl/+</sup> Gdf9-cre* males or females. Typically *Gdf9-cre* is expressed in oocytes, as early as primordial follicles of PD3 ovaries (232) but reports have also suggested paternal leaky expression of *Gdf9-cre* (241). This would explain the possible embryonic lethality of *Med12<sup>fl/+</sup> Gdf9-cre* pups.

As leaky expression of *Gdf9-cre* did not work in favor of generating *Med12<sup>fl/-</sup>* mice, we decided to use *Zp3-cre* as an alternative. *Zp3-cre* is expressed at PD10 in the primary follicles of the ovary(240). We generated *Med12<sup>fl/+</sup> Zp3-cre* females (Figure 2.5B), where about 50% of the follicles would lack *Med12* and the rest 50% would have wild-type *Med12*. Using the *Med12<sup>fl/+</sup> Zp3-cre* females we again failed to generate *Med12<sup>fl/-</sup>* females, suggesting embryonic lethality of pups lacking maternal *Med12*. We tried an alternative strategy to generate *Med12<sup>fl/fl</sup> Zp3-cre* by utilizing *Med12<sup>fl/y</sup> Zp3-cre* males and mating them with *Med12<sup>fl/fl</sup>* females. Using this strategy

we were able to generate *Med12<sup>fl/fl</sup> Zp3-cre* females (primary oocytes will lack *Med12*). Interestingly, the *Med12<sup>fl/fl</sup> Zp3-cre* (n=2) when mated with wild-type proven male studs did not give rise to any pups either. We evaluated the ovarian histology of *Med12<sup>fl/fl</sup> Zp3-cre* females to see if normal oogenesis could occur in the absence of *Med12* from the oocytes. Remarkably, adult *Med12<sup>fl/fl</sup> Zp3-cre* ovaries looked normal with follicles of all developmental stages present (Figure 2.5 C, D). The likely explanation for the *Med12<sup>fl/fl</sup> Zp3-cre* female infertility is the embryonic lethality of pups lacking maternal *Med12*. These results are consistent with the interpretation that *Med12* is a maternal effect gene.

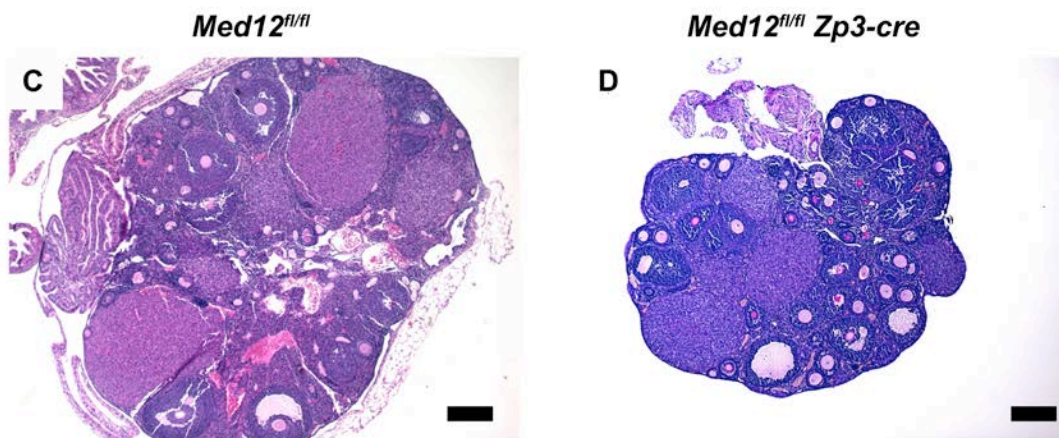
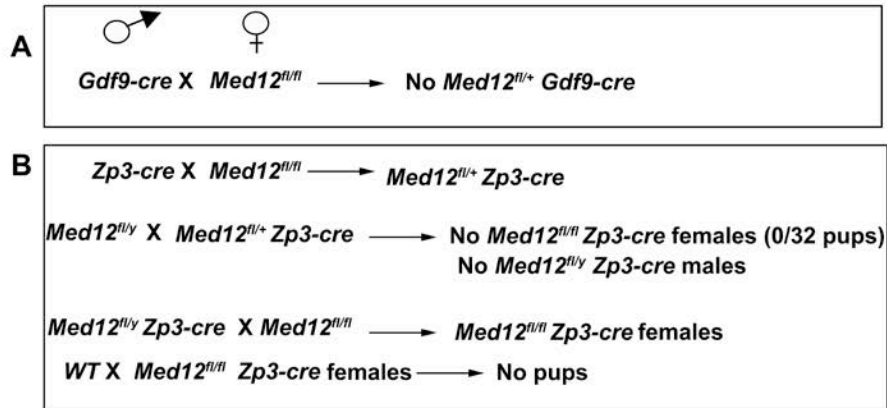


**Figure 2.5. Breeding schemes to generate *Med12<sup>fl/-</sup>* females and evaluation of *Med12<sup>fl/fl</sup> Zp3-cre* ovaries**

(A) Breeding scheme used to generate *Med12<sup>fl/+</sup> Gdf9-cre* mice. (B) Illustration of breeding schemes used to generate *Med12<sup>fl/fl</sup> Zp3-cre* mice. We were unable to generate *Med12<sup>fl/-</sup>* females using the above two strategies. (C) Histology of 12-week control, *Med12<sup>fl/fl</sup>* ovaries and (D) 12 week *Med12<sup>fl/fl</sup> Zp3-cre* ovaries exhibiting normal oogenesis and ovarian histology. Scale bars= 0.5  $\mu$ m (C, D).

### 2.3.6 *Med12* cKO uteri infrequently develop tumors other than leiomyomas

Generally the histology of *Med12* cKO uteri revealed hypoplastic uteri but in three of thirty *Med12* cKO uteri, we observed solid tumors other than leiomyomas. In a 16 week *Med12* cKO uterus we observed a solid mass and appeared to be either a leiomyosarcoma or solid tumor of unknown malignant potential (STUMP) (Figure 2.6A, B). Another 16 week *Med12* cKO uteri

presented with changes associated with adenocarcinoma (stroma) and necrosis (Figure 2.6C, D). The third solid tumor was observed in the uteri 24-week old *Med12* cKO female. Upon histological examination it was apparent that the tumor was a teratoma as different organ cell types were present within the same tumor (Figure 2.6 E, F). Therefore, we could conclude that loss of *Med12* does not stimulate leiomyoma formation but occasionally stimulates other types of solid tumors.

***Med12<sup>fl/fl</sup> Amhr2-cre***

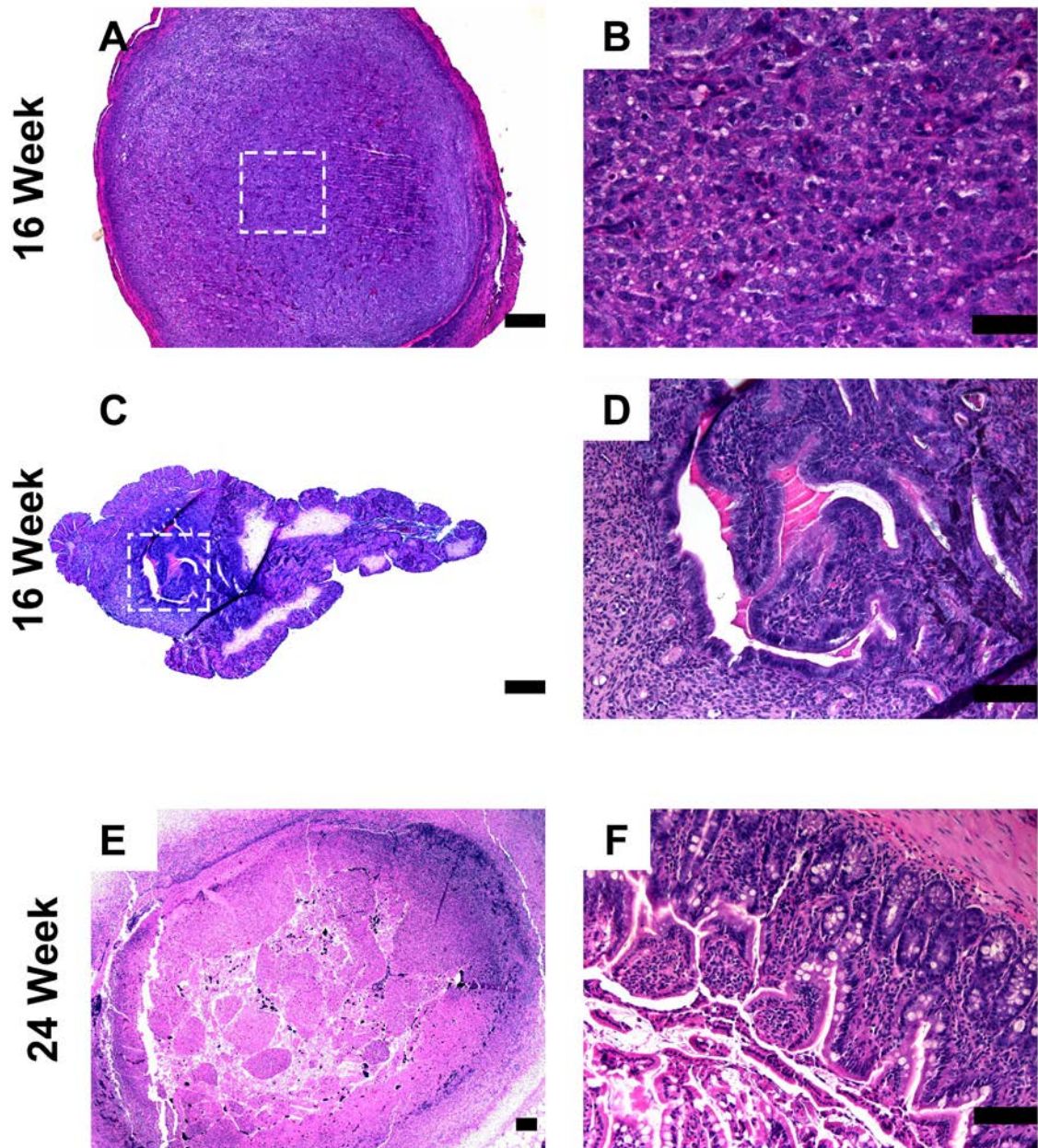


**Figure 2.6. Solid tumors in *Med12* cKO uteri**

(A) A solid tumor in 16 week *Med12* cKO uteri. Higher magnification of the tumor cells from (A) is shown in (B). (C,D) Histology of 16-week *Med12* cKO uteri displaying adenocarcinoma-like phenotype and associated necrosis. (E) Histology of 24-week *Med12* cKO uteri displaying a teratoma. (F) Higher magnification shows different cell types present in the solid tumor, typical of teratoma histology. Scale bars =1000 μm (E), 0.5μm (A,C), 100μm (B,D,F).

## 2.4 DISCUSSION

*Med12* exon 2 mutations occur in about 70% of human leiomyomas, yet the mechanisms of these mutations in tumor formation are not understood (159, 161). *Med12* is known to act as a transcriptional regulator of RNA pol II complex but its role in the uterus or reproductive function is unknown (204). Therefore, understanding the mechanism of *Med12* in tumor causation and reproductive function is important. To address these questions, we generated het cKO and *Med12* cKO females using the *Med12<sup>fl/fl</sup>* (220) and *Amhr2-cre* (226) mice.

The uterine histology of het cKO appeared normal, with the absence of any tumorous lesions. Contrary to the phenotype of het cKO females, the uterine phenotype of *Med12* cKO females was more dramatic with diminished myometrial layers causing hypoplastic uteri. Our results show that the depletion of *Med12* not only caused uterine histological abnormalities in *Med12* cKO females, but also rendered them infertile. Interestingly, the het cKO females were sub-fertile with large variability in the phenotype. This variability in the phenotype can be ascribed to the mosaicism caused due to random X inactivation in the female reproductive tract. In addition, deletion of *Med12* from the interstitial and Leydig cells of the testis (*Med12<sup>fl/y</sup> Amhr2-cre*) causes mild subfertility in males. The sex ratios of pups generated from the *Med12<sup>fl/y</sup> Amhr2-cre* males are also slightly skewed. The reasons for the skewed sex ratios are not clear.

As *Amhr2-cre* is also expressed in the ovarian granulosa cells (226), we considered the possibility that loss of *Med12* in the ovarian granulosa cells could contribute to impaired ovulation in *Med12* cKO females contributing to the infertility phenotype. Though the size of *Med12* cKO ovaries appeared to be normal (histology and morphology), there was an apparent lack of pre-antral, pre-ovulatory follicles and corpora lutea. Instead, a large number of atretic follicles were present in the *Med12* cKO ovaries. These results indicated a block in ovulation at

the antral follicle stage in *Med12* cKO ovaries. Cumulatively, the phenotype observed in the uterus and ovaries of *Med12* cKO females was reminiscent of ER knockout females (242-244). Therefore, it is possible that *Med12* may play a role in steroidogenesis, a role that might explain the recurrence of *Med12* mutations in female specific steroid driven tumors.

In an attempt to improve the cre efficiency we tried generating *Med12*<sup>fl/-</sup> mice using oocyte specific *Zp3-cre* or *Gdf9-cre*, but were unsuccessful in generating any *Med12*<sup>fl/-</sup> pups. It is likely that *Med12*<sup>fl/-</sup> status resulted in embryonic lethality as maternal *Med12* maybe essential to complete fertilization and blastocyst formation. Analysis of *Med12*<sup>fl/fl</sup> *Zp3-cre* ovaries showed that *Med12* was not essential for oogenesis but rather was essential for development, maintenance and functioning of the somatic component supporting oocyte growth (granulosa cells). The *Med12*<sup>fl/fl</sup> *Zp3-cre* females did not give birth to any pups either. This is likely due to the fact that paternal *Med12* expression is not sufficient to pass through embryonic development resulting in lethality. Rocha and colleagues have also observed similar results upon using *CMV-cre* to delete *Med12* floxed sites during embryogenesis (221).

Although we never saw leiomyoma-like lesions, we observed rare occurrences of three different solid tumors (3/30) including similar to a leiomyosarcoma, a teratoma and adenocarcinoma in the *Med12* cKO females. Both Bertsch et al., and Perot et al, have previously shown *Med12* expression to be inhibited in malignant tumors such as STUMP or leiomyosarcomas whereas it was unaltered in benign leiomyomas (164, 172). However it is yet to be determined as to what targets are triggered by the loss of *Med12* leading to the rare occurrence of tumorigenesis in *Med12* cKO females.

In summary, loss of *Med12* does not stimulate uterine leiomyomas but causes infertility, the mechanism of which is to be determined in the future.

### 3.0 *MED12* GAIN OF FUNCTION MUTATION CAUSES LEIOMYOMAS AND GENOMIC INSTABILITY

The majority of the work in Chapter 3 has been published in the Journal of Clinical Investigation.

#### 3.1 INTRODUCTION

The most common *MED12* mutation in leiomyomas among American women is a non-synonymous variant, c.131G>A, predicted to substitute a highly conserved amino acid glycine with aspartic (p.Gly44Asp) (161). We wanted to investigate whether the *MED12* mutations found in women cause leiomyomas and associated instability, by generating a similarly mutated *Med12* knock-in mouse model. Typically, in tumors, a missense variant like p53, can act either via loss of function; gain of function, or in a dominant negative manner (245). Based on the results from Chapter 2, we were able to conclude that *Med12* exon 2 variants do not act through a loss of function mechanism. We needed to develop a mouse model that would allow us to study the mechanism of the *Med12* exon 2 variants either in the presence or in the absence of X-chromosome wild-type *Med12*. We designed a strategy such that the most common human *Med12* exon 2 missense variant (c.131G>A) was engineered into a cDNA and was inserted into the autosomal *ROSA* locus. Using these mice, we generated models where *Med12* missense variant c.131G>A was expressed either with or without X-chromosome wild-type *Med12* and have shown that *Med12* exon 2 variants cause leiomyomas in a gain of function manner. Further,

we have investigated the genomic landscape of these tumors, only to reveal that the *Med12* exon 2 mutations can also cause associated genomic instability, which may ultimately contribute to tumor progression.

## 3.2 MATERIALS AND METHODS

### *Generation of Med12 Rosa knock-in mice*

*Med12* mutated *ROSA* knock-in mice were generated by introducing the most common missense mutation encountered in leiomyomas of American women, c.131G>A (p.Gly44Asp) (161), into the *Med12* cDNA of the mice. Full-length mouse *Med12* cDNA (8.6 kb) was cloned into pEntry vector (Invitrogen) in a stepwise fashion. Initially, a small fragment of *Med12* (1.6 kb) fragment was amplified via PCR from mouse newborn ovary cDNA, using the following primer set:

pEntry-mMed12 F: CACCATGGCGGCTTTTCGGGATCTT and pEntry-mMed12

R1: GCGGCCGCGAATTCTACTCGCTCACTT. The longer fragment of *Med12* (6.5 kb) was then obtained through digestion of the *Med12* EST clone (BC057119, GE Dharmacon) with EcoRI and NOTI. Finally, the smaller fragment was ligated with the larger fragment, and the full-length *Med12* sequence (8.1 kb) was confirmed by Sanger sequencing. Site-directed mutagenesis was performed using QuikChange Multi Site-Directed Mutagenesis Kit

(Stratagene), with Mde12131AF:

ACGGCTTTGAATGTAAAACAAGATTTCAATAACCAGCCTGCTGTC and

Mde12131AR:GACAGCAGGCTGGTTATTGAAATCTTGTTTTACATTCAAAGCCGT

primers used according to manufacturer instructions. pROSA26-DV1 vector was used to target the *ROSA26* genomic locus (246). Mutated *Med12* cDNA was inserted into the pROSA26-DV1

vector, using LR Clonase Enzyme Mix (Invitrogen). Electroporation was performed, using G4 ES cells, at the MWRI transgenic core. Two ES cell clones were selected for blastocyst injection after confirming appropriate integration into the *ROSA26* locus using Rosa26 5' probe (Rosa 5' probe F: GCTCAGAGACTCACGCAGCCCTAGT and Rosa 5' probe R: AGAGTAGGGGGAGGGGAAGAGTCCT) and Rosa26 3' probe (Rosa 3' probe F:CTCCCAAGTGTTGGGAACTAAAGATA and Rosa 3' probe R: GCTACATCCTGATCTAGTCCTGAA) (Figure3.1A, B).

### ***Animal care and experimentation***

All procedures were approved by the University of Pittsburgh Institutional Animal Care and Use Committee and are in accordance with the NIH Guide for the Care and the Use of Laboratory Animals. *Med12 ROSA* knock-in mice were maintained on a FVB/C57BL/6/129SV background. The DNA from tail biopsies was used to confirm the genotypes, using standard PCR protocols. The primer sets used for genotyping *Med12 ROSA* knock in mice include: Rosa A: AAAGTCGCTCTGAGTTGTTAT, Rosa B: GCGAAGAGTTTCTCCTCAACC, and Rosa C: GGAGCGGGAGAAATGGATATG. The genotyping protocol was as follows: 95°C 5:00, 94°C 0:30, 60°C 0:30, 72°C 0:30, 72°C 7:00 for 34 cycles. Breeding pairs were set up at 6 weeks of age, and litters were weaned at 3 weeks. All animals were housed under a 12-hour light, 12-hour dark schedule and provided food and water ad libitum.

### ***Histological Analysis***

Gross morphology and histology assessments were performed on adult female mice. Prior to harvesting the uteri, all females were estrous synchronized with IP injections of 5 IU PMSG

followed by 5 IU of hCG after 48 hours. Females were euthanized 20 hours after hCG administration, and uteri were fixed in 10% formalin, processed, embedded in paraffin, serially sectioned (6  $\mu\text{m}$ ), and stained with hematoxylin and eosin. For frozen sections, tissues were embedded in O.C.T. medium and were, snap-frozen in liquid nitrogen. Sections were obtained using a Leica cryostat (6  $\mu\text{m}$ ). At least three pairs of uteri of each genotype were subjected to gross and microscopic analysis for each time point. Uteri were also subjected to Masson's Trichrome staining (American MasterTech) according to the manufacturer's protocol. Images were acquired using an Axio Scope.A1 microscope (Zeiss) equipped with a digital camera (Zeiss) and an AxioVision (v4.8) imaging software.

### ***Immunohistochemistry and immunofluorescence***

Immunohistochemistry was performed on 6- $\mu\text{m}$  paraffin sections and subjected to antigen retrieval with 10 mM sodium citrate (pH 6.0) for 20 minutes. In order to quench endogenous peroxidase, sections were treated with 3% hydrogen peroxide and then blocked with 3% bovine serum albumin for 45 minutes, followed by incubation with anti- SMA antibody (A5228, Sigma Aldrich) overnight at 4°C. After primary antibody incubation, sections were washed and incubated in biotinylated secondary antibody for 30 minutes, followed by ABC reagent (Vectastain for amplification of signal intensity). DAB Peroxidase Substrate Kit (Vector laboratory) was then used to develop the immunoreactive signals. Immunofluorescence was conducted on 6- $\mu\text{m}$  frozen sections, using a similar protocol, except that the secondary antibodies were Alexa Fluor 488 (Life Technologies) and Alexa Fluor 647 (Life Technologies). Primary Anti-FLAG (F7425, Sigma Aldrich) antibody was used for immunofluorescence. The sections were mounted with Vectashield mounting medium containing DAPI. Images were taken

with a Nikon A1 confocal microscope equipped with a digital camera and NIS-Elements software (Nikon).

### ***Western blot analysis***

For Western blots, Nuclear and cytoplasmic extracts were prepared from pulverized mouse uterine samples as described previously (247). Equal amounts of protein were loaded and resolved on 3-8% Tris-acetate gels (Life Technologies). Membranes were then incubated in either anti-FLAG (F7425, Sigma Aldrich) or  $\beta$ -tubulin antibodies (T0198, Sigma Aldrich) overnight at 4°C. The following day, the membranes were washed and incubated in respective secondary antibodies for 1 hour and developed using ECL-Prime (GE, Amersham).

### ***DNA isolation***

Genomic DNA was isolated from frozen tissue samples using DNeasy Blood & Tissue Kit (Qiagen) according to the manufacturer's protocol and was quantitated using both NanoDrop spectrophotometer (Thermo Scientific) and Qubit (Life Technologies).

### ***Array CGH***

Agilent SurePrint G3 Mouse Genome CGH 180K microarray kits were used to conduct array CGH on mouse uteri. Genomic DNA from uteri of four *Med12<sup>fl/+</sup> Med12R<sup>mt/+</sup> Amhr2-cre* females was used as the “experimental” DNA and corresponding littermate control females without *Amhr2-cre* (*Med12<sup>fl/+</sup> Med12R<sup>mt/+</sup>*) as the “reference” DNA. The samples were labeled, hybridized, and scanned according to the manufacturer's protocol. Briefly, 750 ng of experimental and reference DNA were digested with Alu I and Rsa I (Promega) and labeled with

Cy3-dCTP (experimental) or with Cy5- dCTP (reference). The labeled DNA was purified and hybridized, and the arrays were washed, and scanned using an Agilent G2565CA Microarray Scanner. Raw data were obtained by Agilent Feature Extraction software and imported into the Agilent Genomic Workbench 7.0 software for analysis. DNA copy number changes were detected by Genomic Workbench software. The ADM-2 statistical algorithm was used with a sensitivity of 6.0. The criteria for making aberration calls included positive calls by the software, log<sub>2</sub> ratios of >0.25 or less than <-0.25, and the presence of three consecutive affected probes.

### ***Human syntenic mapping***

Mouse chromosomal aberrations were mapped onto human chromosomal loci using the UCSC genome browser LiftOver tool (<http://genome.ucsc.edu>). The gene lists for the human intervals were determined by the microarray core website developed jointly by the University of Miami and Oklahoma University ([www.ccs.miami.edu/cgi-bin/ROH/ROH\\_analysis\\_tool.cgi](http://www.ccs.miami.edu/cgi-bin/ROH/ROH_analysis_tool.cgi)).

### ***Reverse transcription and Med12 variant expression detection***

Total RNA was isolated from frozen uteri using the RNeasy Mini Kit (Qiagen). One microgram of total RNA was reverse transcribed using Superscript III reverse transcriptase (Invitrogen).

*Med12* exon 2 C.131 G>A variant was evaluated in mutant mouse uteri by performing PCR on cDNA, followed by Sanger sequencing with primers using the following forward and reverse oligonucleotide that flanked the *Med12* exon 2 C.131 G>A variant: Med12 F: ATGGCGGCTTTCGGGATCTT and Med12 R: AGTTGGAAGCTGATCTTGGCAGG primers, designed within Primer3 (<http://bioinfo.ut.ee/primer3-0.4.0>). Sequencing results were analyzed using Sequencher software (Gene Codes Corporation).

### *Statistical analysis*

Two-tailed Student's t-test was applied to determine the difference of means among groups using GraphPad Prism 4.0 software (GraphPad Software, CA, USA). Significance was defined at  $p < 0.05$ .

## 3.3 RESULTS

### 3.3.1 Generation of mutant *Med12 Rosa* knock in mice (c.131G>A)

We investigated whether the *Med12* c.131G>A variant caused leiomyoma formation, by generating a floxed *Med12* mutant knock-in mouse model (Figure 3.1A, B). We engineered the c.131G>A variant into the mouse *Med12* cDNA (*Med12<sup>mt</sup>*) fused with a FLAG tag, subcloned it into the pROSA26-DV1 vector, and integrated it into the autosomal *ROSA26* genomic locus. The presence of the FLAG reporter, allowed us to distinguish the expression of mutant *Med12* from wild-type *Med12* (Figure 3.1D, F). The mice generated were heterozygous for mutant *Med12* cDNA at the *ROSA26* locus (*Med12R<sup>mt/+</sup>*). We mated *Med12R<sup>mt/+</sup>* with *Amhr2-cre* mice to conditionally express mutated *Med12* (c.131G>A) as early as E13.5 in the mouse uterine mesenchyme (226). Upon Cre mediated recombination, mutated *Med12* expression is driven by the *ROSA* promoter at the *ROSA* locus. All the breeding strategies used to generate the mice in this chapter have been shown in Figure 3.2 (C, D).

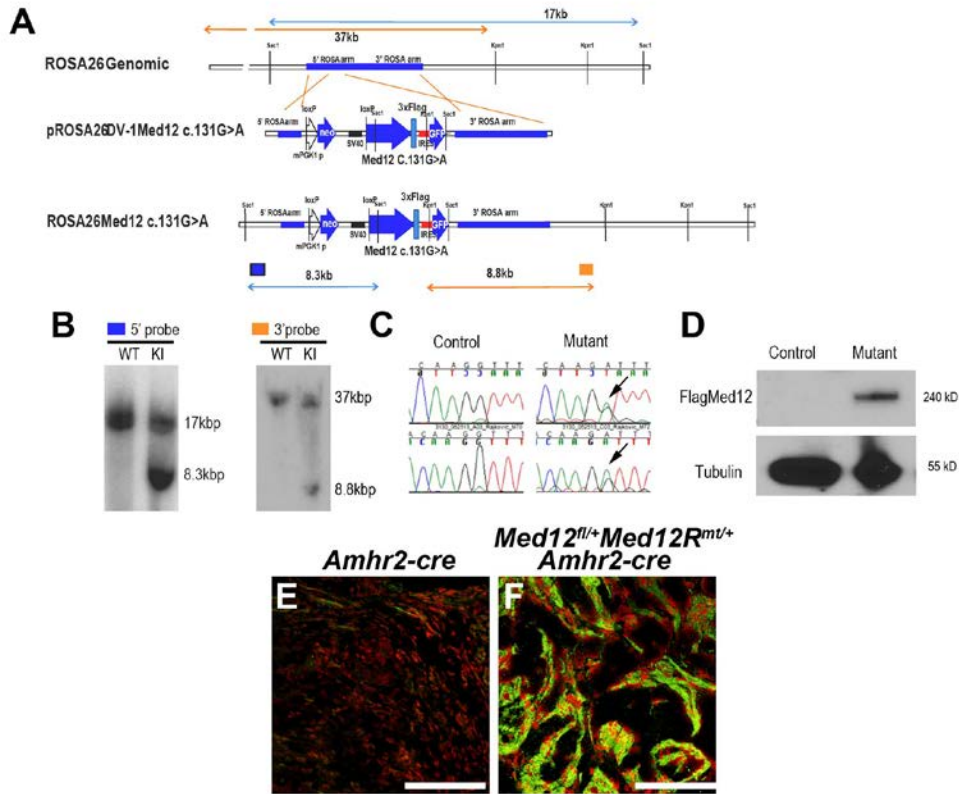


**Figure 3.1. Generation of *ROSA26 Med12* mice that conditionally express *Med12* c.131G>A variant**

(A) Mouse *Med12* cDNA was mutated and inserted into the pROSA26-DV1 vector (pROSA26DV-1 *Med12* c.131G>A) and electroporated into G4 ES cells for homologous recombination with *ROSA26* genomic locus to generate *ROSA26 Med12* c.131G>A mice. Mutated *Med12* transcripts expressed from the *ROSA26* locus are fused with FLAG and GFP. (B) Southern blot on DNA extracted from recombined G4 ES cells shows targeting of mutated *Med12* to the *ROSA26* locus. Probes corresponding to the 5' (blue) and 3' (orange) targeting ends are expected to generate 17-Kb wild-type and 8.4-kb mutant fragments and 37-kb wild-type and 8.8-kb mutant fragments, respectively, when genomic DNA is digested with Sac I and Kpn I enzymes. (C) Uteri from mice that carry the mutation in the absence of *Amhr2-cre* (*Med12<sup>fl/+</sup> Med12<sup>mt/+</sup>*) do not express mutant mRNA, while in the presence of *Amhr2-cre* (*Med12<sup>fl/+</sup> Med12<sup>mt/+</sup> Amhr2-cre*), uteri show significant expression of mutant c.131G>A variant (green chromatogram peak, black arrows). (D) Western blot analysis shows expression of mutant *Med12* protein fused with FLAG in *Med12<sup>mt/+</sup> Amhr2-cre* uteri as compared to control (*Med12<sup>mt/+</sup>*) uteri that are devoid of *Amhr2-cre*. Tubulin is used as a loading control. (E,F) Immunostaining with FLAG antibody shows FLAG expression as a marker for mutant *Med12* expression in uteri of *Med12<sup>fl/+</sup> Med12<sup>mt/+</sup> Amhr2-cre* females but not in control uteri (*Amhr2-cre*). Green: FLAG expression, Red: DAPI staining. Scale bars = 50 $\mu$ m (E,F).

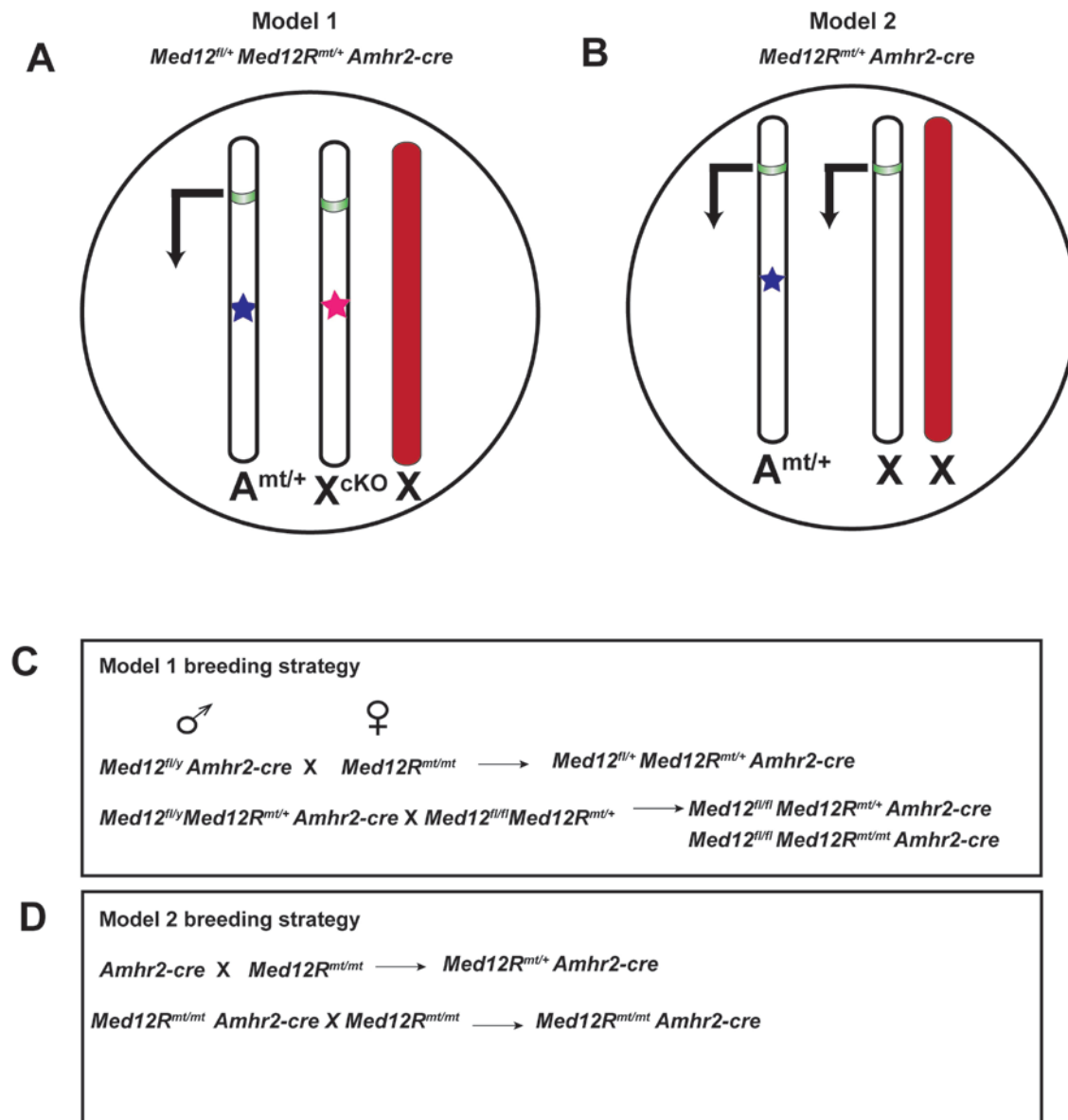


**Figure 3.2 Models and breeding schemes of mice used in Chapter 3**

(A) Mouse model 1 (*Med12<sup>fl/+</sup> Med12R<sup>mt/+</sup> Amhr2-cre*). A subset of cells express *Med12* c.131G>A variant from the autosomal *ROSA* locus while X-chromosome-derived *Med12* will either be conditionally excised at one locus or silenced by X-chromosome inactivation at the other locus. Transcription from mutant autosome (*A<sup>mt/+</sup>*) is shown by the arrow, and the promoter region is depicted in green. The blue star indicates *Med12* c.131G>A variant. The pink star indicates the floxed *Med12* allele on the X-chromosome (*X<sup>ckO</sup>*), which in the presence of *Amhr2-cre* will lose exons 1-7. In the cells where *Med12* floxed allele is subject to X inactivation inactivated, wild-type *Med12* will be expressed. In cells with an active *Med12* floxed allele, only mutant *Med12* will be expressed. The red chromosome indicates the inactivated X. (B) Mouse model 2 (*Med12R<sup>mt/+</sup> Amhr2-cre*). A subset of cells that express *Amhr2-cre* will express *Med12* c.131G>A variant from the autosomal *ROSA* locus in the presence of X-chromosome wild-type *Med12*. Transcription from mutant autosome (*A<sup>mt/+</sup>*) is shown by the arrow, and the promoter region is depicted in

green. *Med12* c.131G>A variant is depicted by a blue star. The red chromosome indicates the inactivated X. (C) Breeding schemes used to generate *Med12<sup>fl/+</sup> Med12R<sup>mt/+</sup> Amhr2-cre*, *Med12<sup>fl/fl</sup> Med12R<sup>mt/+</sup> Amhr2-cre*, *Med12<sup>fl/fl</sup> Med12R<sup>mt/mt</sup> Amhr2-cre*. (D) Breeding schemes used to generate *Med12R<sup>mt/+</sup> Amhr2-cre* and *Med12R<sup>mt/mt</sup> Amhr2-cre* females.

### 3.3.2 Expression of the *Med12* c.131G>A variant on the background of conditional *Med12* knockout causes leiomyomas

We investigated whether uterine leiomyomas will form in mice that express the *Med12* c.131G>A variant on a conditional knockout background (Figure 3.2A). In this model, we generated *Med12<sup>fl/+</sup> Med12R<sup>mt/+</sup> Amhr2-cre* females, such that a subset of uterine cells will express *Med12* c.131G>A on an X-chromosome *Med12*-null background (Figure 3.2A, C). We analyzed the *Med12<sup>fl/+</sup> Med12R<sup>mt/+</sup> Amhr2-cre* female reproductive tracts at 8, 12, 16, 24 weeks of age (n=5 at each time point). Nulliparous *Med12<sup>fl/+</sup> Med12R<sup>mt/+</sup> Amhr2-cre* females presented with pathological changes associated with leiomyoma formation as early as 8 weeks (Figure 3.3 B). Histological evaluation revealed that, beyond 12 weeks, 70% of the uteri contained lesions consistent with leiomyomas (248). These lesions consisted of extracellular matrix (ECM) deposits accompanied by infiltration of fibroblasts and macrophages, hyperplasia, and disorganized muscle fiber arrangement leading to complete destruction of myometrial architecture (Figure 3.3D-N). *Med12<sup>fl/+</sup> Med12R<sup>mt/+</sup> Amhr2-cre* mutant uteri expressed mutant *Med12* as shown by expression of FLAG, which is fused to mutant *Med12* in our *ROSA* construct (Figure 3.1F). The uteri of *Med12<sup>fl/+</sup> Med12R<sup>mt/+</sup> Amhr2-cre* females consistently weighed 40-50% higher (all time points) compared to *Med12<sup>fl/+</sup> Med12R<sup>mt/+</sup>* uteri ( $p<0.05$ ) (Figure 3.O).

It has been noticed that estrogen and progesterone promote leiomyomatous growth, and 30% of leiomyomas in human pregnancies increase in volume as elaborated in section 1.2.1 (45). To corroborate these observations, we studied the effects of mouse parturition on leiomyoma growth. Eighty percent of multiparous *Med12<sup>fl/+</sup> Med12R<sup>mt/+</sup> Amhr2-cre* females had leiomyoma-like lesions. Multiparous *Med12<sup>fl/+</sup> Med12R<sup>mt/+</sup> Amhr2-cre* females often had either grossly visible large leiomyomas (Figure 3.4 A) or multiple small leiomyoma-like nodules (Figure 3.4D). Histology confirmed that these tumors arose from the smooth muscle layer of the uterus and consisted of whorled fascicles of fusiform smooth muscle cells with an abundance of eosinophilic cytoplasm and ECM deposits (Figure 3.4B, C, E, F), consistent with the pathology seen in human uterine leiomyomas. Large tumors were often necrotic, hemorrhagic, and fibrotic. In addition, characteristic of leiomyomas, all tumors stained positive for smooth muscle actin and showed an abundance of collagen deposits when stained with Masson's Trichrome stain (Figure 3.5A, B). These tumors also expressed estrogen receptor ER- $\alpha$ . (Figure 3.5C), supporting our hypothesis that leiomyomas are hormone dependent for their growth (248).

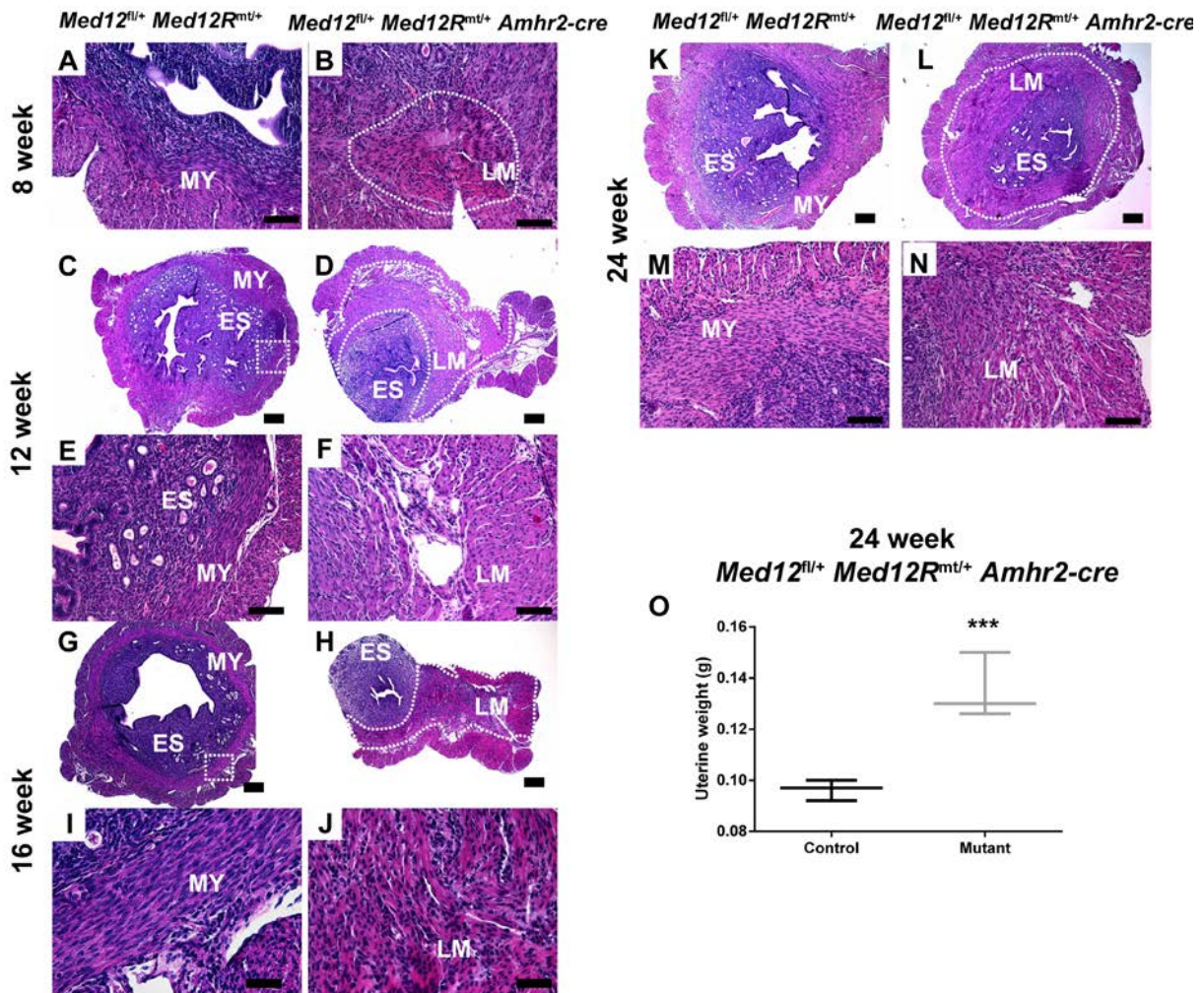


**Figure 3.3. Histological evaluation of uteri from nulliparous *Med12<sup>fl/+</sup> Med12R<sup>mt/+</sup> Amhr2-cre* females**

Control animals (*Med12<sup>fl/+</sup> Med12R<sup>mt/+</sup>*) at each time point show normal uterine histology (A,C,G,K); a magnified view of the white box shows normal endometrial stroma (ES) and myometrium (MY) in (E,I,M). (B) Pathological changes associated with leiomyomas begin as early as 8 weeks of age in the uteri expressing *Med12* c.131G>A variant on the background of conditional loss of *Med12* (*Med12<sup>fl/+</sup> Med12R<sup>mt/+</sup> Amhr2-cre*). These uteri often display characteristic patterns of leiomyoma development, with the presence of ECM deposits and the appearance of dispersed nuclei. Evaluation of uteri at (D,F) 12 week, (H,J) 16 week and at (L,N) 24 weeks of age display leiomyoma-like lesions with features including hyperplasia, fibrosis, ECM deposits and disrupted smooth muscle fibers. The white dotted lines in (D,H,L) outline leiomyomas. (O) Representative of hyperplasia, mutant uteri weights were higher at 24 weeks than controls \*\*\*( $p < 0.001$ ).

Data are presented as mean  $\pm$  SEM. LM-leiomyoma; ES-endometrial stroma; MY-myometrium; EM-endometrium. Scale bars = 0.5 $\mu$ m (C,D,G,H,K,L), 100 $\mu$ m (A,B,E,F,M,N), 50 $\mu$ m (I,J).

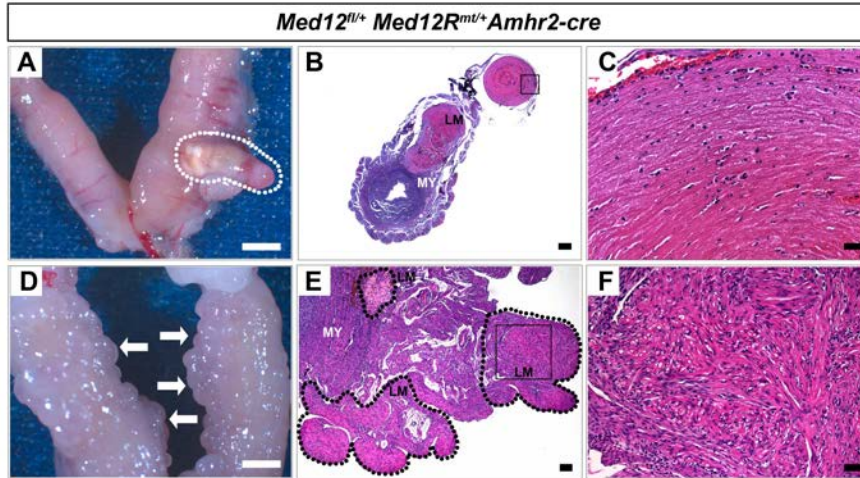


**Figure 3.4. Multiparous *Med12<sup>fl/+</sup> Med12R<sup>mt/+</sup> Amhr2-cre* females develop spectacular leiomyoma-like lesions similar to human leiomyomas**

(A) 18-week multiparous *Med12<sup>fl/+</sup> Med12R<sup>mt/+</sup> Amhr2-cre* reveals a 4-mm tumorous lesion (white dotted lines). (B) Histological examination confirms the presence of a large leiomyoma nodule growing from the smooth muscle layer of the uterus. A higher magnification of the black boxed neoplastic area appears in (C), showing the presence of fascicles with plump spindle cells, eosinophilic cytoplasm and ECM deposits. (D) 24-week-old *Med12<sup>fl/+</sup> Med12R<sup>mt/+</sup> Amhr2-cre* multiparous female exhibiting multiple nodules (white arrows). (E) Multiple leiomyoma nodules are outlined by black dotted lines, the black box, shown at higher magnification in (F), highlighting fibrosis and ECM deposition. About 80% (8/10 females) exhibited leiomyoma-like lesions and hyperplasia. LM-Leiomyoma; ES-Endometrial stroma; MY-Myometrium. Scale bars = 2000 $\mu$ m (A,D), 1000 $\mu$ m(B), 500 $\mu$ m (E),100 $\mu$ m (F), 50  $\mu$ m(C).

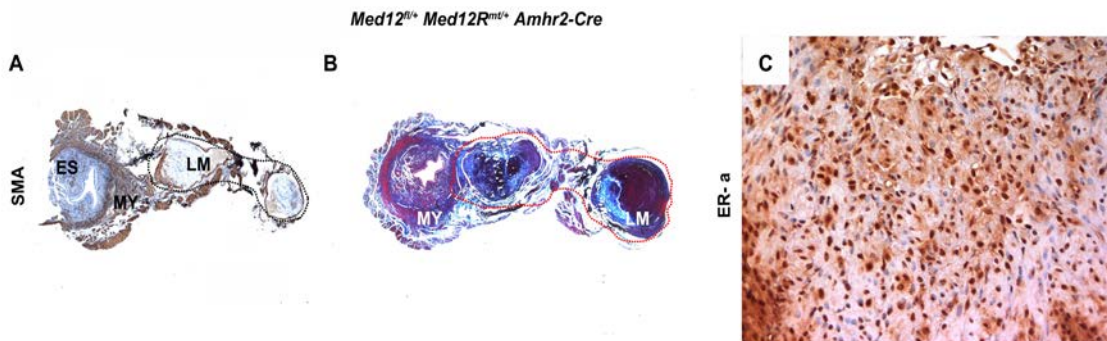


**Figure 3.5. Molecular characterization of leiomyoma-like lesions**

(A) Representative image from *Med12<sup>fl/+</sup> Med12R<sup>mt/+</sup> Amhr2-cre* uteri, showing immunoreactivity to anti-SMA antibodies and staining with Masson's Trichrome. Anti-SMA antibodies show immunoreactivity (brown) in the leiomyoma-like lesion (LM) outlined with a dotted black line. SMA is a marker for smooth muscle cells. (B) Collagen deposits within the uterine tumors stain blue with Masson's Trichrome (B). Red stains show muscle fibers; the blue stain indicates an abundance of collagen deposition in the tumor lesion, a known characteristic of leiomyomas. *Med12<sup>fl/+</sup> Med12R<sup>mt/+</sup> Amhr2-cre* uteri also stain positive for ER- $\alpha$ . ES- endometrial stroma; MY- myometrium; E- endometrium bars = 0.2 $\mu$ m (A), 100 $\mu$ m (B, C).

We also generated more complex mouse models to determine increasing the expression of mutant *Med12* and diminishing the expression of WT *Med12* would result in different phenotypic effects from the above-described outcomes. We generated and analyzed the uterine histology of 16-week *Med12<sup>fl/fl</sup> Med12R<sup>mt/+</sup> Amhr2-cre* (n=4) and *Med12<sup>fl/fl</sup> Med12R<sup>mt/mt</sup> Amhr2-cre* (n=1). We were only able to analyze one female of the *Med12<sup>fl/fl</sup> Med12R<sup>mt/mt</sup> Amhr2-cre* genotype, as the frequency of females born with this genotype was very low. The uteri of 16-week nulliparous *Med12<sup>fl/fl</sup> Med12R<sup>mt/+</sup> Amhr2-cre* (Figure 3.6 C, F) and *Med12<sup>fl/fl</sup> Med12R<sup>mt/mt</sup> Amhr2-cre* females were analyzed and found to have a phenotype (Figure 3.6 I, K) similar to that of *Med12<sup>fl/+</sup> Med12R<sup>mt/+</sup> Amhr2-cre* females with the appearance of dispersed smooth muscle cells interspersed with ECM deposits leading to fibrosis. As reviewed in Chapter 2, *Med12<sup>fl/fl</sup> Amhr2-cre* females are infertile. Interestingly, the *Med12<sup>fl/fl</sup> Med12R<sup>mt/+</sup> Amhr2-cre* females were also infertile and therefore we could only analyze the uteri of nulliparous females. However, a remarkable observation was that the *Med12<sup>fl/fl</sup> Med12R<sup>mt/+</sup> Amhr2-cre* uteri often had hyperplasia with uterine weights 50-60% higher than that of *Med12<sup>fl/fl</sup> Amhr2-cre* uteri ( $p < 0.05$ ) (Figure 3.6 G). This suggested that the mutant *Med12* expression could rescue the histology but not the fertility-related function of WT X-chromosome *Med12*. These results indicate that the *Med12* c.131G>A variant causes leiomyoma-like lesions in mice in a dominant manner, and probably acts via gain of function mechanism with a novel gene function.

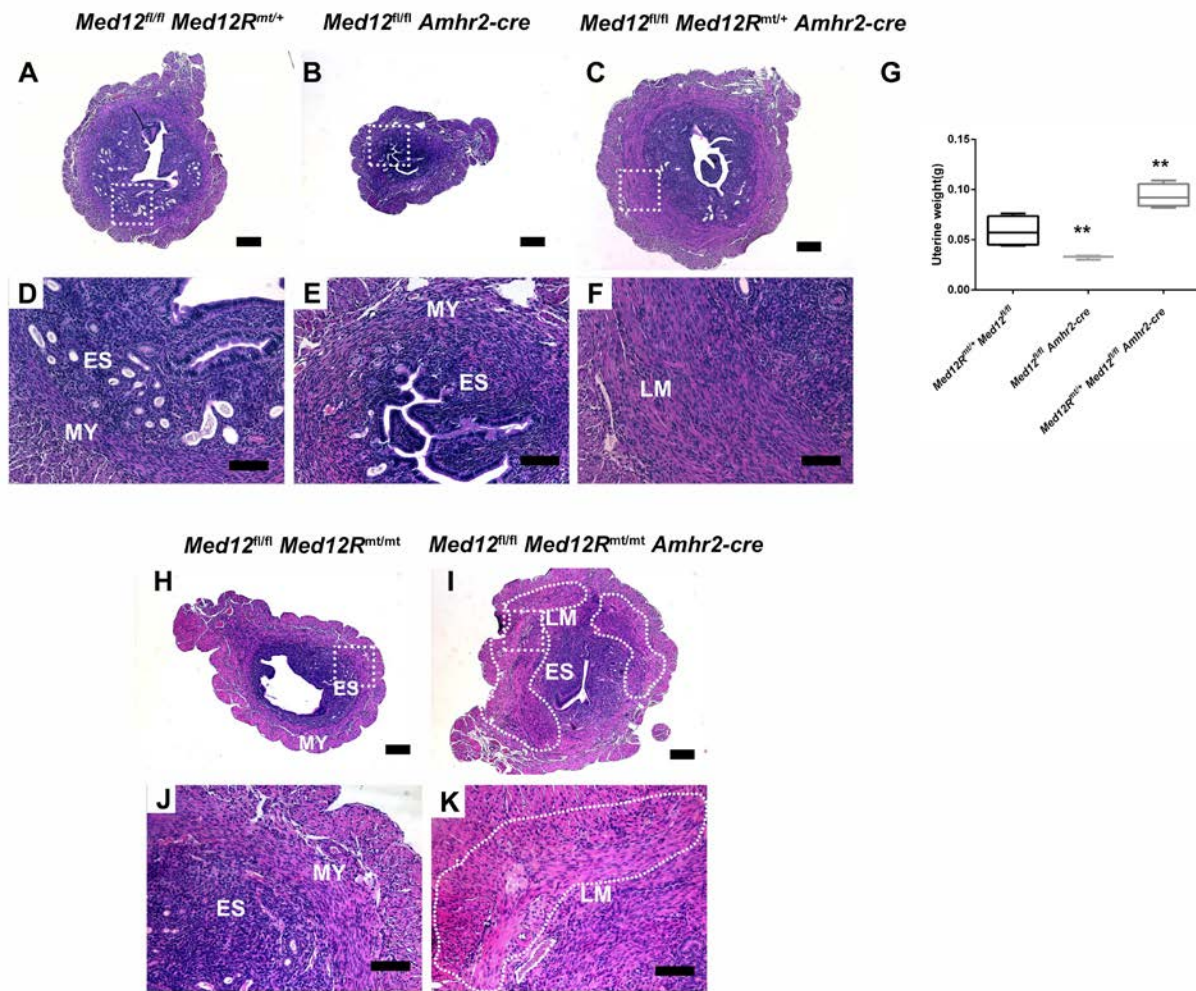


**Figure 3.6. Histological evaluation of uteri from *Med12<sup>fl/fl</sup> Med12R<sup>mt/+</sup> Amhr2-cre*, *Med12<sup>fl/fl</sup> Amhr2-cre* and *Med12<sup>fl/fl</sup> Med12R<sup>mt/mt</sup> Amhr2-cre* females**

(A) 16-week Control animals (*Med12<sup>fl/fl</sup> Med12R<sup>mt/+</sup>*) show normal uterine histology; a magnified view of the white box shows normal endometrial stroma (ES) and myometrium (MY) in (D). (B) *Med12<sup>fl/fl</sup> Amhr2-cre* mice generated on the C57/B6/129Sv/FVB background show hypotrophic uteri, similar to that of *Med12<sup>fl/fl</sup> Amhr2-cre* mice generated on the C57/B6/129Sv background. (C) The uterine histology of *Med12<sup>fl/fl</sup> Med12R<sup>mt/+</sup> Amhr2-cre* mice on the contrary shows hyperplasia with greater myometrial thickness and ECM deposits as observed in (F), compared to the myometrium of *Med12<sup>fl/fl</sup> Amhr2-cre* mice in (E). (G) This difference is quantified by uterine weights shown in (G) where the uterine weights of *Med12<sup>fl/fl</sup> Amhr2-cre* mice are 50% than that of controls; whereas the uterine weights of *Med12<sup>fl/fl</sup> Med12R<sup>mt/+</sup> Amhr2-cre* females is cumulatively 50% greater than that of control and *Med12<sup>fl/fl</sup> Amhr2-cre* mice ( $p < 0.005$ ). (H) Uterine histology of nulliparous 16-week *Med12<sup>fl/fl</sup> Med12R<sup>mt/mt</sup>* female with normal uterine histology with the outlined white box shown at a higher magnification in (J). (I) Uterine histology of 16-week nulliparous *Med12<sup>fl/fl</sup> Med12R<sup>mt/mt</sup> Amhr2-cre* females displaying the presence of leiomyoma-like lesions with the presence of ECM deposits and dispersed pattern of nuclei. Higher magnification of the outlined white dotted lines is shown in (K) where we observe a leiomyoma-like lesion. Error bars represent mean  $\pm$  S.E.M. Asterisk indicates significance using ANOVA test where  $**p < 0.005$ . LM-leiomyoma; ES-endometrial stroma; MY-myometrium; EM-endometrium. Scale bars = 0.5 $\mu$ m (A,B,C,H,I), 100 $\mu$ m (D,E,F,J,K).

### 3.3.3 *Med12* c.131G>A variant can cause uterine leiomyomas on WT background

We investigated if leiomyoma-like lesions were also present when *Med12* c.131G>A variant was expressed on the WT background (Figure 3.1B). To accomplish this, we generated animals that express mutant *Med12* from an autosomal locus in the presence of wild-type *Med12* expressing from the X chromosome (*Med12R<sup>mt/+</sup> Amhr2-cre*) by crossing *Med12R<sup>mt/mt</sup>* and *Amhr2-cre* mice (Figure 3.1B, 3.2D). Uteri from nulliparous *Med12R<sup>mt/+</sup> Amhr2-cre* and control mice (*Med12R<sup>mt/+</sup>*) were examined at 8, 12, 16, 24, and 32 weeks of age, and subjected to histomorphological evaluation. At 8 weeks of age, no leiomyoma-like lesions were observed in *Med12R<sup>mt/+</sup> Amhr2-cre* females (Figure. 3.7 B). Beyond 12 weeks of age, in addition to hyperplasia, we observed leiomyomas in 50% of *Med12R<sup>mt/+</sup> Amhr2-cre* mutant uteri, which were characterized by ECM deposits and disorganized pattern of smooth muscle fiber arrangement (Figure 3.7D-R). No such abnormalities were observed in control nulliparous females (*Med12R<sup>mt/+</sup>*) at any time point (Figure. 3.7 C-Q). Uteri that expressed mutant *Med12* weighed 20-30% more than control uteri with statistical significance ( $P<0.05$ ) (Figure 3.7S). Similar to the previous model, multiparous *Med12R<sup>mt/+</sup> Amhr2-cre* females revealed nodules that histologically resembled human leiomyomas due to deposition of ECM and, whorl formation and, with fewer nuclei present (Figure 3.8B, D). We assessed the uterine histology of both nulliparous and multiparous *Med12R<sup>mt/mt</sup> Amhr2-cre* females (n=4, per group) to explore whether the expression of homozygous *Med12* variant on a WT background would adversely affect the phenotypic outcome. The uterine histology of 16 week *Med12R<sup>mt/mt</sup> Amhr2-cre* revealed no significant differences from the uterine histology (Figure 3.9 B,D,E,G,I) of *Med12R<sup>mt/+</sup> Amhr2-cre* females of the same age, both with presentation of disrupted smooth muscle fibers interspersed with ECM deposits. These results further reinforce the hypothesis that

the *Med12* variant causes leiomyomas in a dominant fashion. In contrast to the previous model, where *Med12* c.131G>A variant was 80% penetrant when expressed on the conditional knockout background (*Med12<sup>fl/+</sup> Med12<sup>mt/+</sup> Amhr2-cre*), the penetrance for leiomyomatous formation of *Med12* c.131G>A variant on WT background was 50%. Moreover, we never observed large leiomyoma-like lesions in *Med12<sup>mt/+</sup> Amhr2-cre* females as we did in *Med12<sup>fl/+</sup> Med12<sup>mt/+</sup> Amhr2-cre* mice (Figure 3.4). Our results show that the *Med12* missense variant c.131G>A causes uterine hyperplasia and leiomyomas in the background of both wild type X chromosomes or conditional *Med12* knockout. In the background of conditional *Med12* deletion, leiomyoma-like lesions tend to have earlier onset and achieved greater size. *Med12* missense variant c.131G>A variant therefore acts as a gain of function mutation.

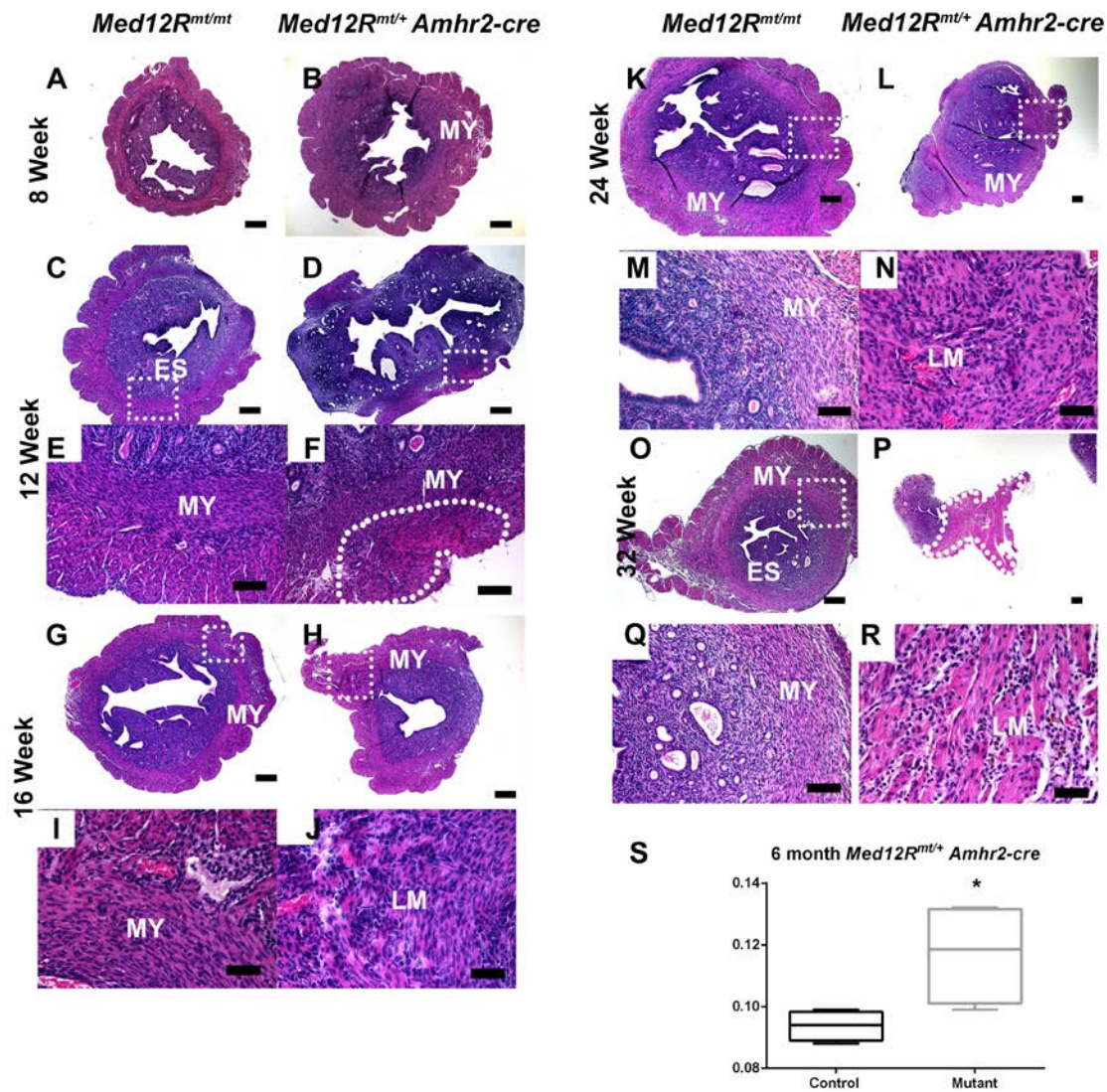


**Figure 3.7. Histological evaluation of uteri from nulliparous *Med12R<sup>mt/+</sup>Amhr2-cre* females**

Control animals (*Med12R<sup>mt/+</sup>*) at each time point show normal uterine histology (A,C,G,K,O) ; a magnified view of the white box shows normal endometrial stroma (ES) and myometrium (MY) in (E,I,M,Q). (B) 8 week old *Med12R<sup>mt/+</sup>Amhr2-cre* mice do not show any distinct pathological changes associated with leiomyoma formation. The uteri of *Med12R<sup>mt/+</sup>Amhr2-cre* females begin to show ECM deposits and dispersed muscle fibers associated with leiomyomas at (D, F) 12-weeks of age. These changes progressively increase with age as observed at (H, J) 16 weeks, (L, N) 24 weeks of age and ultimately give rise to large fibrotic leiomyoma-like lesions as observed at (P,R) 32 weeks of age. The white dotted lines outline leiomyomas IN (F,P) or magnified areas (D,H,L). (S) Representative of hyperplasia, mutant uterine weights were higher at all ages examined as compared to the controls \* ( $p < 0.01$ ). Data are presented as mean  $\pm$  SEM. LM-leiomyoma; ES-endometrial stroma; MY-myometrium; EM-endometrium. Scale bars = 2000 $\mu$ m (L,P) 0.5 $\mu$ m (A,B,C,D,G,H,K,O), 100 $\mu$ m (E,F,M,Q), 50 $\mu$ m (I,J,N,R).

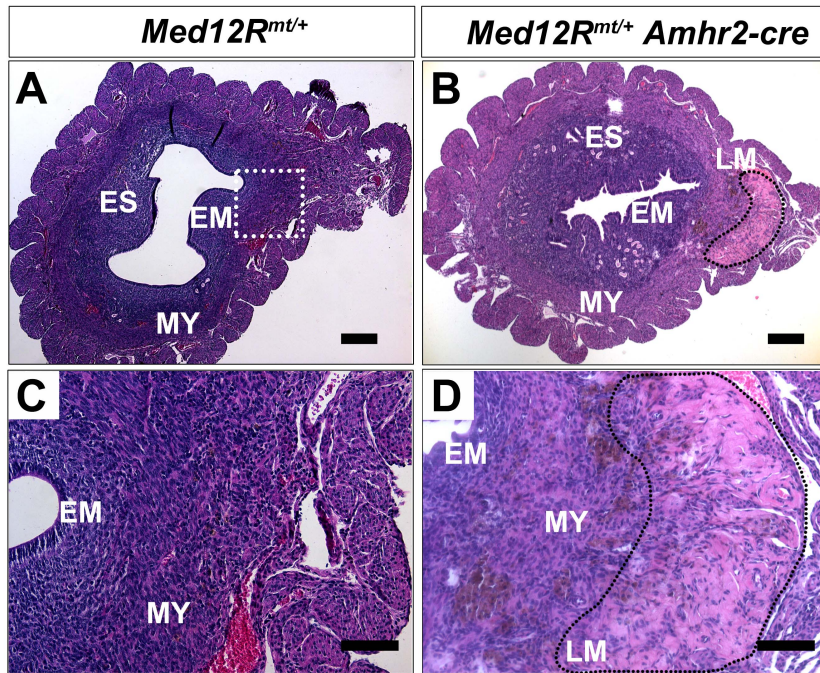


**Figure 3.8** Multiparous *Med12R<sup>mt/+</sup> Amhr2-cre* uteri develop prominent leiomyomas

(A, C) Uteri from control mice, *Med12R<sup>mt/+</sup>*, that, in the absence of *Amhr2-cre*, do not express *Med12* c.131G>A variant and show normal cross-sectional histology. (B, D) Uteri of *Med12R<sup>mt/+</sup> Amhr2-cre* mice that express the *Med12* c.131G>A variant and reveal leiomyoma-like lesions in ~47% females, with typical sparse nuclear arrangement, nodular pattern of cellular growth, and ECM deposition (black dotted lines) LM-Leiomyoma; ES-Endometrial stroma; MY-Myometrium; EM-Endometrium. Scale bars = 500 $\mu$ m (A,B), 100 $\mu$ m (C,D).

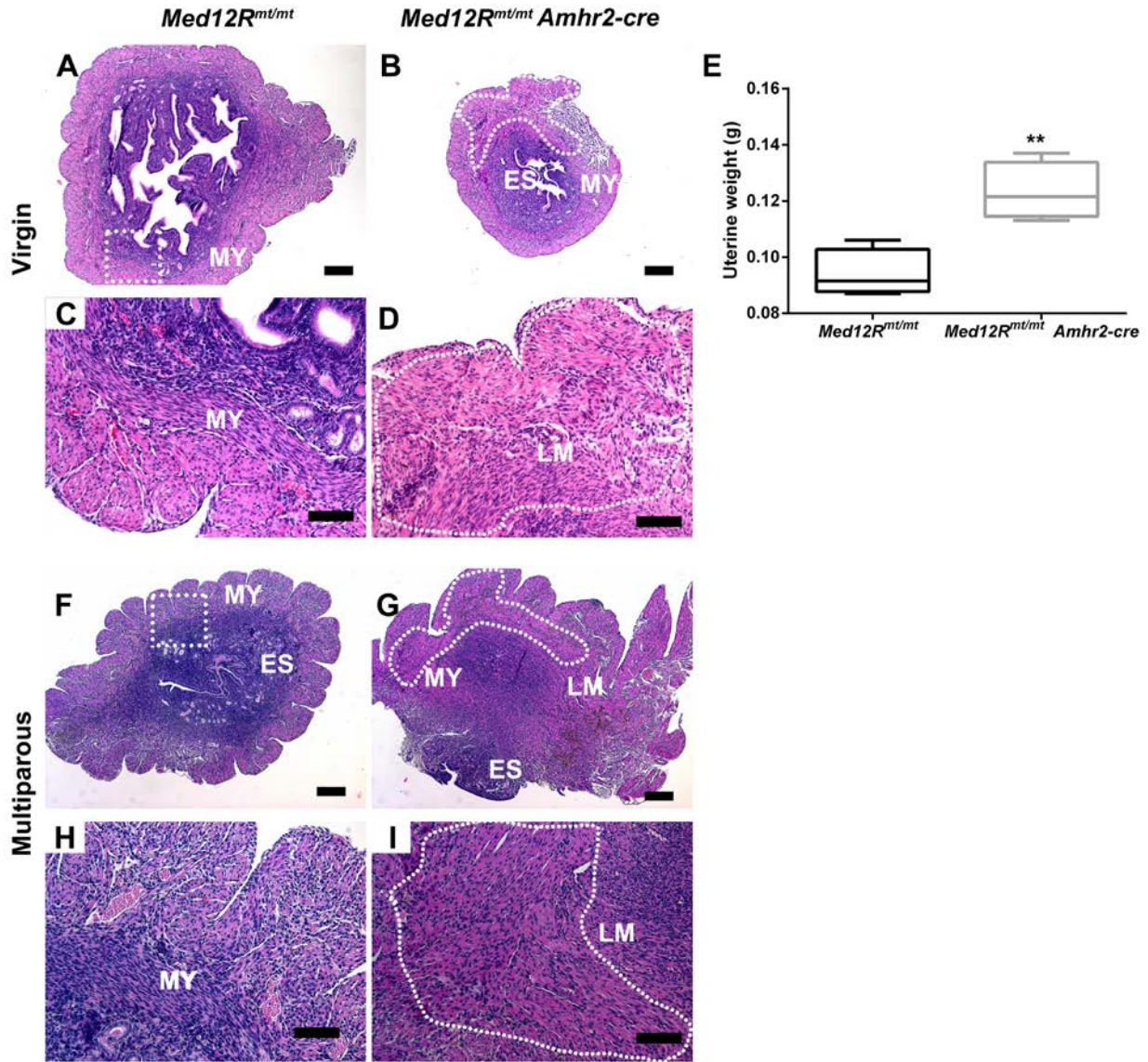


**Figure 3.9** Histological evaluation of uteri from nulliparous and multiparous *Med12R<sup>mt/mt</sup>Amhr2-cre* females

(A, C) Uteri from control mice, *Med12R<sup>mt/mt</sup>*, that, in the absence of *Amhr2-cre*, do not express *Med12* c.131G>A variant and show normal histology. (B, D) 16-week uteri expressing homozygous *Med12* c.131G>A variant, (*Med12R<sup>mt/mt</sup>Amhr2-cre*) develop leiomyoma-like lesions as observed by the presence of ECM deposits and disorganized pattern of nuclei. The incidence and presentation of leiomyomas in the uteri of *Med12R<sup>mt/mt</sup>Amhr2-cre* females was very similar to that of *Med12R<sup>mt/+</sup>Amhr2-cre* females. (E) Representative of hyperplasia, mutant uteri weights was higher in mutant uteri as compared to controls ( $p < 0.01$ ). (G,I) Multiparous *Med12R<sup>mt/mt</sup>Amhr2-cre* uteri also develop prominent leiomyomas as previously observed in the uteri of multiparous *Med12R<sup>mt/+</sup>Amhr2-cre* females. The white dotted lines outline the leiomyoma-like lesions. Data are presented as mean  $\pm$  SEM. LM- Leiomyoma; ES-Endometrial stroma; MY-Myometrium; EM-Endometrium. Scale bars = 500µm (A,B,F,G), 100µm (C,D,H,I).

### 3.3.4 *Med12* mouse mutations and genomic instability

To understand the underlying mechanisms of mutated *Med12* driven tumor development, we investigated the genomic landscape of the mouse tumors by performing array comparative genomic hybridization (aCGH) on four uteri with leiomyoma-like lesions (*Med12*<sup>fl/+</sup>*Med12R*<sup>mt/+</sup>*Amhr2-cre*) and compared them to uteri from littermate controls without *Amhr2-cre* (*Med12*<sup>fl/+</sup>*Med12R*<sup>mt/+</sup>). Aberrations were called as deletions or duplications based on the logarithmic values of probe signal intensities as shown in Table 3.1.

**Table 3.1 Table of logarithmic signal intensity ratios to interpret aCGH data**

Log ratios	Deletion	Duplication
0/2 (-ξ)	homozygous	
1/2 (-1)	heterozygous	
3/2 (0.58)		heterozygous
4/2 (1)		homozygous
>1		Amplification

The log ratios, which were not whole numbers, such as  $\pm 0.3$  or  $\pm 1.25$ , were considered as mosaic aberrations. The tumors from each of the four uteri showed a range of chromosomal abnormalities (approximately 40 abnormalities per tumor), with chromosomes 2, 7, 14 and 17 being most frequently affected (Figure 3.10A). An example of a deletion and duplication seen in the tumors is shown in Figure 3.10B. Genes in these regions were carefully annotated, eliminating common CNVs present in the Wellcome Sanger Trust database. The affected regions often consisted of genes targeting cell cycle checkpoints or common tumor signaling pathways

such as Ras, Wnt/ $\beta$ -catenin, Tp53/Rb, NF-kappa $\beta$ , and Tgf $\beta$  signaling. The complete list of aberrations in the uteri of *Med12<sup>fl/+</sup>Med12R<sup>mt/+</sup> Amhr2-cre* females is shown in Appendix Table 5.2. Microarray analysis on genomic DNA from *Med12<sup>fl/+</sup>Med12R<sup>mt/+</sup> Amhr2-cre* uteri additionally showed a few affected genomic regions with a pattern consistent with focal chromothripsis-like alterations (180) (Figure 3.10C). Chromothripsis has been previously described by Mehine et al in human uterine leiomyomas as well (178).

We also mapped these aberrations to the human genome (hg19) to determine regions of synteny between mouse and human chromosomes. Approximately 50% of the mouse aberrations had syntenic counterparts on human chromosomes (Appendix Table 5.3), and a number of these regions are known to be rearranged in human leiomyomas (Table 3.2). For example, mouse chromosome locus 17qA3.3, duplicated in *Med12<sup>fl/+</sup>Med12R<sup>mt/+</sup> Amhr2-cre* uteri (Figure 3.11A), maps to the human 6p21 locus. Similarly, in another *Med12<sup>fl/+</sup>Med12R<sup>mt/+</sup> Amhr2-cre* uterus, a deletion of the 4qD2.3 locus is syntenic to the human 1p36.1-p35 region (Figure 3.11B). Genomic rearrangements in 6p21 and 1p36.1-p35 are common in human leiomyomas. These results suggest that *Med12* exon 2 mutations are precursors to genomic rearrangements and therefore can lead to an unstable genome and which drives tumor progression.

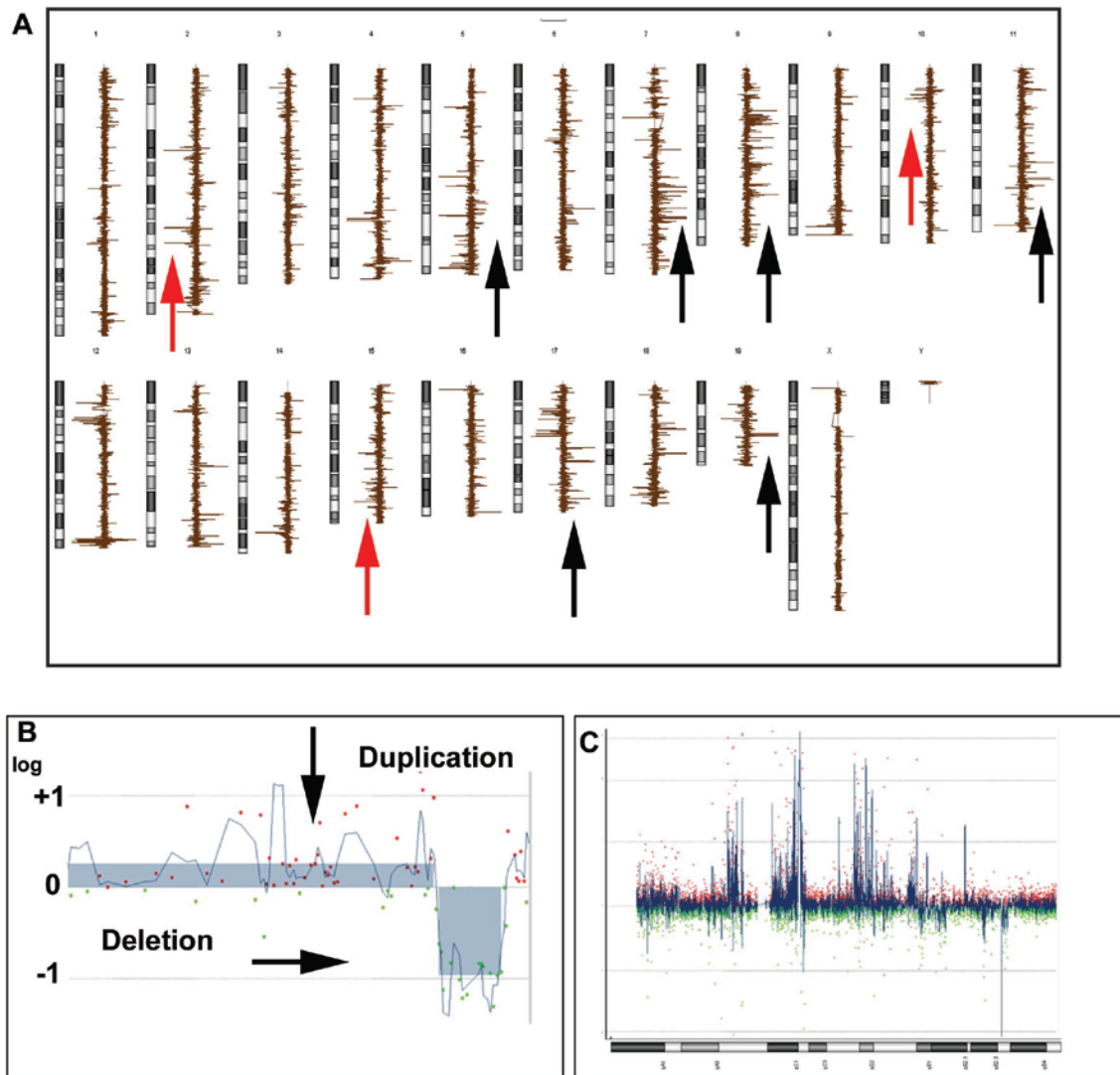


**Figure 3.10 Representative array profiles of  $Med12^{fl/+}Med12R^{mt/+}Amhr2-cre$  tumors**

(A) Representative genomic view of a  $Med12^{fl/+}Med12R^{mt/+}Amhr2-cre$  tumor showing 19 mouse chromosomes on the left and the log of signal intensity ratios on the right. We observe numerous deletions (Red arrows) and duplications (black arrows) throughout the genome of this tumor. (B) Representative example of mosaic gain followed by a loss of region 18qA1 (chr18: 8457226- 10017847). This region of approximately 345 kb encompasses the genes *Fzd8*, *Ccny*, *Cetn1*, *Thoc1*, *Usp14*, and *Colec12*. (C) Chromosome view of mouse chromosome 14 of  $Med12^{fl/+}Med12R^{mt/+}Amhr2-cre$  uteri showing chromothripsis.

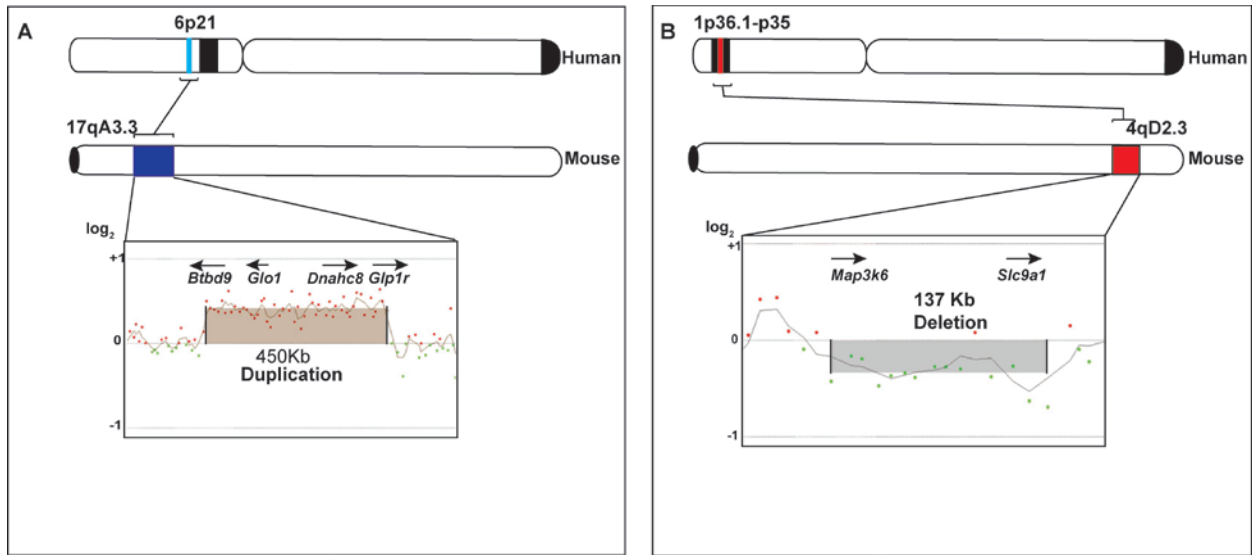


**Figure 3.11** Representation of human syntenic mapping of uterine rearrangements in mouse *Med12<sup>fl/+</sup> Med12<sup>R<sup>mt/+</sup></sup> Amhr2-cre* females

(A) Genomic duplication observed on mouse chromosome locus 17qA3.3 is syntenic to the human 6p21 locus, shown in blue. Representative array profile of the 17qA3.3 region, highlighting the 450 kb duplication (chr17: 30586287- 31049473), is also shown. (B) Genomic deletion observed on mouse 4qD2.3 locus is syntenic to the human chromosome locus 1p36.1-p35. The mouse deletion encompasses 137 kb and is shown in the respective array profile (chr4: 132799884-132936192). Positions are displayed approximately to scale according to the hg19 and mm9 physical maps, respectively.

**Table 3.2 Regions shared between human and mouse leiomyomas**

Chr	Gain/Loss	Size (kb)	Genes in region	Human Syntenic loci
1qH5	Mosaic gain	104	<i>Rab3gap2</i> -TgfB signaling, <i>Iars2</i> - cell cycle checkpoint network <i>Bpnt1</i> -estrogen metabolism <i>Mir194, Mir195</i>	1q41
1qD	Mosaic loss	108	<i>Hjrp</i> - maintenance of genomic stability	2q37.1
4qD2.3	Mosaic Loss	137	<i>Slc9A1, Map3k6</i> - Mapk/c-Jun signaling	1p36.1-p35
6qB1	Mosaic gain	105	<i>Prss1</i> - ECM receptors <i>Prss3</i> - cell division	7q34
14qD2	Gain	40	<i>Adam28</i> - fibronectin receptor, <i>Adam 7</i> - collagen receptors	8p21.2
14qD3	Gain	133	<i>Pcdh17</i>	13q21.1
17qA3.3	Mosaic gain	450	<i>Btbd9</i> -Tp53 network, <i>Glo1</i> -NFkappaB network, <i>Glp1r</i> -cAMP signaling	6p21.1-p21.3
18qA1	Mosaic gain	133	<i>Fzd8</i> -Wnt /beta catenin network, <i>Ccny</i> - cell cycle regulator <i>Cetn1</i> - chromosome segregation	10p11.21
18qA1	Loss	212	<i>Thoc1</i> - G2/M cell cycle checkpoint activator/apoptosis pathway, <i>Usp14, Colec12</i>	18p11.32

*Med12<sup>fl/+</sup> Med12<sup>mt/+</sup> Amhr2-cre* uteri chromosomal aberrations and corresponding human syntenic regions implicated in human leiomyomas.

### 3.3.5 Expression of mutant *Med12* in myometrial cells using the Myosin heavy chain 11-cre (*Myh11-cre*)

We had shown earlier in Chapter 2 that the *Amhr2-cre* recombination efficiency was approximately 50%. We also wanted to investigate the penetrance and the effects of mutant *Med12* expression on the phenotype and the penetrance of the *Med12 Rosa* knock-in model by

using another smooth muscle specific-cre. We chose to use *Myosin heavy chain 11* driven Cre that is expressed in all smooth muscle tissues, including the uterine myometrium starting at E13.5 (249). We generated the *Med12R<sup>mt/+</sup> Myh11-cre* by crossing *Med12R<sup>mt/mt</sup>* and *Myh11-cre* mice and evaluated the uterine histology and morphology at 12 weeks of age. The histological presentation of *Med12R<sup>mt/+</sup> Myh11-cre* was not dramatically different from that of *Med12R<sup>mt/+</sup> Amhr2-cre* uteri, with the presence of ECM deposits and disorganized smooth muscle fibers (Figure 3.12 B, D). This suggested to us that the phenotype and the penetrance observed in the previous models was independent of the type of specific smooth muscle cre allele used to recombine the floxed sites.

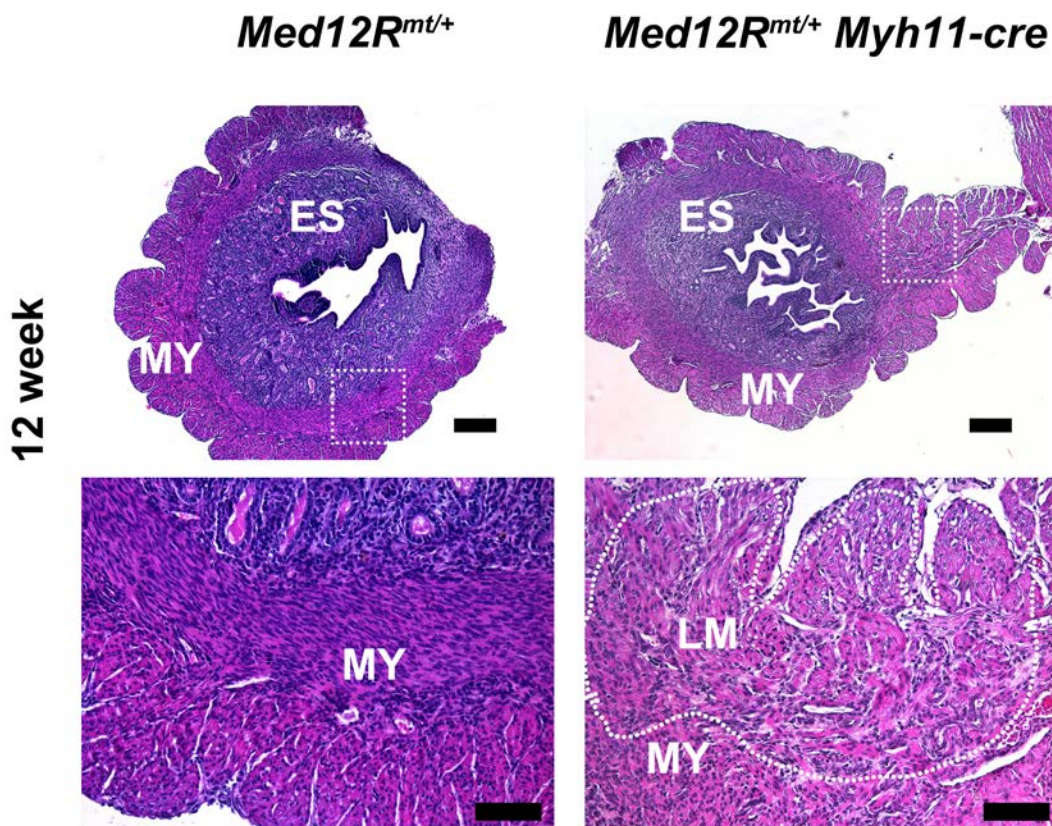


Figure 3.12 Evaluation of 12-week *Med12R<sup>mt/+</sup> Myh11-cre* uteri

(A,C) 12-week control animals (*Med12R<sup>mt/+</sup>*) show normal uterine histology. (B) 12-week *Med12R<sup>mt/+</sup> Myh11-cre* shows the development of leiomyoma-like lesions with the outlined white dotted box shown at a higher magnification in (D) highlighting the dispersed pattern of nuclei and ECM deposits (white dotted lines). The size or the presentation of lesions in *Med12R<sup>mt/+</sup> Myh11-cre* did not differ from that of 12-week old *Med12R<sup>mt/+</sup> Amhr2-cre* females. Scale bars=0.5 $\mu$ m (A,B), 100 $\mu$ m (C,D).

### 3.4 DISCUSSION

Recurrent human *MED12* exon 2 mutations have been associated with benign tumors such as uterine leiomyomas (161), breast fibroadenomas (186) and phyllodes tumors (187, 190); however, their etiology, genetic mechanism of action, and role in genomic instability are unknown. To study the role of *Med12* mutations in uterine leiomyomas, we generated a mouse model which would conditionally express the most common human *Med12* c.131G>A variant from the autosomal *ROSA26* locus and allow us to study its effects in a tissue-specific manner in the uterus. Our strategy allowed us flexibility, to develop mouse models where mutated *Med12* was expressed either in the absence (gain of function) or presence (dominant negative) of X-chromosome WT *Med12*. We found that expression of mutated *Med12* in the absence or presence of X-chromosome *Med12* gave rise to leiomyoma-like lesions, regardless of the background, although the age of onset and the presentation of leiomyomas were different between the two models. Remarkably, the mouse leiomyomas shared histological features of human uterine leiomyomas.

Parity appeared to have an adverse effect on leiomyomatous growth, as multiparous females in both models presented with the larger and more distinct leiomyoma-like lesions as compared to nulliparous females. This may be explained by the exposure of the *Med12* mutated uterus, to a milieu of steroid hormones during pregnancy, therefore driving growth of

leiomyomas. This finding is in agreement with human data, as reports have suggested that pregnancy often has dramatic effects on human fibroids (45).

In comparison to the dominant negative model, leiomyoma-like lesions in the gain-of-function model were often larger, more penetrant, and presented as early as 8-weeks of age. These findings suggest that the *Med12* c.131G>A variant alone drives tumor formations via gain-of-function mechanism.

We also examined the phenotypes of animals expressing homozygous mutant *Med12* c.131G>A variant, on a background of *Med12* cKO (*Med12<sup>fl/fl</sup>*) mice (*Med12<sup>fl/fl</sup> Med12R<sup>mt/+</sup> Amhr2-cre* and *Med12<sup>fl/fl</sup> Med12R<sup>mt/mt</sup> Amhr2-cre*). Although the penetrance and the size of leiomyoma-like lesions was similar to the previous models (*Med12<sup>fl/fl</sup> Med12R<sup>mt/+</sup> Amhr2-cre* and *Med12R<sup>mt/+</sup> Amhr2-cre*), yet the expression of the mutant *Med12* was able to rescue the histology of the *Med12<sup>fl/fl</sup> Amhr2-cre* (*Med12* cKO) uteri as observed by the heavier uterine weights of *Med12<sup>fl/fl</sup> Med12R<sup>mt/+</sup> Amhr2-cre* females. The fact that the *Med12<sup>fl/fl</sup> Med12R<sup>mt/+</sup> Amhr2-cre* females still remain infertile indicates that the mutant *Med12* may have a role distinct of the X-chromosome *Med12* (neomorph). A caveat applies to the models on the background of *Med12* cKO as the tumorigenic changes occurring have to be evaluated against a hypoplastic background, making data interpretation difficult.

There are three published transgenic mouse models of uterine leiomyomas; these include transgenic overexpression of hGPR10-driven with calbindin-D9K promoter (227), conditional deletion of *Tsc2* (224), and conditional expression of a gain-of-function mutant form of  $\beta$ -catenin (225). The phenotype in these mice is confined to increased myometrial thickness and formation of small nodules, but none show the dramatic tumors we report here (Figure 3.4). Interestingly, *Amhr2-cre* drives mutant *Med12* expression in both uterine smooth muscle tissue (myometrium)

and stroma, yet we only observed tumors deriving from the mouse myometrium. In contrast, *Amhr2*-cre-driven expression of the gain-of-function mutant form of  $\beta$ -catenin causes tumors both in the mouse myometrium and in the stroma (225). These results indicate that *Med12* exon 2 mutations have specific tumorigenic effects in smooth muscle cells.

Studies published on human leiomyomas were unable to establish a correlation between *MED12* positive leiomyomas and underlying cytogenetic changes, which are often observed in about 40% of human leiomyomas. We utilized our mouse models to explore this further. Array CGH on *Med12* c.131G>A mouse uteri revealed genome-wide aberrations affecting regions containing genes belonging to a variety of tumor pathways including Ras, Wnt/ $\beta$ -catenin, Tp53/Rb, NF-kappa $\beta$ , and Tgf $\beta$  signaling. We also observed complex chromosomal alterations such as chromothripsis. Recently, chromothripsis was reported in human leiomyomas and proposed as a possible mechanism of tumor progression (91). This suggests a role of *Med12* as a global transcriptional regulator and guardian of genome integrity.

Another key feature of the mouse leiomyomas, is that some of the chromosomal aberrations occurring in these regions, also occur in regions syntenic to human 1p, 1q, 2q, 6p21, and 18p loci. It was previously shown that 60% of human leiomyomas with 6p21 rearrangements harbored *MED12* exon 2 mutations (163).

Previous reports had suggested that the *MED12* exon 2 mutations uncouple Cyclin C–CDK8/19 interface leading to diminished CDK8 activity (250). Interestingly, in our array data we did not observe any changes in *Cdk8*, *Cyclin C*, *Med13* or *Cdk19*, rather we observed more global genome-wide changes. The *CDK8* and *MED12* studies were conducted on baculovirus systems (*in-vitro*) whereas our mechanistic studies were conducted on *in-vivo* mouse models

making it evolutionarily more relevant to the role of human *MED12* exon 2 mutations in tumorigenesis.

Overall, we have successfully created the first animal models for uterine leiomyomas harboring *Med12* exon 2 mutations. This model will be a valuable tool not only to understand the genesis of uterine leiomyomas but also other steroid influenced tumors such as breast fibroadenomas, and phyllodes tumors, as well. These models will also provide a platform to test therapeutic targets to treat uterine leiomyomas as an alternative to hysterectomy.

The limitations of our model include regulatory differences that may exist in the expression of *Med12* on the X chromosome versus an autosome. The autosomal *Med12* is under the control of *ROSA* promoter, which probably differs from the native *Med12* promoter. In addition to the model itself, factors such as random X-chromosome inactivation influencing the *Med12* floxed allele expression and *Amhr2*-cre mediated allelic recombination add to the complexities of this study. Nonetheless, we have successfully created the first animal model for uterine leiomyomas and *Med12* exon 2 mutations. Our model mimics the human condition and shows that *Med12* variants can act through a gain-of-function mechanism.

### 3.5 ACKNOWLEDGEMENTS

We thank Dr. Yonghyun Shin for generating the *ROSA* Knock-in mice. We thank Drs. Y. Ren, A. Kishore and Ms. K.J. Golnoski for their technical assistance. We thank our collaborators, Drs. Carlos Castro (pathology) from MWRI, Svetlana Yatsenko, and Urvashi Surti from the Magee-Womens Hospital Cytogenetics Laboratory for their assistance with the aCGH studies. We thank Gabriel Rajkovic for his assistance with the generation of the *Med12* antibody. We also thank

Magee-Womens Research Institute (MWRI) Transgenic and Molecular Core and the Histology core facilities. We would like to thank Dr. Heinrich Schrewe for generously donating us the *Med12<sup>fl/fl</sup>* mice, and Dr. Richard Behringer and Stephanie Pangas for the *Amhr2-cre* mice. I would like to acknowledge the MWRI startup and RO1: 4010 grants as the funding sources for the *MED12* project.

#### 4.0 OVERALL SUMMARY AND CONCLUSIONS

Ever since studies first associated *MED12* exon 2 variants with human uterine leiomyomas (159) (161), numerous studies have replicated the association of *MED12* exon 2 variants with leiomyomas from women of ethnically diverse backgrounds. The *MED12* exon 2 variant studies have now been extended to many different types of benign and malignant tumors . Since its discovery using whole exome sequencing, *MED12* exon 2 variants have been classified as the most frequently occurring variants associated with gynecological tumors.

Over the years, many groups have speculated on the possible mechanisms of *MED12* exon 2 variants in tumor causation, but such mechanisms are difficult to study *in vivo* in human tissues. Animal models expressing and analyzing *in-vivo* functions of *Med12* exon 2 variants have been lacking. Our own observations of the *MED12* exon 2 variants in the mixed North American women population convinced us of the importance of this gene in leiomyoma biology. The high frequency of *MED12* mutations in leiomyomas, clustering of the mutations in an evolutionary conserved region of the gene, and its location on the X-chromosome made *MED12* an ideal candidate gene for generating animal models and studying its role in tumorigenesis.

The overarching goal of my thesis work was to investigate the role of *MED12* exon 2 variants, in leiomyoma initiation and to determine the role of *MED12* in normal uterine function.

As the *Med12* gene is highly conserved between humans and mice, it gave us the opportunity to model this gene *in-vivo* using mouse models. As typical of modeling any driver

mutations in tumors (example: p53) (245), we chose to generate loss of function, gain of function and dominant negative models of *Med12* exon 2 variants. The first of this thesis entailed characterization of *Med12* cKO females (loss of function) using the *Med12<sup>fllox</sup>* (220) and *Amhr2-cre* (226) mice. Loss of function did not stimulate leiomyomas. On the contrary, *Med12* cKO females appeared to have hypoplastic uteri, and were infertile. Although, young *Med12* cKO ovaries were capable of ovulating under external gonadotropic stimulus, adult *Med12* cKO ovaries lacked large follicles and had the appearance of hyperchromatic “follicular nests”. Such structures have also been reported in the ovaries of mutant *beta-catenin* females (225) (239). The global phenotype observed in the reproductive tracts of the *Med12* cKO female point towards a defect in estrogen and progesterone synthesis. It is possible that either *Med12* directly or indirectly targets steroid hormones and their receptors, or simply, the loss of granulosa cells in *Med12* cKO ovaries may result in reduced steroid hormone synthesis. Based on the phenotypic similarities between *beta-catenin* cKO (239) (225) and *Med12* cKO reproductive tracts, one could infer that loss of beta-catenin may in part contribute to the infertility phenotype. In the future, experiments aimed to assay serum estrogen, progesterone levels, cumulus cell expansion, fertilization potential, uterine implantation and decidualization will be important to determine the cause of infertility. In addition, determining the expression of beta-catenin and hormone receptors will also be important. As part of this aim, I also synthesized a new *Med12* antibody to quantitate *Med12* expression and localization. In addition to protein expression studies, this antibody will be a valuable resource to conduct experiments such as IP and ChIP-seq. Alternatively, the FLAG reporter fused to *Med12* cDNA at the *ROSA* locus may also be used to conduct ChIP-seq experiments. Thus, data from our loss of function mouse model indicates that loss of *Med12* is not the likely mechanism of *Med12* exon 2 variants for leiomyomagenesis,

contrary to previous reports based on in-vitro data (250). This model will be a useful tool to help understand the function of *MED12* in uterine biology and pregnancy.

To examine the gain of function or dominant negative effects of *Med12*, we developed the conditionally floxed *Med12 ROSA* knock in mouse model, giving us the opportunity to express mutated *Med12* from the *ROSA* locus, either in the absence (gain-of-function) or in the presence of X-chromosome wild-type *Med12*. Thus, the latter half of my thesis focused on developing and characterizing various genotypes associated with the gain of function and dominant negative mouse models. We remarkably observed leiomyoma-like lesions, in about 87% of females expressing mutated *Med12* in the absence of wild-type *Med12* and in about 50% of females expressing mutated *Med12* in the presence of wild-type *Med12*, showing that *Med12* c.131G>A alone can cause leiomyomas in a dominant manner. As concomitant deletion of *Med12* did not ameliorate the phenotype of *Med12* knock in mice, but made it worse, we conclude that the c.131G>A mutation represents a gain of new function (neomorph) rather than a gain of existing function (hypermorph) (248). In both the models, appearance of the most distinct leiomyomas was observed in multiparous females, suggesting a role of *Med12* in steroid driven leiomyomagenesis. This may also explain the presence of recurrent *MED12* exon 2 variants in other steroid driven tumors such as fibroadenomas (186) and phyllodes tumors (187) of the breasts. Our data indicates a link between *Med12*, steroidogenesis, infertility and tumorigenesis. In the future, these models could be used to decipher the specific roles of estrogen and progesterone in tumor initiation and progression by performing ovariectomy followed by estrogen and progesterone supplementation. Testing gonadotropic antagonists on the *Med12* gain of function models might be another way to examine their individual roles in tumorigenesis.

Not only did the *Med12* exon 2 variants cause leiomyomas, they also led to genomic instability in the leiomyomas. Moreover, the genomic instability outcomes affected several pathways, therefore reflecting the role of *MED12* as a global regulator of genome stability (204). In the future, it is crucial to determine the specific targets of the exon 2 variants through RNA-seq or ChIPseq, to help design small molecule inhibitors that will modulate the activity of pathways associated with *MED12* mutated leiomyomagenesis. Interestingly, several regions previously implicated in human leiomyomas were also shared by the mouse leiomyomas, revealing the similarities between human and mouse leiomyomas. This data suggests that *Med12* exon 2 mutations are precursors to genomic rearrangements and hence can cause an unstable genome and drive tumor progression. The results from this thesis collectively provide novel insights into the mechanism of *Med12* exon 2 variants in leiomyoma causation, and also establish a unique link between *Med12*, steroidogenesis and fertility. Deciphering the functions of *Med12* from the loss of function mouse model may be a means to further understand the roles of *Med12* in tumorigenesis.

Although there are limitations to our model as explained in section 3.4, we have successfully generated a novel model for leiomyomas which successfully replicates the human condition with shared pathological and cytogenetic features between mouse and human leiomyomas. These models will also serve as a platform to help identify drug targets to develop and test small molecule therapeutics, to move the field of leiomyoma research forward. Further, these models will help us in understanding the mechanism of *Med12* exon 2 variants in other benign tumors such as fibroadenomas and phyllodes tumors of the breasts.

## APPENDIX: ABBREVIATIONS AND TABLES

**Table 4.1 List of abbreviations**

bFGF	basic fibroblast growth factor
BHD	Birt-Hogg-Dubé syndrome
bp	base pair
BRAF	v-raf murine sarcoma viral oncogene homolog
C	cytosine
cDNA	complementary deoxyribonucleic acid
CDK19	cyclin-dependent kinase 19
CDK8	cyclin-dependent kinase 8
CUX1	cut-like homeobox 1
D	aspartic acid
DNA	deoxyribonucleic acid
DAPI	4',6- Diamidino-2-2phenylindole, Dihydrochloride
G	Glutamine
ECM	extracellular matrix
ER	estrogen receptor
FH	fumarate hydratase
G	guanine
HE	hematoxylin-eosin
HLRCC	hereditary leiomyomatosis and renal cell cancer
HMGA	high mobility group A

**Table 4.1 continued**

HMGA1	high mobility group AT-hook 1
HMGA2	high mobility group AT-hook 2
hCG	human chorionic gonadotropin
IGF	insulin-like growth factor ins insertion
IP	intra peritoneum
IU	International Unit
KAT6B	K(lysine) acetyltransferase 6B
let-7	lethal-7
LOH	loss of heterozygosity
LS	leucine-serine-rich
MED12	Mediator complex subunit 12
MED12L	Mediator complex subunit 12-like
MED13	Mediator complex subunit 13
MED13L	Mediator complex subunit 13-like
MIM	Mendelian Inheritance in Man
MRI	magnetic resonance imaging
p	short arm of a chromosome
PCR	polymerase chain reaction
PMSG	Pregnyl mare serum gonadotropin
Pol II	RNA polymerase II
PR	Progesterone receptor
q	long arm of a chromosome
RAD51B	RAD51 paralog B
RAS	rat sarcoma RB1 retinoblastoma 1
RB1	retinoblastoma 1
REST	RE1-silencing transcription factor
RNA	ribonucleic acid

**Table 4.1 continued**

SNP	single-nucleotide polymorphism
t	translocation
TCA	tricarboxylic acid cycle
TGF- $\beta$	transforming growth factor beta
TP53	tumor protein 53
TSC	tuberous sclerosis
TSC2	tuberous sclerosis 2
VEGF	vascular endothelial growth factor
WHO	the World Health Organization
WNT4	wingless-type MMTV integration site family, member 4

**Table 4.2 Regions of aberrations in mouse leiomyomas**

<b>Chr</b>	<b>Cytoband</b>	<b>Start</b>	<b>Stop</b>	<b>Aberration size (Kb)</b>	<b>Gain/Loss</b>	<b>Region of Aberration</b>
chr1	qD	90115633	90193738	78.105	deletion	3
chr1	qE1.1	101591968	101656500	64.532	gain	1
chr1	qH4	179805696	179926632	120.936	deletion	1
chr1	qH5	187079059	187183640	104.581	gain	1
chr2	qA1	3947206	4016684	69.478	deletion	3
chr2	qC1.3	62554677	62580394	25.717	deletion	4
chr2	qD	85849412	85920056	70.644	gain	4
chr2	qH2	161545931	161698753	152.822	gain	1
chr3	qF1	87188304	87211687	23.383	gain	1
chr3	qF1	87267733	87302881	35.148	gain	1
chr3	qF3	110878881	110995945	117.064	gain	1
chr4	qD1	111726014	113251939	1525.925	deletion	4
chr4	qD1	111742887	112273763	530.876	deletion	4
chr4	qD1	111962345	112065411	103.066	deletion	4
chr4	qD1	112289418	112504314	214.896	deletion	3
chr4	qD1	112510205	112564300	54.095	deletion	4
chr4	qD1	112665000	112793116	128.116	deletion	4
chr4	qD1	112821289	112915923	94.634	deletion	4
chr4	qD1	113001582	113251939	250.357	deletion	2
chr4	qD1	113286238	113658273	372.035	deletion	1
chr4	qD2.2	121649423	122218644	569.221	deletion	1
chr4	qD2.3	132799884	132936192	136.308	deletion	1
chr4	qE1	145001092	146793868	1792.776	deletion	3
chr5	qC3.1	69891606	70097860	206.254	gain	3
chr5	qE5	105142362	105237345	94.983	gain	1
chr6	qA1	8556759	8575270	18.511	gain	1
chr6	qB1	41010073	41112757	102.684	gain	1
chr6	qB1	41306470	41412425	105.955	gain	2
chr7	qA2	18382929	18426616	43.687	gain	1
chr7	qB4	54844755	54883844	39.089	deletion	2
chr7	qB4	55466579	55715246	248.667	gain	1
chr7	qC	67475144	67731725	256.581	deletion	1
chr7	qE3	111430424	111507023	76.599	deletion	1
chr7	qF1	123631491	123927328	295.837	deletion	2

**Table 4.2 continued**

chr7	qF3	136825759	137141925	316.166	gain	1
chr8	qA1.2	16763830	16826155	62.325	gain	1
chr8	qA4	40187843	40274870	87.027	gain	1
chr9	qA3	21968269	22021024	52.755	deletion	1
chr9	qA5.3	46697499	46906183	208.684	deletion	0
chr10	qA3	17697339	17744401	47.062	deletion	1
chr10	qA3	22006887	22072759	65.872	gain	1
chr12	qE	105048428	105263855	215.427	deletion	2
chr12	qF1	114886825	114956321	69.496	gain	4
chr12	qF1 - qF2	115427710	115487987	60.277	deletion	4
chr12	qF2	115667710	115852666	184.956	gain	4
chr12	qF2	116155408	116261498	106.09	deletion	4
chr12	qF2	116515691	116624944	109.253	deletion	4
chr12	qF2	116840011	117047397	207.386	gain	
chr12	qF2	117198164	117274793	76.629	deletion	
chr13	qA1	12690823	12723384	32.561	Deletion	2
chr13	qB3	61743712	62048006	304.294	gain	1
chr13	qC1	75983645	76020728	37.083	Deletion	1
chr13	qD1	101053361	101110842	57.481	deletion	1
chr14	qC1	44380406	44579789	199.383	Gain	1
chr14	qC2	54320774	54422503	101.729	gain	1
chr14	qD1	69019011	69103662	84.651	gain	1
chr14	qD2	69209459	69249991	40.532	gain	1
chr14	qD2	69876584	70090608	214.024	deletion	2
chr14	qD2	72891034	72930683	39.649	gain	1
chr14	qD3	84908855	85042415	133.56	gain	1
chr14	qE1	86407031	86441138	34.107	gain	1
chr14	qE3	110472070	111123931	651.861	deletion	1
chr14	qE3 - qE4	110015732	111565569	1549.837	deletion	1
chr15	qA1	14992022	15100240	108.218	gain	
chr15	qE1	77310653	77364452	53.799	gain	3
chr16	qB3	35483725	35550180	66.455	gain	1
chr16	qB3	36245661	36336077	90.416	deletion	1
chr16	qB4	44819587	44909082	89.495	gain	1
chr17	qA3.3	30586287	31049473	463.186	gain	4
chr17	qB1	36199712	36245963	46.251	gain	1
chr17	qB1	36860348	36909276	48.928	deletion	1
chr17	qB1	38635045	38791870	156.825	gain	1
chr17	qB1 - qB2	40082709	40241053	158.344	deletion	4
chr18	qA1	8457226	9788370	1331.144	gain	1
chr18	qA1	9813671	10017847	204.176	deletion	3

**Table 4.2 continued**

chr19	qD3	60897053	60945155	48.102	Gain	1
-------	-----	----------	----------	--------	------	---

Chromosomal aberration list of all four-mouse tumors with the interval, number of genes and critical genes in each region

**Table 4.3 Syntenic regions between mouse aberrations and human chromosomes**

Mouse Chromosome	Human chromosomal locus	Human		Orthologous genes			
		Start	Stop	Tumor 1	Tumor 2	Tumor 3	Tumor 4
4qD2.3	chr1	27470631	27690372			SLC9A1,CHC HD3P3,WDC1, SYTL1, MAP3K6	
3qF3	chr1	106701046	106830733	-	-		
3qF1	chr1	157764252	157772664			FCRL1	
1qH5	chr1	220229780	220359711	BPNT1, IARS2, MIR215, MIR194-1, RAB3GAP2			
13qA1	chr1	236368354	236390748			ERO1LB, GPR137B	ERO1LB, GPR137B
1qH4	chr1	244734347	244817416		DESI2, COX20		
1qE1.1	chr2	124573472	124762072				
2qC1.3	chr2	163236878	163260207				
1qD	chr2	234682002	234812683		HJURP, TRPM8, SPP2	HJURP, MSL3P1	HJURP, MSL3P1, TRPM8
16qB3	chr3	122738925	122793361			SEMA5B, PDIA5	
5qC3.1	chr4	44613169	44931460		GNPDA2	YIPF7, GUF1, GNPDA2	YIPF7, GUF1, GNPDA2
8qA4	chr4	190221667	190228149				
13qC1	chr5	95111576	95153221			RHOBTB3, GLRX	
15qA1	chr5	29027869	29199306				
13qD2.3	chr5	45614983	45626841	HCN1	HCN1		
13qD1	chr5	66052023	66071066				
13qD1	chr5	70265907	70308766		NAIP		
17qA3.3	chr6	38457579	39028735	BTBD9, GLO1, DNAH8, GLP1R	BTBD9, GLO1, DNAH8, GLP1R	BTBD9, GLO1, DNAH8	BTBD9, GLO1, DNAH8, GLP1R
10qA3	chr6	139348580	139403048			ABRACL	ABRACL
6qA1	chr7	8134096	8148036				
6qB1	chr7	142190236	142250584				
8qA4	chr8	15586895	15636766		TUSC3		
14qD2	chr8	23158977	23414178		LOXL2, ENTPD4, SLC		

**Table 4.3 continued**

					25A37		
14qD2	chr8	24187964	24229697	ADAM28			
14qD1	chr8	24383271	24461193				
14qD2	chr8	36716399	36733668	KCNU1			
8qA1.2	chr8	3989107	4060094				
2qA1	chr10	14283901	14363312			FRMD4A	FRMD4A
18qA1	chr10	35739803	36669673	CCNY,GJ D4,FZD8			
19qD3	chr10	120876971	120932106				SFXN4, COXPD13, PRDX3
7qF3	chr10	122740826	123058528				
2qD	chr11	56216083	56241010		SLC25A37		
9qA5.3	chr11	115811243	116008575	KCNU1			
14qD3	chr13	58275467	58409706	PCDH17			
14qE1	chr13	59632641	59660044				
14qE3 - 14qE4	chr13	85181293	87535910			SLITRK6, MOB1AP1, DDX6P2, TXNL1P1	
14qE3	chr13	85660155	86345915				
12qE	chr14	94879399	94946027			SERPINA11, SERPINA9	
12qF1	chr14	106209967	106242264				
7qF1	chr16	18175137	18325190				
11qB5	chr17	2938562	2948297				
11qB4	chr17	5417772	5463831		NLRP1		
18qA1	chr18	179212	391932	USP14,TH OC1,COLE C12	USP14,TH OC1,COLE C12		USP14,THOC1,C OLEC12
2qH2	chr20	40900568	41046759				PTPRT

List of human chromosomal intervals that are syntenic to mouse chromosomal aberration intervals and conserved orthologous genes in the conserved regions

## BIBLIOGRAPHY

1. Wallach EE, and Vlahos NF. Uterine myomas: an overview of development, clinical features, and management. *Obstetrics and gynecology*. 2004;104(2):393-406.
2. Cramer SF, and Patel A. The frequency of uterine leiomyomas. *American journal of clinical pathology*. 1990;94(4):435-8.
3. Blaustein A, and Kurman RJ. *Blaustein's pathology of the female genital tract*. New York: Springer; 2002.
4. Stewart EA. Uterine fibroids. *Lancet*. 2001;357(9252):293-8.
5. Garcia CR, and Tureck RW. Submucosal leiomyomas and infertility. *Fertil Steril*. 1984;42(1):16-9.
6. Bukulmez O, and Doody KJ. Clinical features of myomas. *Obstetrics and gynecology clinics of North America*. 2006;33(1):69-84.
7. Gupta S, Jose J, and Manyonda I. Clinical presentation of fibroids. *Best Pract Res Clin Obstet Gynaecol*. 2008;22(4):615-26.
8. Wu JM, Wechter ME, Geller EJ, Nguyen TV, and Visco AG. Hysterectomy rates in the United States, 2003. *Obstetrics and gynecology*. 2007;110(5):1091-5.
9. Marshall LM, Spiegelman D, Barbieri RL, Goldman MB, Manson JE, Colditz GA, Willett WC, and Hunter DJ. Variation in the incidence of uterine leiomyoma among premenopausal women by age and race. *Obstetrics and gynecology*. 1997;90(6):967-73.
10. Flake GP, Andersen J, and Dixon D. Etiology and pathogenesis of uterine leiomyomas: a review. *Environmental health perspectives*. 2003;111(8):1037-54.
11. Marshall LM, Spiegelman D, Goldman MB, Manson JE, Colditz GA, Barbieri RL, Stampfer MJ, and Hunter DJ. A prospective study of reproductive factors and oral contraceptive use in relation to the risk of uterine leiomyomata. *Fertil Steril*. 1998;70(3):432-9.
12. Ross RK, Pike MC, Vessey MP, Bull D, Yeates D, and Casagrande JT. Risk factors for uterine fibroids: reduced risk associated with oral contraceptives. *Br Med J (Clin Res Ed)*. 1986;293(6543):359-62.
13. Parazzini F, Negri E, La Vecchia C, Chatenoud L, Ricci E, and Guarnerio P. Reproductive factors and risk of uterine fibroids. *Epidemiology*. 1996;7(4):440-2.
14. Terry KL, De Vivo I, Hankinson SE, and Missmer SA. Reproductive characteristics and risk of uterine leiomyomata. *Fertil Steril*. 2010;94(7):2703-7.
15. Baird DD, Dunson DB, Hill MC, Cousins D, and Schectman JM. High cumulative incidence of uterine leiomyoma in black and white women: ultrasound evidence. *American journal of obstetrics and gynecology*. 2003;188(1):100-7.

16. Kjerulff KH, Langenberg P, Seidman JD, Stolley PD, and Guzinski GM. Uterine leiomyomas. Racial differences in severity, symptoms and age at diagnosis. *J Reprod Med.* 1996;41(7):483-90.
17. Huyck KL, Panhuysen CI, Cuenco KT, Zhang J, Goldhammer H, Jones ES, Somasundaram P, Lynch AM, Harlow BL, Lee H, et al. The impact of race as a risk factor for symptom severity and age at diagnosis of uterine leiomyomata among affected sisters. *American journal of obstetrics and gynecology.* 2008;198(2):168 e1-9.
18. Taioli E, Garte SJ, Trachman J, Garbers S, Sepkovic DW, Osborne MP, Mehl S, and Bradlow HL. Ethnic differences in estrogen metabolism in healthy women. *J Natl Cancer Inst.* 1996;88(9):617.
19. Vikhlyaeva EM, Khodzhaeva ZS, and Fantschenko ND. Familial predisposition to uterine leiomyomas. *Int J Gynaecol Obstet.* 1995;51(2):127-31.
20. Shikora SA, Niloff JM, Bistrrian BR, Forse RA, and Blackburn GL. Relationship between obesity and uterine leiomyomata. *Nutrition.* 1991;7(4):251-5.
21. Wise LA, Palmer JR, Harlow BL, Spiegelman D, Stewart EA, Adams-Campbell LL, and Rosenberg L. Risk of uterine leiomyomata in relation to tobacco, alcohol and caffeine consumption in the Black Women's Health Study. *Hum Reprod.* 2004;19(8):1746-54.
22. Wise LA, Palmer JR, Spiegelman D, Harlow BL, Stewart EA, Adams-Campbell LL, and Rosenberg L. Influence of body size and body fat distribution on risk of uterine leiomyomata in U.S. black women. *Epidemiology.* 2005;16(3):346-54.
23. Summers WE, Watson RL, Wooldridge WH, and Langford HG. Hypertension, obesity, and fibromyomata uteri, as a syndrome. *Arch Intern Med.* 1971;128(5):750-4.
24. Faerstein E, Szklo M, and Rosenshein N. Risk factors for uterine leiomyoma: a practice-based case-control study. I. African-American heritage, reproductive history, body size, and smoking. *Am J Epidemiol.* 2001;153(1):1-10.
25. Chiaffarino F, Parazzini F, La Vecchia C, Chatenoud L, Di Cintio E, and Marsico S. Diet and uterine myomas. *Obstetrics and gynecology.* 1999;94(3):395-8.
26. Houston KD, Hunter DS, Hodges LC, and Walker CL. Uterine leiomyomas: mechanisms of tumorigenesis. *Toxicol Pathol.* 2001;29(1):100-4.
27. Saxena SP, Khare C, Farooq A, Murugesan K, Buckshee K, and Chandra J. DDT and its metabolites in leiomyomatous and normal human uterine tissue. *Arch Toxicol.* 1987;59(6):453-5.
28. Newbold RR, Moore AB, and Dixon D. Characterization of uterine leiomyomas in CD-1 mice following developmental exposure to diethylstilbestrol (DES). *Toxicol Pathol.* 2002;30(5):611-6.
29. Baird DD, and Newbold R. Prenatal diethylstilbestrol (DES) exposure is associated with uterine leiomyoma development. *Reprod Toxicol.* 2005;20(1):81-4.
30. Parker WH. Etiology, symptomatology, and diagnosis of uterine myomas. *Fertil Steril.* 2007;87(4):725-36.
31. Dueholm M, Lundorf E, Hansen ES, Ledertoug S, and Olesen F. Accuracy of magnetic resonance imaging and transvaginal ultrasonography in the diagnosis, mapping, and measurement of uterine myomas. *American journal of obstetrics and gynecology.* 2002;186(3):409-15.
32. Khan AT, Shehmar M, and Gupta JK. Uterine fibroids: current perspectives. *Int J Womens Health.* 2014;6(95-114).

33. Dueholm M, Lundorf E, Hansen ES, Ledertoug S, and Olesen F. Evaluation of the uterine cavity with magnetic resonance imaging, transvaginal sonography, hysterosonographic examination, and diagnostic hysteroscopy. *Fertil Steril*. 2001;76(2):350-7.
34. Somigliana E, Vercellini P, Daguati R, Pasin R, De Giorgi O, and Crosignani PG. Fibroids and female reproduction: a critical analysis of the evidence. *Hum Reprod Update*. 2007;13(5):465-76.
35. Murphy AA, Kettel LM, Morales AJ, Roberts VJ, and Yen SS. Regression of uterine leiomyomata in response to the antiprogestosterone RU 486. *J Clin Endocrinol Metab*. 1993;76(2):513-7.
36. Donnez J, Tatarchuk TF, Bouchard P, Puscasiu L, Zakharenko NF, Ivanova T, Ugocsai G, Mara M, Jilla MP, Bestel E, et al. Ulipristal acetate versus placebo for fibroid treatment before surgery. *N Engl J Med*. 2012;366(5):409-20.
37. Banu NS, Gaze DC, Bruce H, Collinson PO, Belli AM, and Manyonda IT. Markers of muscle ischemia, necrosis, and inflammation following uterine artery embolization in the treatment of symptomatic uterine fibroids. *American journal of obstetrics and gynecology*. 2007;196(3):213 e1-5.
38. van der Kooij SM, Ankum WM, and Hehenkamp WJ. Review of nonsurgical/minimally invasive treatments for uterine fibroids. *Curr Opin Obstet Gynecol*. 2012;24(6):368-75.
39. Salama SS, and Kilic GS. Uterine fibroids and current clinical challenges. *J Turk Ger Gynecol Assoc*. 2013;14(1):40-5.
40. Oliva E. Cellular mesenchymal tumors of the uterus: a review emphasizing recent observations. *Int J Gynecol Pathol*. 2014;33(4):374-84.
41. Hashimoto K, Azuma C, Kamiura S, Kimura T, Nobunaga T, Kanai T, Sawada M, Noguchi S, and Saji F. Clonal determination of uterine leiomyomas by analyzing differential inactivation of the X-chromosome-linked phosphoglycerokinase gene. *Gynecol Obstet Invest*. 1995;40(3):204-8.
42. Linder D, and Gartler SM. Glucose-6-phosphate dehydrogenase mosaicism: utilization as a cell marker in the study of leiomyomas. *Science*. 1965;150(3692):67-9.
43. Mashal RD, Fejzo ML, Friedman AJ, Mitchner N, Nowak RA, Rein MS, Morton CC, and Sklar J. Analysis of androgen receptor DNA reveals the independent clonal origins of uterine leiomyomata and the secondary nature of cytogenetic aberrations in the development of leiomyomata. *Genes, chromosomes & cancer*. 1994;11(1):1-6.
44. Townsend DE, Sparkes RS, Baluda MC, and McClelland G. Unicellular histogenesis of uterine leiomyomas as determined by electrophoresis by glucose-6-phosphate dehydrogenase. *American journal of obstetrics and gynecology*. 1970;107(8):1168-73.
45. Bulun SE. Uterine Fibroids. *New Engl J Med*. 2013;369(14):1344-55.
46. Rosati P, Exacoustos C, and Mancuso S. Longitudinal evaluation of uterine myoma growth during pregnancy. A sonographic study. *J Ultrasound Med*. 1992;11(10):511-5.
47. Rein MS. Advances in uterine leiomyoma research: the progesterone hypothesis. *Environmental health perspectives*. 2000;108 Suppl 5(791-3).
48. Richards PA, and Tiltman AJ. Anatomical variation of the oestrogen receptor in the non-neoplastic myometrium of fibromyomatous uteri. *Virchows Arch*. 1996;428(6):347-51.
49. Pollow K, Sinnecker G, Boquoi E, and Pollow B. In vitro conversion of estradiol-17beta into estrone in normal human myometrium and leiomyoma. *J Clin Chem Clin Biochem*. 1978;16(9):493-502.

50. Shozu M, Murakami K, and Inoue M. Aromatase and leiomyoma of the uterus. *Semin Reprod Med.* 2004;22(1):51-60.
51. Otubu JA, Buttram VC, Besch NF, and Besch PK. Unconjugated steroids in leiomyomas and tumor-bearing myometrium. *American journal of obstetrics and gynecology.* 1982;143(2):130-3.
52. Folkerd EJ, Newton CJ, Davidson K, Anderson MC, and James VH. Aromatase activity in uterine leiomyomata. *J Steroid Biochem.* 1984;20(5):1195-200.
53. Ishikawa H, Ishi K, Serna VA, Kakazu R, Bulun SE, and Kurita T. Progesterone is essential for maintenance and growth of uterine leiomyoma. *Endocrinology.* 2010;151(6):2433-42.
54. Kim JJ, and Sefton EC. The role of progesterone signaling in the pathogenesis of uterine leiomyoma. *Molecular and cellular endocrinology.* 2012;358(2):223-31.
55. Yin P, Lin Z, Cheng YH, Marsh EE, Utsunomiya H, Ishikawa H, Xue Q, Reierstad S, Innes J, Thung S, et al. Progesterone receptor regulates Bcl-2 gene expression through direct binding to its promoter region in uterine leiomyoma cells. *J Clin Endocrinol Metab.* 2007;92(11):4459-66.
56. Hyder SM, and Stancel GM. Regulation of angiogenic growth factors in the female reproductive tract by estrogens and progestins. *Molecular endocrinology.* 1999;13(6):806-11.
57. Lyons RM, and Moses HL. Transforming growth factors and the regulation of cell proliferation. *Eur J Biochem.* 1990;187(3):467-73.
58. Stewart EA, and Nowak RA. Leiomyoma-related bleeding: a classic hypothesis updated for the molecular era. *Hum Reprod Update.* 1996;2(4):295-306.
59. Ono M, Maruyama T, Masuda H, Kajitani T, Nagashima T, Arase T, Ito M, Ohta K, Uchida H, Asada H, et al. Side population in human uterine myometrium displays phenotypic and functional characteristics of myometrial stem cells. *Proc Natl Acad Sci U S A.* 2007;104(47):18700-5.
60. Szotek PP, Chang HL, Zhang L, Preffer F, Dombkowski D, Donahoe PK, and Teixeira J. Adult mouse myometrial label-retaining cells divide in response to gonadotropin stimulation. *Stem Cells.* 2007;25(5):1317-25.
61. Ono M, Qiang W, Serna VA, Yin P, Coon JSt, Navarro A, Monsivais D, Kakinuma T, Dyson M, Druschitz S, et al. Role of stem cells in human uterine leiomyoma growth. *PLoS one.* 2012;7(5):e36935.
62. Mas A, Cervello I, Gil-Sanchis C, Faus A, Ferro J, Pellicer A, and Simon C. Identification and characterization of the human leiomyoma side population as putative tumor-initiating cells. *Fertil Steril.* 2012;98(3):741-51 e6.
63. Stewart EA, and Nowak RA. New concepts in the treatment of uterine leiomyomas. *Obstetrics and gynecology.* 1998;92(4 Pt 1):624-7.
64. Zhou S, Yi T, Shen K, Zhang B, Huang F, and Zhao X. Hypoxia: the driving force of uterine myometrial stem cells differentiation into leiomyoma cells. *Med Hypotheses.* 2011;77(6):985-6.
65. Rein MS, Friedman AJ, Barbieri RL, Pavelka K, Fletcher JA, and Morton CC. Cytogenetic abnormalities in uterine leiomyomata. *Obstetrics and gynecology.* 1991;77(6):923-6.
66. Nibert M, and Heim S. Uterine leiomyoma cytogenetics. *Genes, chromosomes & cancer.* 1990;2(1):3-13.

67. Brosens I, Deprest J, Dal Cin P, and Van den Berghe H. Clinical significance of cytogenetic abnormalities in uterine myomas. *Fertil Steril*. 1998;69(2):232-5.
68. Rein MS, Powell WL, Walters FC, Weremowicz S, Cantor RM, Barbieri RL, and Morton CC. Cytogenetic abnormalities in uterine myomas are associated with myoma size. *Mol Hum Reprod*. 1998;4(1):83-6.
69. Hennig Y, Deichert U, Bonk U, Thode B, Bartnitzke S, and Bullerdiek J. Chromosomal translocations affecting 12q14-15 but not deletions of the long arm of chromosome 7 associated with a growth advantage of uterine smooth muscle cells. *Mol Hum Reprod*. 1999;5(12):1150-4.
70. Meloni AM, Surti U, Contento AM, Davare J, and Sandberg AA. Uterine leiomyomas: cytogenetic and histologic profile. *Obstetrics and gynecology*. 1992;80(2):209-17.
71. Kazmierczak B, Hennig Y, Wanschura S, Rogalla P, Bartnitzke S, Van de Ven W, and Bullerdiek J. Description of a novel fusion transcript between HMGI-C, a gene encoding for a member of the high mobility group proteins, and the mitochondrial aldehyde dehydrogenase gene. *Cancer Res*. 1995;55(24):6038-9.
72. Kurose K, Mine N, Doi D, Ota Y, Yoneyama K, Konishi H, Araki T, and Emi M. Novel gene fusion of COX6C at 8q22-23 to HMGIC at 12q15 in a uterine leiomyoma. *Genes, chromosomes & cancer*. 2000;27(3):303-7.
73. Markowski DN, Nimzyk R, Belge G, Loning T, Helmke BM, and Bullerdiek J. Molecular topography of the MED12-deleted region in smooth muscle tumors: a possible link between non-B DNA structures and hypermutability. *Mol Cytogenet*. 2013;6(1):23.
74. Mine N, Kurose K, Konishi H, Araki T, Nagai H, and Emi M. Fusion of a sequence from HEI10 (14q11) to the HMGIC gene at 12q15 in a uterine leiomyoma. *Jpn J Cancer Res*. 2001;92(2):135-9.
75. Quade BJ, Weremowicz S, Neskey DM, Vanni R, Ladd C, Dal Cin P, and Morton CC. Fusion transcripts involving HMGA2 are not a common molecular mechanism in uterine leiomyomata with rearrangements in 12q15. *Cancer Res*. 2003;63(6):1351-8.
76. Velagaleti GV, Tonk VS, Hakim NM, Wang X, Zhang H, Erickson-Johnson MR, Medeiros F, and Oliveira AM. Fusion of HMGA2 to COG5 in uterine leiomyoma. *Cancer genetics and cytogenetics*. 2010;202(1):11-6.
77. Wanschura S, Dal Cin P, Kazmierczak B, Bartnitzke S, Van den Berghe H, and Bullerdiek J. Hidden paracentric inversions of chromosome arm 12q affecting the HMGIC gene. *Genes, chromosomes & cancer*. 1997;18(4):322-3.
78. Sandberg AA. Updates on the cytogenetics and molecular genetics of bone and soft tissue tumors: leiomyoma. *Cancer genetics and cytogenetics*. 2005;158(1):1-26.
79. Ashar HR, Fejzo MS, Tkachenko A, Zhou X, Fletcher JA, Weremowicz S, Morton CC, and Chada K. Disruption of the architectural factor HMGI-C: DNA-binding AT hook motifs fused in lipomas to distinct transcriptional regulatory domains. *Cell*. 1995;82(1):57-65.
80. Schoenmakers EF, Wanschura S, Mols R, Bullerdiek J, Van den Berghe H, and Van de Ven WJ. Recurrent rearrangements in the high mobility group protein gene, HMGI-C, in benign mesenchymal tumours. *Nature genetics*. 1995;10(4):436-44.
81. Fusco A, and Fedele M. Roles of HMGA proteins in cancer. *Nat Rev Cancer*. 2007;7(12):899-910.
82. Grosschedl R, Giese K, and Pagel J. HMG domain proteins: architectural elements in the assembly of nucleoprotein structures. *Trends Genet*. 1994;10(3):94-100.

83. Reeves R. Molecular biology of HMGA proteins: hubs of nuclear function. *Gene*. 2001;277(1-2):63-81.
84. Gattas GJ, Quade BJ, Nowak RA, and Morton CC. HMGIC expression in human adult and fetal tissues and in uterine leiomyomata. *Genes, chromosomes & cancer*. 1999;25(4):316-22.
85. Gross KL, Neskey DM, Manchanda N, Weremowicz S, Kleinman MS, Nowak RA, Ligon AH, Rogalla P, Drechsler K, Bullerdiek J, et al. HMGA2 expression in uterine leiomyomata and myometrium: quantitative analysis and tissue culture studies. *Genes, chromosomes & cancer*. 2003;38(1):68-79.
86. Rogalla P, Drechsler K, Frey G, Hennig Y, Helmke B, Bonk U, and Bullerdiek J. HMGI-C expression patterns in human tissues. Implications for the genesis of frequent mesenchymal tumors. *The American journal of pathology*. 1996;149(3):775-9.
87. Schoenberg Fejzo M, Ashar HR, Krauter KS, Powell WL, Rein MS, Weremowicz S, Yoon SJ, Kucherlapati RS, Chada K, and Morton CC. Translocation breakpoints upstream of the HMGIC gene in uterine leiomyomata suggest dysregulation of this gene by a mechanism different from that in lipomas. *Genes, chromosomes & cancer*. 1996;17(1):1-6.
88. Klemke M, Meyer A, Hashemi Nezhad M, Belge G, Bartnitzke S, and Bullerdiek J. Loss of let-7 binding sites resulting from truncations of the 3' untranslated region of HMGA2 mRNA in uterine leiomyomas. *Cancer genetics and cytogenetics*. 2010;196(2):119-23.
89. Mayr C, Hemann MT, and Bartel DP. Disrupting the pairing between let-7 and Hmga2 enhances oncogenic transformation. *Science*. 2007;315(5818):1576-9.
90. Peng Y, Laser J, Shi G, Mittal K, Melamed J, Lee P, and Wei JJ. Antiproliferative effects by Let-7 repression of high-mobility group A2 in uterine leiomyoma. *Mol Cancer Res*. 2008;6(4):663-73.
91. Mehine M, Kaasinen E, Makinen N, Katainen R, Kampjarvi K, Pitkanen E, Heinonen HR, Butzow R, Kilpivaara O, Kuosmanen A, et al. Characterization of Uterine Leiomyomas by Whole-Genome Sequencing. *New Engl J Med*. 2013;369(1):43-53.
92. Wang T, Zhang X, Obijuru L, Laser J, Aris V, Lee P, Mittal K, Soteropoulos P, and Wei JJ. A micro-RNA signature associated with race, tumor size, and target gene activity in human uterine leiomyomas. *Genes, chromosomes & cancer*. 2007;46(4):336-47.
93. Heim S, Nilbert M, Vanni R, Floderus UM, Mandahl N, Liedgren S, Lecca U, and Mitelman F. A specific translocation, t(12;14)(q14-15;q23-24), characterizes a subgroup of uterine leiomyomas. *Cancer genetics and cytogenetics*. 1988;32(1):13-7.
94. Turc-Carel C, Dal Cin P, Boghosian L, Terk-Zakarian J, and Sandberg AA. Consistent breakpoints in region 14q22-q24 in uterine leiomyoma. *Cancer genetics and cytogenetics*. 1988;32(1):25-31.
95. Ingraham SE, Lynch RA, Kathiresan S, Buckler AJ, and Menon AG. hREC2, a RAD51-like gene, is disrupted by t(12;14)(q15;q24.1) in a uterine leiomyoma. *Cancer genetics and cytogenetics*. 1999;115(1):56-61.
96. Schoenmakers EF, Huysmans C, and Van de Ven WJ. Allelic knockout of novel splice variants of human recombination repair gene RAD51B in t(12;14) uterine leiomyomas. *Cancer Res*. 1999;59(1):19-23.
97. Thacker J. The RAD51 gene family, genetic instability and cancer. *Cancer Lett*. 2005;219(2):125-35.

98. Takahashi T, Nagai N, Oda H, Ohama K, Kamada N, and Miyagawa K. Evidence for RAD51L1/HMGIC fusion in the pathogenesis of uterine leiomyoma. *Genes, chromosomes & cancer*. 2001;30(2):196-201.
99. Klemke M, Meyer A, Nezhad MH, Bartnitzke S, Drieschner N, Frantzen C, Schmidt EH, Belge G, and Bullerdiek J. Overexpression of HMGA2 in uterine leiomyomas points to its general role for the pathogenesis of the disease. *Genes, chromosomes & cancer*. 2009;48(2):171-8.
100. Saito E, Okamoto A, Saito M, Shinozaki H, Takakura S, Yanaihara N, Ochiai K, and Tanaka T. Genes associated with the genesis of leiomyoma of the uterus in a commonly deleted chromosomal region at 7q22. *Oncol Rep*. 2005;13(3):469-72.
101. Sell SM, Altungoz O, Prowse AA, Meloni AM, Surti U, and Sandberg AA. Molecular analysis of chromosome 7q21.3 in uterine leiomyoma: analysis using markers with linkage to insulin resistance. *Cancer genetics and cytogenetics*. 1998;100(2):165-8.
102. van der Heijden O, Chiu HC, Park TC, Takahashi H, LiVolsi VA, Risinger JI, Barrett JC, Berchuck A, Evans AC, Behbakht K, et al. Allelotype analysis of uterine leiomyoma: localization of a potential tumor suppressor gene to a 4-cM region of chromosome 7q. *Mol Carcinog*. 1998;23(4):243-7.
103. Vanharanta S, Wortham NC, Laiho P, Sjoberg J, Aittomaki K, Arola J, Tomlinson IP, Karhu A, Arango D, and Aaltonen LA. 7q deletion mapping and expression profiling in uterine fibroids. *Oncogene*. 2005;24(43):6545-54.
104. Zeng WR, Scherer SW, Koutsilieris M, Huizenga JJ, Filteau F, Tsui LC, and Nepveu A. Loss of heterozygosity and reduced expression of the CUTL1 gene in uterine leiomyomas. *Oncogene*. 1997;14(19):2355-65.
105. Hulea L, and Nepveu A. CUX1 transcription factors: from biochemical activities and cell-based assays to mouse models and human diseases. *Gene*. 2012;497(1):18-26.
106. Vadnais C, Davoudi S, Afshin M, Harada R, Dudley R, Clermont PL, Drobetsky E, and Nepveu A. CUX1 transcription factor is required for optimal ATM/ATR-mediated responses to DNA damage. *Nucleic acids research*. 2012;40(10):4483-95.
107. Mc Nerney ME, Brown CD, Wang X, Bartom ET, Karmakar S, Bandlamudi C, Yu S, Ko J, Sandall BP, Stricker T, et al. CUX1 is a haploinsufficient tumor suppressor gene on chromosome 7 frequently inactivated in acute myeloid leukemia. *Blood*. 2013;121(6):975-83.
108. Wong CC, Martincorena I, Rust AG, Rashid M, Alifrangis C, Alexandrov LB, Tiffen JC, Kober C, Chronic Myeloid Disorders Working Group of the International Cancer Genome C, Green AR, et al. Inactivating CUX1 mutations promote tumorigenesis. *Nature genetics*. 2014;46(1):33-8.
109. Ishiai M, Dean FB, Okumura K, Abe M, Moon KY, Amin AA, Kagotani K, Taguchi H, Murakami Y, Hanaoka F, et al. Isolation of human and fission yeast homologues of the budding yeast origin recognition complex subunit ORC5: human homologue (ORC5L) maps to 7q22. *Genomics*. 1997;46(2):294-8.
110. Ligon AH, Scott IC, Takahara K, Greenspan DS, and Morton CC. PCOLCE deletion and expression analyses in uterine leiomyomata. *Cancer genetics and cytogenetics*. 2002;137(2):133-7.
111. Schoenmakers EF, Bunt J, Hermers L, Schepens M, Merckx G, Janssen B, Kersten M, Huys E, Pauwels P, Debiec-Rychter M, et al. Identification of CUX1 as the recurrent

- chromosomal band 7q22 target gene in human uterine leiomyoma. *Genes, chromosomes & cancer*. 2013;52(1):11-23.
112. Sait SN, Dal Cin P, Ovanessoff S, and Sandberg AA. A uterine leiomyoma showing both t(12;14) and del(7) abnormalities. *Cancer genetics and cytogenetics*. 1989;37(2):157-61.
  113. Xing YP, Powell WL, and Morton CC. The del(7q) subgroup in uterine leiomyomata: genetic and biologic characteristics. Further evidence for the secondary nature of cytogenetic abnormalities in the pathobiology of uterine leiomyomata. *Cancer genetics and cytogenetics*. 1997;98(1):69-74.
  114. Nilbert M, Heim S, Mandahl N, Floderus UM, Willen H, and Mitelman F. Different karyotypic abnormalities, t(1;6) and del(7), in two uterine leiomyomas from the same patient. *Cancer genetics and cytogenetics*. 1989;42(1):51-3.
  115. Kiechle-Schwarz M, Sreekantaiah C, Berger CS, Pedron S, Medchill MT, Surti U, and Sandberg AA. Nonrandom cytogenetic changes in leiomyomas of the female genitourinary tract. A report of 35 cases. *Cancer genetics and cytogenetics*. 1991;53(1):125-36.
  116. Ozisik YY, Meloni AM, Altungoz O, Surti U, and Sandberg AA. Translocation (6;10)(p21;q22) in uterine leiomyomas. *Cancer genetics and cytogenetics*. 1995;79(2):136-8.
  117. Sornberger KS, Weremowicz S, Williams AJ, Quade BJ, Ligon AH, Pedoutour F, Vanni R, and Morton CC. Expression of HMGIY in three uterine leiomyomata with complex rearrangements of chromosome 6. *Cancer genetics and cytogenetics*. 1999;114(1):9-16.
  118. Kazmierczak B, Wanschura S, Rommel B, Bartnitzke S, and Bullerdiek J. Ten pulmonary chondroid hamartomas with chromosome 6p21 breakpoints within the HMGI(Y) gene or its immediate surroundings. *J Natl Cancer Inst*. 1996;88(17):1234-6.
  119. Williams AJ, Powell WL, Collins T, and Morton CC. HMGI(Y) expression in human uterine leiomyomata. Involvement of another high-mobility group architectural factor in a benign neoplasm. *The American journal of pathology*. 1997;150(3):911-8.
  120. Dal Cin P, Wanschura S, Christiaens MR, Van den Berghe I, Moerman P, Polito P, Kazmierczak B, Bullerdiek J, and Van den Berghe H. Hamartoma of the breast with involvement of 6p21 and rearrangement of HMGIY. *Genes, chromosomes & cancer*. 1997;20(1):90-2.
  121. Xiao S, Lux ML, Reeves R, Hudson TJ, and Fletcher JA. HMGI(Y) activation by chromosome 6p21 rearrangements in multilineage mesenchymal cells from pulmonary hamartoma. *The American journal of pathology*. 1997;150(3):901-10.
  122. Cleynen I, and Van de Ven WJ. The HMGA proteins: a myriad of functions (Review). *Int J Oncol*. 2008;32(2):289-305.
  123. Nilbert M, Heim S, Mandahl N, Floderus UM, Willen H, and Mitelman F. Trisomy 12 in uterine leiomyomas. A new cytogenetic subgroup. *Cancer genetics and cytogenetics*. 1990;45(1):63-6.
  124. Moore SD, Herrick SR, Ince TA, Kleinman MS, Dal Cin P, Morton CC, and Quade BJ. Uterine leiomyomata with t(10;17) disrupt the histone acetyltransferase MORF. *Cancer Res*. 2004;64(16):5570-7.
  125. Ligon AH, and Morton CC. Genetics of uterine leiomyomata. *Genes, chromosomes & cancer*. 2000;28(3):235-45.
  126. Morey C, and Avner P. The demoiselle of X-inactivation: 50 years old and as trendy and mesmerising as ever. *PLoS genetics*. 2011;7(7):e1002212.

127. Zhang P, Zhang C, Hao J, Sung CJ, Quddus MR, Steinhoff MM, and Lawrence WD. Use of X-chromosome inactivation pattern to determine the clonal origins of uterine leiomyoma and leiomyosarcoma. *Hum Pathol.* 2006;37(10):1350-6.
128. Bowden W, Skorupski J, Kovanci E, and Rajkovic A. Detection of novel copy number variants in uterine leiomyomas using high-resolution SNP arrays. *Mol Hum Reprod.* 2009;15(9):563-8.
129. Levy B, Mukherjee T, and Hirschhorn K. Molecular cytogenetic analysis of uterine leiomyoma and leiomyosarcoma by comparative genomic hybridization. *Cancer genetics and cytogenetics.* 2000;121(1):1-8.
130. Meadows KL, Andrews DM, Xu Z, Carswell GK, Laughlin SK, Baird DD, and Taylor JA. Genome-wide analysis of loss of heterozygosity and copy number amplification in uterine leiomyomas using the 100K single nucleotide polymorphism array. *Exp Mol Pathol.* 2011;91(1):434-9.
131. Packenham JP, du Manoir S, Schrock E, Risinger JI, Dixon D, Denz DN, Evans JA, Berchuck A, Barrett JC, Devereux TR, et al. Analysis of genetic alterations in uterine leiomyomas and leiomyosarcomas by comparative genomic hybridization. *Mol Carcinog.* 1997;19(4):273-9.
132. Launonen V, Vierimaa O, Kiuru M, Isola J, Roth S, Pukkala E, Sistonen P, Herva R, and Aaltonen LA. Inherited susceptibility to uterine leiomyomas and renal cell cancer. *Proc Natl Acad Sci U S A.* 2001;98(6):3387-92.
133. Lehtonen HJ. Hereditary leiomyomatosis and renal cell cancer: update on clinical and molecular characteristics. *Fam Cancer.* 2011;10(2):397-411.
134. Smit DL, Mensenkamp AR, Badeloe S, Breuning MH, Simon ME, van Spaendonck KY, Aalfs CM, Post JG, Shanley S, Krapels IP, et al. Hereditary leiomyomatosis and renal cell cancer in families referred for fumarate hydratase germline mutation analysis. *Clin Genet.* 2011;79(1):49-59.
135. Csatlos E, Rigo J, Laky M, Brubel R, and Joo GJ. The role of the alcohol dehydrogenase-1 (ADH1) gene in the pathomechanism of uterine leiomyoma. *Eur J Obstet Gynecol Reprod Biol.* 2013;170(2):492-6.
136. Ishikawa H, Shozu M, Okada M, Inukai M, Zhang B, Kato K, Kasai T, and Inoue M. Early growth response gene-1 plays a pivotal role in down-regulation of a cohort of genes in uterine leiomyoma. *J Mol Endocrinol.* 2007;39(5):333-41.
137. Tomlinson IP, Alam NA, Rowan AJ, Barclay E, Jaeger EE, Kelsell D, Leigh I, Gorman P, Lamlum H, Rahman S, et al. Germline mutations in FH predispose to dominantly inherited uterine fibroids, skin leiomyomata and papillary renal cell cancer. *Nature genetics.* 2002;30(4):406-10.
138. Bayley JP, Launonen V, and Tomlinson IP. The FH mutation database: an online database of fumarate hydratase mutations involved in the MCUL (HLRCC) tumor syndrome and congenital fumarase deficiency. *BMC Med Genet.* 2008;9(20).
139. Kiuru M, Launonen V, Hietala M, Aittomaki K, Vierimaa O, Salovaara R, Arola J, Pukkala E, Sistonen P, Herva R, et al. Familial cutaneous leiomyomatosis is a two-hit condition associated with renal cell cancer of characteristic histopathology. *The American journal of pathology.* 2001;159(3):825-9.
140. Pollard PJ, Briere JJ, Alam NA, Barwell J, Barclay E, Wortham NC, Hunt T, Mitchell M, Olpin S, Moat SJ, et al. Accumulation of Krebs cycle intermediates and over-expression

- of HIF1alpha in tumours which result from germline FH and SDH mutations. *Hum Mol Genet.* 2005;14(15):2231-9.
141. Pollard P, Wortham N, Barclay E, Alam A, Elia G, Manek S, Poulson R, and Tomlinson I. Evidence of increased microvessel density and activation of the hypoxia pathway in tumours from the hereditary leiomyomatosis and renal cell cancer syndrome. *J Pathol.* 2005;205(1):41-9.
  142. Isaacs JS, Jung YJ, Mole DR, Lee S, Torres-Cabala C, Chung YL, Merino M, Trepel J, Zbar B, Toro J, et al. HIF overexpression correlates with biallelic loss of fumarate hydratase in renal cancer: novel role of fumarate in regulation of HIF stability. *Cancer Cell.* 2005;8(2):143-53.
  143. Kiuru M, Lehtonen R, Arola J, Salovaara R, Jarvinen H, Aittomaki K, Sjoberg J, Visakorpi T, Knuutila S, Isola J, et al. Few FH mutations in sporadic counterparts of tumor types observed in hereditary leiomyomatosis and renal cell cancer families. *Cancer Res.* 2002;62(16):4554-7.
  144. Lehtonen R, Kiuru M, Vanharanta S, Sjoberg J, Aaltonen LM, Aittomaki K, Arola J, Butzow R, Eng C, Husgafvel-Pursiainen K, et al. Biallelic inactivation of fumarate hydratase (FH) occurs in nonsyndromic uterine leiomyomas but is rare in other tumors. *The American journal of pathology.* 2004;164(1):17-22.
  145. Vaidya S, Shaik NA, Latha M, Chava S, Mohiuddin K, Yalla A, Rao KP, Kodati VL, and Hasan Q. No evidence for the role of somatic mutations and promoter hypermethylation of FH gene in the tumorigenesis of nonsyndromic uterine leiomyomas. *Tumour Biol.* 2012;33(5):1411-8.
  146. van Slechtenhorst M, de Hoogt R, Hermans C, Nellist M, Janssen B, Verhoef S, Lindhout D, van den Ouweland A, Halley D, Young J, et al. Identification of the tuberous sclerosis gene TSC1 on chromosome 9q34. *Science.* 1997;277(5327):805-8.
  147. Everitt JI, Wolf DC, Howe SR, Goldsworthy TL, and Walker C. Rodent model of reproductive tract leiomyomata. Clinical and pathological features. *The American journal of pathology.* 1995;146(6):1556-67.
  148. Walker CL, Hunter D, and Everitt JI. Uterine leiomyoma in the Eker rat: a unique model for important diseases of women. *Genes, chromosomes & cancer.* 2003;38(4):349-56.
  149. Lingaas F, Comstock KE, Kirkness EF, Sorensen A, Aarskaug T, Hitte C, Nickerson ML, Moe L, Schmidt LS, Thomas R, et al. A mutation in the canine BHD gene is associated with hereditary multifocal renal cystadenocarcinoma and nodular dermatofibrosis in the German Shepherd dog. *Hum Mol Genet.* 2003;12(23):3043-53.
  150. Liaw D, Marsh DJ, Li J, Dahia PL, Wang SI, Zheng Z, Bose S, Call KM, Tsou HC, Peacocke M, et al. Germline mutations of the PTEN gene in Cowden disease, an inherited breast and thyroid cancer syndrome. *Nature genetics.* 1997;16(1):64-7.
  151. Hobert JA, and Eng C. PTEN hamartoma tumor syndrome: an overview. *Genet Med.* 2009;11(10):687-94.
  152. Cha PC, Takahashi A, Hosono N, Low SK, Kamatani N, Kubo M, and Nakamura Y. A genome-wide association study identifies three loci associated with susceptibility to uterine fibroids. *Nature genetics.* 2011;43(5):447-50.
  153. Eggert SL, Huyck KL, Somasundaram P, Kavalla R, Stewart EA, Lu AT, Painter JN, Montgomery GW, Medland SE, Nyholt DR, et al. Genome-wide linkage and association analyses implicate FASN in predisposition to Uterine Leiomyomata. *Am J Hum Genet.* 2012;91(4):621-8.

154. Wise LA, Ruiz-Narvaez EA, Palmer JR, Cozier YC, Tandon A, Patterson N, Radin RG, Rosenberg L, and Reich D. African ancestry and genetic risk for uterine leiomyomata. *Am J Epidemiol.* 2012;176(12):1159-68.
155. Edwards TL, Hartmann KE, and Velez Edwards DR. Variants in BET1L and TNRC6B associate with increasing fibroid volume and fibroid type among European Americans. *Human genetics.* 2013;132(12):1361-9.
156. Liu H, Liu JY, Wu X, and Zhang JT. Biochemistry, molecular biology, and pharmacology of fatty acid synthase, an emerging therapeutic target and diagnosis/prognosis marker. *Int J Biochem Mol Biol.* 2010;1(1):69-89.
157. Pizer ES, Chrest FJ, DiGiuseppe JA, and Han WF. Pharmacological inhibitors of mammalian fatty acid synthase suppress DNA replication and induce apoptosis in tumor cell lines. *Cancer Res.* 1998;58(20):4611-5.
158. Pizer ES, Jackisch C, Wood FD, Pasternack GR, Davidson NE, and Kuhajda FP. Inhibition of fatty acid synthesis induces programmed cell death in human breast cancer cells. *Cancer Res.* 1996;56(12):2745-7.
159. Makinen N, Mehine M, Tolvanen J, Kaasinen E, Li Y, Lehtonen HJ, Gentile M, Yan J, Enge M, Taipale M, et al. MED12, the mediator complex subunit 12 gene, is mutated at high frequency in uterine leiomyomas. *Science.* 2011;334(6053):252-5.
160. Makinen N, Heinonen HR, Moore S, Tomlinson IPM, van der Spuy ZM, and Aaltonen LA. MED12 exon 2 mutations are common in uterine leiomyomas from South African patients. *Oncotarget.* 2011;2(12):966-9.
161. McGuire MM, Yatsenko A, Hoffner L, Jones M, Surti U, and Rajkovic A. Whole exome sequencing in a random sample of North American women with leiomyomas identifies MED12 mutations in majority of uterine leiomyomas. *PloS one.* 2012;7(3):e33251.
162. Je EM, Kim MR, Min KO, Yoo NJ, and Lee SH. Mutational analysis of MED12 exon 2 in uterine leiomyoma and other common tumors. *Int J Cancer.* 2012;131(6):E1044-E7.
163. Markowski DN, Bartnitzke S, Loning T, Drieschner N, Helmke BM, and Bullerdiek J. MED12 mutations in uterine fibroids-their relationship to cytogenetic subgroups. *Int J Cancer.* 2012;131(7):1528-36.
164. Perot G, Croce S, Ribeiro A, Lagarde P, Velasco V, Neuville A, Coindre JM, Stoeckle E, Floquet A, MacGrogan G, et al. MED12 alterations in both human benign and malignant uterine soft tissue tumors. *PloS one.* 2012;7(6):e40015.
165. Ravegnini G, Marino-Enriquez A, Slater J, Eilers G, Wang Y, Zhu M, Nucci MR, George S, Angelini S, Raut CP, et al. MED12 mutations in leiomyosarcoma and extrauterine leiomyoma. *Mod Pathol.* 2013;26(5):743-9.
166. Matsubara A, Sekine S, Yoshida M, Yoshida A, Taniguchi H, Kushima R, Tsuda H, and Kanai Y. Prevalence of MED12 mutations in uterine and extrauterine smooth muscle tumours. *Histopathology.* 2013;62(4):657-61.
167. Markowski DN, Huhle S, Nimzyk R, Stenman G, Loning T, and Bullerdiek J. MED12 mutations occurring in benign and malignant mammalian smooth muscle tumors. *Genes, chromosomes & cancer.* 2013;52(3):297-304.
168. Makinen N, Vahteristo P, Kampjarvi K, Arola J, Butzow R, and Aaltonen LA. MED12 exon 2 mutations in histopathological uterine leiomyoma variants. *Eur J Hum Genet.* 2013;21(11):1300-3.

169. de Graaff MA, Cleton-Jansen AM, Szuhai K, and Bovee JV. Mediator complex subunit 12 exon 2 mutation analysis in different subtypes of smooth muscle tumors confirms genetic heterogeneity. *Hum Pathol.* 2013;44(8):1597-604.
170. Rieker RJ, Agaimy A, Moskalev EA, Hebele S, Hein A, Mehlhorn G, Beckmann MW, Hartmann A, and Haller F. Mutation status of the mediator complex subunit 12 (MED12) in uterine leiomyomas and concurrent/metachronous multifocal peritoneal smooth muscle nodules (leiomyomatosis peritonealis disseminata). *Pathology.* 2013;45(4):388-92.
171. Schwetye KE, Pfeifer JD, and Duncavage EJ. MED12 exon 2 mutations in uterine and extrauterine smooth muscle tumors. *Hum Pathol.* 2014;45(1):65-70.
172. Bertsch E, Qiang W, Zhang Q, Espona-Fiedler M, Druschitz S, Liu Y, Mittal K, Kong B, Kurita T, and Wei JJ. MED12 and HMGA2 mutations: two independent genetic events in uterine leiomyoma and leiomyosarcoma. *Mod Pathol.* 2014;27(8):1144-53.
173. Heinonen HR, Sarvilinna NS, Sjoberg J, Kampjarvi K, Pitkanen E, Vahteristo P, Makinen N, and Aaltonen LA. MED12 mutation frequency in unselected sporadic uterine leiomyomas. *Fertil Steril.* 2014;102(4):1137-42.
174. Halder SK, Laknaur A, Miller J, Layman LC, Diamond M, and Al-Hendy A. Novel MED12 gene somatic mutations in women from the Southern United States with symptomatic uterine fibroids. *Mol Genet Genomics.* 2015;290(2):505-11.
175. Kampjarvi K, Park MJ, Mehine M, Kim NH, Clark AD, Butzow R, Bohling T, Bohm J, Mecklin JP, Jarvinen H, et al. Mutations in Exon 1 highlight the role of MED12 in uterine leiomyomas. *Hum Mutat.* 2014;35(9):1136-41.
176. Mäkinen N. Helsinki: University of Helsinki,; 2014:1 verkkojulkaisu (86 s.).
177. Garraway LA, and Lander ES. Lessons from the cancer genome. *Cell.* 2013;153(1):17-37.
178. Mehine M, Kaasinen E, and Aaltonen LA. Chromothripsis in uterine leiomyomas. *N Engl J Med.* 2013;369(22):2160-1.
179. Forment JV, Kaidi A, and Jackson SP. Chromothripsis and cancer: causes and consequences of chromosome shattering. *Nat Rev Cancer.* 2012;12(10):663-70.
180. Forment JV, Kaidi A, and Jackson SP. Chromothripsis and cancer: causes and consequences of chromosome shattering. *Nat Rev Cancer.* 2012;12(10):663-70.
181. Lee WY, Tzeng CC, and Chou CY. Uterine leiomyosarcomas coexistent with cellular and atypical leiomyomata in a young woman during the treatment with luteinizing hormone-releasing hormone agonist. *Gynecol Oncol.* 1994;52(1):74-9.
182. Mittal K, and Joutovsky A. Areas with benign morphologic and immunohistochemical features are associated with some uterine leiomyosarcomas. *Gynecol Oncol.* 2007;104(2):362-5.
183. Mittal KR, Chen F, Wei JJ, Rihvani K, Kurvathi R, Streck D, Dermody J, and Toruner GA. Molecular and immunohistochemical evidence for the origin of uterine leiomyosarcomas from associated leiomyoma and symplastic leiomyoma-like areas. *Mod Pathol.* 2009;22(10):1303-11.
184. Yanai H, Wani Y, Notohara K, Takada S, and Yoshino T. Uterine leiomyosarcoma arising in leiomyoma: clinicopathological study of four cases and literature review. *Pathol Int.* 2010;60(7):506-9.
185. Kampjarvi K, Kim NH, Keskitalo S, Clark AD, von Nandelstadh P, Turunen M, Heikkinen T, Park MJ, Makinen N, Kivinummi K, et al. Somatic MED12 mutations in

- prostate cancer and uterine leiomyomas promote tumorigenesis through distinct mechanisms. *Prostate*. 2015.
186. Lim WK, Ong CK, Tan J, Thike AA, Ng CC, Rajasegaran V, Myint SS, Nagarajan S, Nasir ND, McPherson JR, et al. Exome sequencing identifies highly recurrent MED12 somatic mutations in breast fibroadenoma. *Nature genetics*. 2014;46(8):877-80.
  187. Yoshida M, Sekine S, Ogawa R, Yoshida H, Maeshima A, Kanai Y, Kinoshita T, and Ochiai A. Frequent MED12 mutations in phyllodes tumours of the breast. *Br J Cancer*. 2015;112(10):1703-8.
  188. Piscuoglio S, Murray M, Fusco N, Marchio C, Loo FL, Martelotto LG, Schultheis AM, Akram M, Weigelt B, Brogi E, et al. MED12 somatic mutations in fibroadenomas and phyllodes tumours of the breast. *Histopathology*. 2015.
  189. Pfarr N, Kriegsmann M, Sinn P, Klauschen F, Endris V, Herpel E, Muckenhuber A, Jesinghaus M, Klosterhalfen B, Penzel R, et al. Distribution of MED12 mutations in fibroadenomas and phyllodes tumors of the breast--implications for tumor biology and pathological diagnosis. *Genes, chromosomes & cancer*. 2015;54(7):444-52.
  190. Mishima C, Kagara N, Tanei T, Naoi Y, Shimoda M, Shimomura A, Shimazu K, Kim SJ, and Noguchi S. Mutational analysis of MED12 in fibroadenomas and phyllodes tumors of the breast by means of targeted next-generation sequencing. *Breast Cancer Res Treat*. 2015;152(2):305-12.
  191. Shah SP, Roth A, Goya R, Oloumi A, Ha G, Zhao Y, Turashvili G, Ding J, Tse K, Haffari G, et al. The clonal and mutational evolution spectrum of primary triple-negative breast cancers. *Nature*. 2012;486(7403):395-9.
  192. Schuh A, Becq J, Humphray S, Alexa A, Burns A, Clifford R, Feller SM, Grocock R, Henderson S, Khrebtukova I, et al. Monitoring chronic lymphocytic leukemia progression by whole genome sequencing reveals heterogeneous clonal evolution patterns. *Blood*. 2012;120(20):4191-6.
  193. Barbieri CE, Baca SC, Lawrence MS, Demichelis F, Blattner M, Theurillat JP, White TA, Stojanov P, Van Allen E, Stransky N, et al. Exome sequencing identifies recurrent SPOP, FOXA1 and MED12 mutations in prostate cancer. *Nature genetics*. 2012;44(6):685-9.
  194. Assie G, Letouze E, Fassnacht M, Jouinot A, Luscap W, Barreau O, Omeiri H, Rodriguez S, Perlemoine K, Rene-Corail F, et al. Integrated genomic characterization of adrenocortical carcinoma. *Nature genetics*. 2014;46(6):607-12.
  195. Risheg H, Graham JM, Jr., Clark RD, Rogers RC, Opitz JM, Moeschler JB, Peiffer AP, May M, Joseph SM, Jones JR, et al. A recurrent mutation in MED12 leading to R961W causes Opitz-Kaveggia syndrome. *Nature genetics*. 2007;39(4):451-3.
  196. Rump P, Niessen RC, Verbruggen KT, Brouwer OF, de Raad M, and Hordijk R. A novel mutation in MED12 causes FG syndrome (Opitz-Kaveggia syndrome). *Clin Genet*. 2011;79(2):183-8.
  197. Schwartz CE, Tarpey PS, Lubs HA, Verloes A, May MM, Risheg H, Friez MJ, Futreal PA, Edkins S, Teague J, et al. The original Lujan syndrome family has a novel missense mutation (p.N1007S) in the MED12 gene. *J Med Genet*. 2007;44(7):472-7.
  198. Vulto-van Silfhout AT, de Vries BB, van Bon BW, Hoischen A, Ruitkamp-Versteeg M, Gilissen C, Gao F, van Zwam M, Harteveld CL, van Essen AJ, et al. Mutations in MED12 cause X-linked Ohdo syndrome. *Am J Hum Genet*. 2013;92(3):401-6.

199. Ding N, Zhou H, Esteve PO, Chin HG, Kim S, Xu X, Joseph SM, Friez MJ, Schwartz CE, Pradhan S, et al. Mediator links epigenetic silencing of neuronal gene expression with x-linked mental retardation. *Molecular cell*. 2008;31(3):347-59.
200. Kitano T, Schwarz C, Nickel B, and Paabo S. Gene diversity patterns at 10 X-chromosomal loci in humans and chimpanzees. *Mol Biol Evol*. 2003;20(8):1281-9.
201. Philibert RA, Winfield SL, Damschroder-Williams P, Tengstrom C, Martin BM, and Ginns EI. The genomic structure and developmental expression patterns of the human OPA-containing gene (HOPA). *Human genetics*. 1999;105(1-2):174-8.
202. Philibert RA, King BH, Winfield S, Cook EH, Lee YH, Stubblefield B, Damschroder-Williams P, Dea C, Palotie A, Tengstrom C, et al. Association of an X-chromosome dodecamer insertional variant allele with mental retardation. *Mol Psychiatry*. 1998;3(4):303-9.
203. Lariviere L, Seizl M, and Cramer P. A structural perspective on Mediator function. *Curr Opin Cell Biol*. 2012;24(3):305-13.
204. Borggreffe T, and Yue X. Interactions between subunits of the Mediator complex with gene-specific transcription factors. *Semin Cell Dev Biol*. 2011;22(7):759-68.
205. Conaway RC, and Conaway JW. Function and regulation of the Mediator complex. *Curr Opin Genet Dev*. 2011;21(2):225-30.
206. Samuelsen CO, Baraznenok V, Khorosjutina O, Spahr H, Kieselbach T, Holmberg S, and Gustafsson CM. TRAP230/ARC240 and TRAP240/ARC250 Mediator subunits are functionally conserved through evolution. *Proc Natl Acad Sci U S A*. 2003;100(11):6422-7.
207. Wang X, Sun Q, Ding Z, Ji J, Wang J, Kong X, Yang J, and Cai G. Redefining the modular organization of the core Mediator complex. *Cell Res*. 2014;24(7):796-808.
208. Knuesel MT, Meyer KD, Bernecky C, and Taatjes DJ. The human CDK8 subcomplex is a molecular switch that controls Mediator coactivator function. *Genes & development*. 2009;23(4):439-51.
209. Hengartner CJ, Myer VE, Liao SM, Wilson CJ, Koh SS, and Young RA. Temporal regulation of RNA polymerase II by Srb10 and Kin28 cyclin-dependent kinases. *Molecular cell*. 1998;2(1):43-53.
210. Borggreffe T, Davis R, Erdjument-Bromage H, Tempst P, and Kornberg RD. A complex of the Srb8, -9, -10, and -11 transcriptional regulatory proteins from yeast. *The Journal of biological chemistry*. 2002;277(46):44202-7.
211. Tsai KL, Tomomori-Sato C, Sato S, Conaway RC, Conaway JW, and Asturias FJ. Subunit architecture and functional modular rearrangements of the transcriptional mediator complex. *Cell*. 2014;157(6):1430-44.
212. Knuesel MT, Meyer KD, Donner AJ, Espinosa JM, and Taatjes DJ. The human CDK8 subcomplex is a histone kinase that requires Med12 for activity and can function independently of mediator. *Molecular and cellular biology*. 2009;29(3):650-61.
213. Belakavadi M, and Fondell JD. Role of the mediator complex in nuclear hormone receptor signaling. *Rev Physiol Biochem Pharmacol*. 2006;156(23-43).
214. Kim S, Xu X, Hecht A, and Boyer TG. Mediator is a transducer of Wnt/beta-catenin signaling. *The Journal of biological chemistry*. 2006;281(20):14066-75.
215. Zhou H, Kim S, Ishii S, and Boyer TG. Mediator modulates Gli3-dependent Sonic hedgehog signaling. *Molecular and cellular biology*. 2006;26(23):8667-82.

216. Zhou H, Spaeth JM, Kim NH, Xu X, Friez MJ, Schwartz CE, and Boyer TG. MED12 mutations link intellectual disability syndromes with dysregulated GLI3-dependent Sonic Hedgehog signaling. *Proc Natl Acad Sci U S A*. 2012;109(48):19763-8.
217. Zhou R, Bonneaud N, Yuan CX, de Santa Barbara P, Boizet B, Schomber T, Scherer G, Roeder RG, Poulat F, and Berta P. SOX9 interacts with a component of the human thyroid hormone receptor-associated protein complex. *Nucleic acids research*. 2002;30(14):3245-52.
218. Rau MJ, Fischer S, and Neumann CJ. Zebrafish Trap230/Med12 is required as a coactivator for Sox9-dependent neural crest, cartilage and ear development. *Developmental biology*. 2006;296(1):83-93.
219. Vogl MR, Reiprich S, Kuspert M, Kosian T, Schrewe H, Nave KA, and Wegner M. Sox10 cooperates with the mediator subunit 12 during terminal differentiation of myelinating glia. *J Neurosci*. 2013;33(15):6679-90.
220. Rocha PP, Scholze M, Bleiss W, and Schrewe H. Med12 is essential for early mouse development and for canonical Wnt and Wnt/PCP signaling. *Development*. 2010;137(16):2723-31.
221. Rocha PP, Bleiss W, and Schrewe H. Mosaic expression of Med12 in female mice leads to exencephaly, spina bifida, and craniorachischisis. *Birth defects research Part A, Clinical and molecular teratology*. 2010;88(8):626-32.
222. Sato S, Tomomori-Sato C, Parmely TJ, Florens L, Zybilov B, Swanson SK, Banks CA, Jin J, Cai Y, Washburn MP, et al. A set of consensus mammalian mediator subunits identified by multidimensional protein identification technology. *Molecular cell*. 2004;14(5):685-91.
223. Bourbon HM. Comparative genomics supports a deep evolutionary origin for the large, four-module transcriptional mediator complex. *Nucleic acids research*. 2008;36(12):3993-4008.
224. Prizant H, Sen A, Light A, Cho SN, DeMayo FJ, Lydon JP, and Hammes SR. Uterine-specific loss of Tsc2 leads to myometrial tumors in both the uterus and lungs. *Molecular endocrinology*. 2013;27(9):1403-14.
225. Tanwar PS, Lee HJ, Zhang L, Zukerberg LR, Taketo MM, Rueda BR, and Teixeira JM. Constitutive activation of Beta-catenin in uterine stroma and smooth muscle leads to the development of mesenchymal tumors in mice. *Biology of reproduction*. 2009;81(3):545-52.
226. Jamin SP, Arango NA, Mishina Y, Hanks MC, and Behringer RR. Requirement of Bmpr1a for Mullerian duct regression during male sexual development. *Nature genetics*. 2002;32(3):408-10.
227. Varghese BV, Koohestani F, McWilliams M, Colvin A, Gunewardena S, Kinsey WH, Nowak RA, Nothnick WB, and Chennathukuzhi VM. Loss of the repressor REST in uterine fibroids promotes aberrant G protein-coupled receptor 10 expression and activates mammalian target of rapamycin pathway. *P Natl Acad Sci USA*. 2013;110(6):2187-92.
228. Farquhar C, Brown PM, and Furness S. Cost effectiveness of pre-operative gonadotrophin releasing analogues for women with uterine fibroids undergoing hysterectomy or myomectomy. *BJOG*. 2002;109(11):1273-80.
229. Farquhar CM, and Steiner CA. Hysterectomy rates in the United States 1990-1997. *Obstetrics and gynecology*. 2002;99(2):229-34.

230. Cardozo ER, Clark AD, Banks NK, Henne MB, Stegmann BJ, and Segars JH. The estimated annual cost of uterine leiomyomata in the United States. *American journal of obstetrics and gynecology*. 2012;206(3):211 e1-9.
231. Nadine Markowski D, Tadayyon M, Bartnitzke S, Belge G, Maria Helmke B, and Bullerdiek J. Cell cultures in uterine leiomyomas: rapid disappearance of cells carrying MED12 mutations. *Genes, chromosomes & cancer*. 2014;53(4):317-23.
232. Lan ZJ, Xu X, and Cooney AJ. Differential oocyte-specific expression of Cre recombinase activity in GDF-9-iCre, Zp3cre, and Msx2Cre transgenic mice. *Biology of reproduction*. 2004;71(5):1469-74.
233. Myers M, Britt KL, Wreford NG, Ebling FJ, and Kerr JB. Methods for quantifying follicular numbers within the mouse ovary. *Reproduction*. 2004;127(5):569-80.
234. Wutz A. Gene silencing in X-chromosome inactivation: advances in understanding facultative heterochromatin formation. *Nat Rev Genet*. 2011;12(8):542-53.
235. Muzumdar MD, Tasic B, Miyamichi K, Li L, and Luo L. A global double-fluorescent Cre reporter mouse. *Genesis*. 2007;45(9):593-605.
236. Heffner CS, Herbert Pratt C, Babiuk RP, Sharma Y, Rockwood SF, Donahue LR, Eppig JT, and Murray SA. Supporting conditional mouse mutagenesis with a comprehensive cre characterization resource. *Nat Commun*. 2012;3(1218).
237. Huang S, Holzel M, Knijnenburg T, Schlicker A, Roepman P, McDermott U, Garnett M, Grenrum W, Sun C, Prahallad A, et al. MED12 controls the response to multiple cancer drugs through regulation of TGF-beta receptor signaling. *Cell*. 2012;151(5):937-50.
238. Jeyasuria P, Ikeda Y, Jamin SP, Zhao L, De Rooij DG, Themmen AP, Behringer RR, and Parker KL. Cell-specific knockout of steroidogenic factor 1 reveals its essential roles in gonadal function. *Molecular endocrinology*. 2004;18(7):1610-9.
239. Boerboom D, Paquet M, Hsieh M, Liu J, Jamin SP, Behringer RR, Sirois J, Taketo MM, and Richards JS. Misregulated Wnt/beta-catenin signaling leads to ovarian granulosa cell tumor development. *Cancer Res*. 2005;65(20):9206-15.
240. de Vries WN, Binns LT, Fancher KS, Dean J, Moore R, Kemler R, and Knowles BB. Expression of Cre recombinase in mouse oocytes: a means to study maternal effect genes. *Genesis*. 2000;26(2):110-2.
241. Douglas NC, Arora R, Chen CY, Sauer MV, and Papaioannou VE. Investigating the role of *tbx4* in the female germline in mice. *Biology of reproduction*. 2013;89(6):148.
242. Walker VR, and Korach KS. Estrogen receptor knockout mice as a model for endocrine research. *ILAR J*. 2004;45(4):455-61.
243. Couse JF, and Korach KS. Reproductive phenotypes in the estrogen receptor-alpha knockout mouse. *Ann Endocrinol (Paris)*. 1999;60(2):143-8.
244. Couse JF, and Korach KS. Estrogen receptor null mice: what have we learned and where will they lead us? *Endocr Rev*. 1999;20(3):358-417.
245. Willis A, Jung EJ, Wakefield T, and Chen X. Mutant p53 exerts a dominant negative effect by preventing wild-type p53 from binding to the promoter of its target genes. *Oncogene*. 2004;23(13):2330-8.
246. Nyabi O, Naessens M, Haigh K, Gembarska A, Goossens S, Maetens M, De Clercq S, Drogat B, Haenebalcke L, Bartunkova S, et al. Efficient mouse transgenesis using Gateway-compatible ROSA26 locus targeting vectors and F1 hybrid ES cells. *Nucleic acids research*. 2009;37(7):e55.

247. Jeyasuria P, Wetzel J, Bradley M, Subedi K, and Condon JC. Progesterone-regulated caspase 3 action in the mouse may play a role in uterine quiescence during pregnancy through fragmentation of uterine myocyte contractile proteins. *Biology of reproduction*. 2009;80(5):928-34.
248. Mittal P, Shin YH, Yatsenko SA, Castro CA, Surti U, and Rajkovic A. Med12 gain-of-function mutation causes leiomyomas and genomic instability. *J Clin Invest*. 2015;125(8):3280-4.
249. Xin HB, Deng KY, Rishniw M, Ji G, and Kotlikoff MI. Smooth muscle expression of Cre recombinase and eGFP in transgenic mice. *Physiol Genomics*. 2002;10(3):211-5.
250. Turunen M, Spaeth JM, Keskitalo S, Park MJ, Kivioja T, Clark AD, Makinen N, Gao FJ, Palin K, Nurkkala H, et al. Uterine Leiomyoma-Linked MED12 Mutations Disrupt Mediator-Associated CDK Activity. *Cell Rep*. 2014;7(3):654-60.